

Calibration system for the Tracking Accuracy
Measurement System (TAMS) using differential GPS
(dGPS)

Alan Neil Mountain

A dissertation submitted to the Department of Electrical Engineering,
University of Cape Town, in fulfilment of the requirements
for the degree of Master of Science in Engineering.

Cape Town, March 2004

Declaration

I declare that this dissertation is my own, unaided work. It is being submitted for the degree of Master of Science in Engineering in the University of Cape Town. It has not been submitted before for any degree or examination in any other university.

Signature of Author

Cape Town

1 March 2004

Abstract

The accuracy of a combined Optronics and Radar Tracker system is investigated in this dissertation. The Tracking Accuracy Measurement (TAMS) was designed to exploit the positional accuracy of differential Global Positioning System (dGPS) technology to qualify a 60km range X-band combined Optronic and Radar Tracker System.

In essence, a roving GPS receiver, capable of measuring high dynamic movement, is mounted on-board an airplane and records target position as it is tracked by the sensor. At the sensor, a similar recording station records the GPS position of the sensor, and is carefully surveyed into the co-ordinate system of the sensor. The TAMS also records the sensor output, which is carefully time-stamped with GPS time. Post mission, the raw GPS is differentially corrected.

An algorithm was written in *Matlab* for the purpose of comparing the dGPS measurements and the sensor measurements, once suitable interpolation and correction for sensor latency has taken place. The accuracy of the sensor latencies were investigated, and it was found that the latencies for both the Optronic and Radar sensors were off by a marginal time delay. It was concluded that the direction and speed of the airplane would account for this anomaly, but a more in-depth investigation should be considered.

The accuracy of the Tracker was calculated using statistical methods, and the accuracy computed for the data received for this dissertation was compared to the required Tracker specifications. Because only data from the 5km and 10km range bin was available for the analysis, the Tracker could only be qualified at these range bins. The result of the statistical analysis showed that the Tracker system meets specification at the 5km and 10km range bin.

Acknowledgements

The author would like to thank the following for their assistance with this dissertation:

- Professor Inggs for his continued advice and guidance throughout this dissertation;
- Dr. Richard Lord for his patient guidance and assistance with this document;
- Marie-Louise Barry from the CSIR for sponsoring this project;
- Thomas Bennett for helping out with hardware issues;
- Oladipo Fadiran for laying the foundation upon which this dissertation is based;
- My special friend Annie Parsons for her continual support and proof-reading;
- All the friends I have made in the Radar lab;
- My friends for their continual mockery of my extended academic career;
- My parents and brother for their continued support. This is for you.

Contents

Declaration	i
Abstract	ii
Acknowledgements	iii
Contents	iv
List of Figures	vii
List of Tables	xi
List of Symbols	xiv
Nomenclature	xv
1 Introduction	1
1.1 Background	1
1.2 User Requirements	1
1.2.1 dGPS base accuracy measurement	1
1.2.2 Calibration Software	2
1.3 Tracker Accuracy Requirements	2
1.4 Previous Work on the Calibration Software	4
1.5 Scope and Limitations	4
1.6 Dissertation Overview	5

2	Theory of DGPS, radar and statistical methods	10
2.1	dGPS	10
2.1.1	Basic Concept	10
2.2	Time Conversion	11
2.3	Co-ordinate Transformation	12
2.4	Summary of Chapter	12
3	Components of the Tracking Accuracy Measurement System (TAMS)	14
3.1	Concept of the Tracking Accuracy Measurement System	14
3.2	RTS 6400 Optronics and Radar Tracking System	15
3.3	GPS System	16
3.4	System Latencies	20
3.4.1	Radar	20
3.4.2	Optronics	21
3.5	Summary of Chapter	22
4	Software Background and Considerations	23
4.1	Tracker and Differential GPS Data files	23
4.1.1	Obtaining differential GPS data	24
4.2	Data Format	25
4.3	Co-ordinate system of Tracker and GPS system	25
4.4	Time Conversion	26
4.5	GPS data characteristics	26
4.5.1	PDOP and Space vehicles (SV's)	26
4.5.2	Discontinuities in dGPS time-stamp	26
4.5.3	Sectioning the dGPS data	27
4.6	Tracker data characteristics	29
4.6.1	Zero values for Azimuth, Elevation and Range	29
4.6.2	Gaps in Time Base	29
4.6.3	Optronic Data Update Rate	29
4.7	Interpolation of dGPS data	29
4.8	Summary of Chapter	31

5	Calibration Software	32
5.1	User variables	32
5.2	dGPS, Radar and Optronics data files	33
5.3	Repository for Results	33
5.4	Software Structure	34
5.4.1	User Menu	34
5.4.2	Section the Rad/Opt and dGPS data files	35
5.4.3	Radar or Optronics	35
5.4.4	Radar/Optronics data	35
5.4.5	Interpolation of dGPS data	35
5.4.6	Producing Results	36
5.5	Software Internals	36
5.6	Summary of Chapter	37
6	Results	43
6.1	Optronics vs dGPS	43
6.1.1	Overview of Optronics Data	43
6.1.2	Results Overview	45
6.1.3	Calibration software results	46
6.2	Radar vs dGPS	48
6.2.1	Overview of Radar Data	48
6.2.2	Results Overview	50
6.2.3	Calibration software results	51
6.3	Verification of Latency values	53
6.3.1	Latency test	53
6.4	Comments on Results	57
6.5	Summary of Chapter	57
7	Statistical Analysis	59
7.1	Effect of Co-ordinate transformation on GPS error distribution	59
7.2	Calculating Tracker <i>variance</i> and <i>standard deviation</i>	64
7.3	Summary of Chapter	68

8	Conclusions and Recommendations	70
8.1	Conclusions	70
8.1.1	Tracker system meets specification	70
8.1.2	Minimal Tracker data limits analysis	70
8.1.3	Insufficient data at particular range bins	71
8.1.4	Latency values	71
8.2	Recommendations	71
8.2.1	Test software by simulating data in radar simulator	71
8.2.2	Collect data at all range bins to qualify Tracker	71
8.2.3	Perform radial test flights to increase data at particular range bins	71
A	Optronics Results	75
A.1	Overview of Optronics Data	75
A.2	Results Overview	83
A.3	Results for ITB FAT - TAMS using LL data	90
A.3.1	Optronics tracking accuracies for optronics data latency compensation of 0 ms	90
A.3.2	Optronics tracking accuracies for optronics angle and range data latency compensation, of -230 and -240 ms respectively	92
B	Radar Appendices	94
B.1	Overview of Radar Data	94
B.2	Results Overview	106
B.3	Results for ITB FAT - TAMS using LL data	117
B.3.1	Radar tracking accuracies for radar data latency compensation of 0 ms	117
B.3.2	Radar tracking accuracies for radar data latency compensation of -204 ms . .	119
C	Polynomial Coefficients	121

List of Figures

1.1	Block diagram of the calibration system.	3
2.1	Concept of dGPS [10, pg 136].	11
2.2	Relationships of the various co-ordinate systems.	13
3.1	Picture of the RTS 6400 [27] Optronics and Radar Tracker System.	15
3.2	Ellipsoid of accuracy for 68% confidence level, in the Cartesian CRF.	18
3.3	Polar CRF for azimuth and elevation, with range of 2000m.	18
3.4	Dimensions of the aircraft used to collect the GPS data, with the GPS antenna mounted 1.6m from nose.	20
4.1	Sectioning the dGPS data.	28
4.2	Methods of Interpolation.	31
5.1	System level flow-diagram of TAMS software (1st part).	38
5.2	System level flow-diagram of TAMS software (2nd part).	39
5.3	Flow-diagram of GPS segmentation.	40
5.4	Flow-diagram of Optronics input.	41
5.5	Flow-diagram of GPS data interpolated to optronics time.	42
6.1	Optronics Segment 1 (ITB_FAT_WPN_Wed_12_09_22_1): Plots of optronics range, elevation and azimuth data. The GPS-derived range data is also shown for comparison.	44
6.2	Optronics Segment 1: Difference between optronics data and GPS-derived data for range, azimuth and elevation measurements (no latency compensation).	45
6.3	Radar Segment 1 (ITB_FAT_WPN_Wed_10_07_23): Plots of radar range, elevation and azimuth data. The GPS-derived range data is also shown for comparison.	49

6.4	Radar Segment 1: Difference between radar data and GPS-derived data for range, azimuth and elevation measurements (no latency compensation).	50
6.5	Plot of latency (s) vs. mean range (m), to verify the latency value of -204ms (radar inbound).	55
6.6	Plot of latency (s) vs. mean range (m), to verify the latency value of -204ms (radar outbound).	55
6.7	Plot of latency (s) vs. mean range (m), to verify the latency value of -240ms (optronics inbound).	56
6.8	Plot of latency (s) vs. mean range (m), to verify the latency value of -240ms (optronics outbound).	56
7.2	Input and Output variables of the Transformation.	59
7.1	Diagram depicting the effect of the Transformation on the GPS distribution.	60
7.3	Normal plot and histogram for closest range bin (639.09m).	62
7.4	Normal plot and histogram for mean range bin (6414.68m).	63
7.5	Normal plot and histogram for furthest range bin (18234.357m).	63
7.6	Diagram of differential data Z computed from the dGPS and Tracker Data.	64
7.7	Fitted mean curve to reflect data trend.	65
7.8	Flow diagram to compute Tracker Accuracy.	69
A.1	Optronics Segment 1 (ITB_FAT_WPN_Wed_12_09_22_1): Plots of optronics range, elevation and azimuth data. The GPS-derived range data is also shown for comparison.	76
A.2	Optronics Segment 2 (ITB_FAT_WPN_Wed_12_11_36_1): Plots of optronics range, elevation and azimuth data. The GPS-derived range data is also shown for comparison.	77
A.3	Optronics Segment 3 (ITB_FAT_WPN_Wed_12_17_04_1): Plots of optronics range, elevation and azimuth data. The GPS-derived range data is also shown for comparison.	78
A.4	Optronics Segment 4 (ITB_FAT_WPN_Wed_12_18_48_1): Plots of optronics range, elevation and azimuth data. The GPS-derived range data is also shown for comparison.	79
A.5	Optronics Segment 5 (ITB_FAT_WPN_Wed_12_24_59_1): Plots of optronics range, elevation and azimuth data. The GPS-derived range data is also shown for comparison.	80
A.6	Optronics Segment 6 (ITB_FAT_WPN_Wed_12_27_09_1): Plots of optronics range, elevation and azimuth data. The GPS-derived range data is also shown for comparison.	81
A.7	Optronics Segment 7 (ITB_FAT_WPN_Wed_12_29_28_1): Plots of optronics range, elevation and azimuth data. The GPS-derived range data is also shown for comparison.	82

A.8	Optronics Segment 1: Difference between optronics data and GPS-derived data for range, azimuth and elevation measurements (no latency compensation).	83
A.9	Optronics Segment 2: Difference between optronics data and GPS-derived data for range, azimuth and elevation measurements (no latency compensation).	84
A.10	Optronics Segment 3: Difference between optronics data and GPS-derived data for range, azimuth and elevation measurements (no latency compensation).	85
A.11	Optronics Segment 4: Difference between optronics data and GPS-derived data for range, azimuth and elevation measurements (no latency compensation).	86
A.12	Optronics Segment 5: Difference between optronics data and GPS-derived data for range, azimuth and elevation measurements (no latency compensation).	87
A.13	Optronics Segment 6: Difference between optronics data and GPS-derived data for range, azimuth and elevation measurements (no latency compensation).	88
A.14	Optronics Segment 7: Difference between optronics data and GPS-derived data for range, azimuth and elevation measurements (no latency compensation).	89
B.1	Radar Segment 1 (ITB_FAT_WPN_Wed_10_07_23): Plots of radar range, elevation and azimuth data. The GPS-derived range data is also shown for comparison.	95
B.2	Radar Segment 2 (ITB_FAT_WPN_Wed_10_11_13): Plots of radar range, elevation and azimuth data. The GPS-derived range data is also shown for comparison.	96
B.3	Radar Segment 3 (ITB_FAT_WPN_Wed_10_11_13): Plots of radar range, elevation and azimuth data. The GPS-derived range data is also shown for comparison.	97
B.4	Radar Segment 4 (ITB_FAT_WPN_Wed_10_15_54): Plots of radar range, elevation and azimuth data. The GPS-derived range data is also shown for comparison.	98
B.5	Radar Segment 5 (ITB_FAT_WPN_Wed_10_19_56): Plots of radar range, elevation and azimuth data. The GPS-derived range data is also shown for comparison.	99
B.6	Radar Segment 6 (ITB_FAT_WPN_Wed_10_19_56): Plots of radar range, elevation and azimuth data. The GPS-derived range data is also shown for comparison.	100
B.7	Radar Segment 7 (ITB_FAT_WPN_Wed_10_19_56): Plots of radar range, elevation and azimuth data. The GPS-derived range data is also shown for comparison.	101
B.8	Radar Segment 8 (ITB_FAT_WPN_Wed_10_25_04): Plots of radar range, elevation and azimuth data. The GPS-derived range data is also shown for comparison.	102
B.9	Radar Segment 10 (ITB_FAT_WPN_Wed_10_43_27): Plots of radar range, elevation and azimuth data. The GPS-derived range data is also shown for comparison.	103

B.10 Radar Segment 11 (ITB_FAT_WPN_Wed_10_48_28): Plots of radar range, elevation and azimuth data. The GPS-derived range data is also shown for comparison.	104
B.11 Radar Segment 12 (ITB_FAT_WPN_Wed_10_53_19): Plots of radar range, elevation and azimuth data. The GPS-derived range data is also shown for comparison.	105
B.12 Radar Segment 1: Difference between radar data and GPS-derived data for range, azimuth and elevation measurements (no latency compensation).	106
B.13 Radar Segment 2: Difference between radar data and GPS-derived data for range, azimuth and elevation measurements (no latency compensation).	107
B.14 Radar Segment 3: Difference between radar data and GPS-derived data for range, azimuth and elevation measurements (no latency compensation).	108
B.15 Radar Segment 4: Difference between radar data and GPS-derived data for range, azimuth and elevation measurements (no latency compensation).	109
B.16 Radar Segment 5: Difference between radar data and GPS-derived data for range, azimuth and elevation measurements (no latency compensation).	110
B.17 Radar Segment 6: Difference between radar data and GPS-derived data for range, azimuth and elevation measurements (no latency compensation).	111
B.18 Radar Segment 7: Difference between radar data and GPS-derived data for range, azimuth and elevation measurements (no latency compensation).	112
B.19 Radar Segment 8: Difference between radar data and GPS-derived data for range, azimuth and elevation measurements (no latency compensation).	113
B.20 Radar Segment 10: Difference between radar data and GPS-derived data for range, azimuth and elevation measurements (no latency compensation).	114
B.21 Radar Segment 11: Difference between radar data and GPS-derived data for range, azimuth and elevation measurements (no latency compensation).	115
B.22 Radar Segment 12: Difference between radar data and GPS-derived data for range, azimuth and elevation measurements (no latency compensation).	116

List of Tables

3.1	Azimuth and Elevation accuracies vs Range for 68% confidence.	19
3.2	Azimuth and Elevation accuracies vs Range for 95% confidence.	19
6.1	Accuracy of azimuth data, optronics angle time delay = -230 ms, optronics range time delay = -240 ms.	46
6.2	Accuracy of elevation data, optronics angle time delay = -230 ms, optronics range time delay = -240 ms.	46
6.3	Accuracy of range data, optronics angle time delay = -230 ms, optronics range time delay = -240 ms.	47
6.4	Accuracies over all inbound flights, optronics angle time delay = -230 ms, optronics range time delay = -240 ms.	47
6.5	Accuracies over all outbound flights, optronics angle time delay = -230 ms, optronics range time delay = -240 ms.	47
6.6	Accuracy of azimuth data, radar time delay = -204 ms.	51
6.7	Accuracy of elevation data, radar time delay = -204 ms.	51
6.8	Accuracy of range data, radar time delay = -204 ms.	52
6.9	Accuracies over all inbound flights, radar time delay = -204 ms.	52
6.10	Accuracies over all outbound flights, radar time delay = -204 ms.	52
6.11	Range differences for Optronics and Radar.	53
7.1	Coefficients of dGPS range data for Optronics 5km range bin.	66
7.2	Coefficients of dGPS range data for Radar 5km range bin.	66
7.3	Coefficients of dGPS range data for Radar 10km range bin.	67
7.4	Optronics standard deviations (σ_y).	67
7.5	Radar standard deviations (σ_y).	68

A.1	Accuracy of azimuth data, optronics time delay = 0 ms.	90
A.2	Accuracy of elevation data, optronics time delay = 0 ms.	90
A.3	Accuracy of range data, optronics time delay = 0 ms.	90
A.4	Accuracies over all inbound flights, optronics time delay = 0 ms.	91
A.5	Accuracies over all outbound flights, optronics time delay = 0 ms.	91
A.6	Accuracy of azimuth data, optronics angle time delay = -230 ms, optronics range time delay = -240 ms.	92
A.7	Accuracy of elevation data, optronics angle time delay = -230 ms, optronics range time delay = -240 ms.	92
A.8	Accuracy of range data, optronics angle time delay = -230 ms, optronics range time delay = -240 ms.	92
A.9	Accuracies over all inbound flights, optronics angle time delay = -230 ms, optronics range time delay = -240 ms.	93
A.10	Accuracies over all outbound flights, optronics angle time delay = -230 ms, optronics range time delay = -240 ms.	93
B.1	Accuracy of azimuth data, radar time delay = 0 ms.	117
B.2	Accuracy of elevation data, radar time delay = 0 ms.	117
B.3	Accuracy of range data, radar time delay = 0 ms.	118
B.4	Accuracies over all inbound flights, radar time delay = 0 ms.	118
B.5	Accuracies over all outbound flights, radar time delay = 0 ms.	118
B.6	Accuracy of azimuth data, radar time delay = -204 ms.	119
B.7	Accuracy of elevation data, radar time delay = -204 ms.	119
B.8	Accuracy of range data, radar time delay = -204 ms.	120
B.9	Accuracies over all inbound flights, radar time delay = -204 ms.	120
B.10	Accuracies over all outbound flights, radar time delay = -204 ms.	120
C.1	Coefficients of dGPS elevation data for Optronics 5km range bin.	121
C.2	Coefficients of dGPS elevation data for Radar 5km range bin.	121
C.3	Coefficients of dGPS elevation data for Radar 10km range bin.	121
C.4	Coefficients of dGPS azimuth data for Optronics 5km range bin.	122
C.5	Coefficients of dGPS azimuth data for Radar 5km range bin.	122
C.6	Coefficients of dGPS azimuth data for Radar 10km range bin.	122

List of Symbols

σ — standard deviation (square root of variance)

σ^2 —variance

μ — mean

Nomenclature

Azimuth—Angle in a horizontal plane, relative to a fixed reference, usually north or the longitudinal reference axis of the aircraft or satellite.

Baseline—In differential or relative positioning in GPS surveying, co-ordinates are in relation to some other fixed point. The line joining these co-ordinates are known as the baseline [32].

dGPS—*differential* GPS. dGPS uses range corrections determined at a known position (s) (base station (s)), and is more accurate than GPS.

Elevation—Angle in the vertical plane, relative to the fixed reference. The elevation angle is measured from the horizon upwards.

GPS—*Global Positioning System*. GPS is a worldwide radio-navigation system, that uses ranges measured from 27 satellites with known positions in the WGS84 co-ordinate system.

Latency—time delay measured in system between transmission and reception of pulses.

Laser—(*light amplification by stimulated emission of radiation*) Device that utilizes the natural oscillations of atoms or molecules between energy levels for generating coherent electromagnetic radiation [18, url].

Optronics—Target detection system that consists of a number of sensors, usually including an automatic video tracker (AVT), and a laser rangefinder. The AVT measures azimuth and elevation, and the laser measures range [3, url].

PDOP—(*Position Dilution of Precision*) This value represents the strength of the geometric fix of the GPS. A smaller value represents more favourable conditions. With clear visibility, the PDOP value should be 6 or less.

PRF—*Pulse Repetition Frequency*.

Range—The radial distance from a radar to a target.

RRSG—*Radar Remote Sensing Group*.

Selective Availability—internationally imposed degradation of civilian GPS accuracy by the U.S. Department of Defence. Turned off in May 2000.

TAMS—*Tracking Accuracy Measurement System.*

TWT—(*travelling-wave tube*) A specialized vacuum tube used in wireless communications, especially in satellite systems. The TWT is capable of amplifying or generating microwave signals.

UCT—*University of Cape Town.*

UTC—*Universal Time Coordinated.*

WGS-84—*World Geodetic System 1984.* The co-ordinate system used for GPS satellites, and also used in South Africa as the official co-ordinate system.

Chapter 1

Introduction

1.1 Background

Hardware and software are required to calibrate an Optronics and Radar Tracker system, using differential Global Positioning System (dGPS). The objective of this project is to determine the base accuracy of the dGPS measurement system and compare measurements made simultaneously with the Optronics and Radar Tracker system, thereby determining the accuracy of the Tracker system.

The RTS 6400 is the Optronics and Radar Tracker system used. The RTS 6400 is a 60 km range X-band combined Optronics and Radar Tracking System [27]. The data from the Tracker system comes from three sensors, namely the :

- X-band radar sensor (50Hz)
- laser rangefinder (12.5Hz)
- video autotracker (50Hz).

1.2 User Requirements

1.2.1 dGPS base accuracy measurement

The base accuracy of the dGPS measurement must be appraised through field tests, to determine whether the GPS system meets the manufacturer's specifications. Further analysis of the dGPS data, including statistical distributions, need to be investigated to determine the Tracker accuracy.

1.2.2 Calibration Software

Software needs to be written to simultaneously compare measurements made by the Optronics/Radar system and the dGPS measurements, to determine the accuracy of the Tracker System. The calibration software must meet certain requirements. The following requirements were specified for the calibration system:

- The software must be capable of reading in time-stamped dGPS and Optronics/Radar data.
- The dGPS time-stamp format must be converted to the format compatible with the Optronics/Radar time-stamp.
- The corrected GPS data needs to be interpolated for correct time-matching and calibration.
- The latency values given in Chapter 3, for the Tracker and GPS systems, must be verified.
- The effect of the co-ordinate transformation on the GPS error distribution must be determined.
- The software must determine whether the Tracker system meets the specified accuracy defined in Section 1.3.

The block diagram (in Figure 1.1 overleaf) depicts the calibration system from the initial input of raw data to the statistical analysis that is investigated in this dissertation.

1.3 Tracker Accuracy Requirements

The specified accuracies for the Tracker system, to be verified by the calibration system, are given in [23]:

1. 5m in *range*
2. 1.5mrad in *azimuth* and *elevation* angle from 500m to 25km

The accuracies stipulated in [23], do not state whether the accuracies represent the standard deviation. For the purposes of this dissertation, it is assumed that the accuracies represent the standard deviations.

The accuracy of the dGPS system must be more accurate than the Tracker system, to verify the accuracy of the Optronics Tracker system. It was decided that the GPS system needs to be three times more accurate than the Tracker system [19], ie. the equivalent range accuracy (one sigma level) of the verification system should be 1.5m or better.

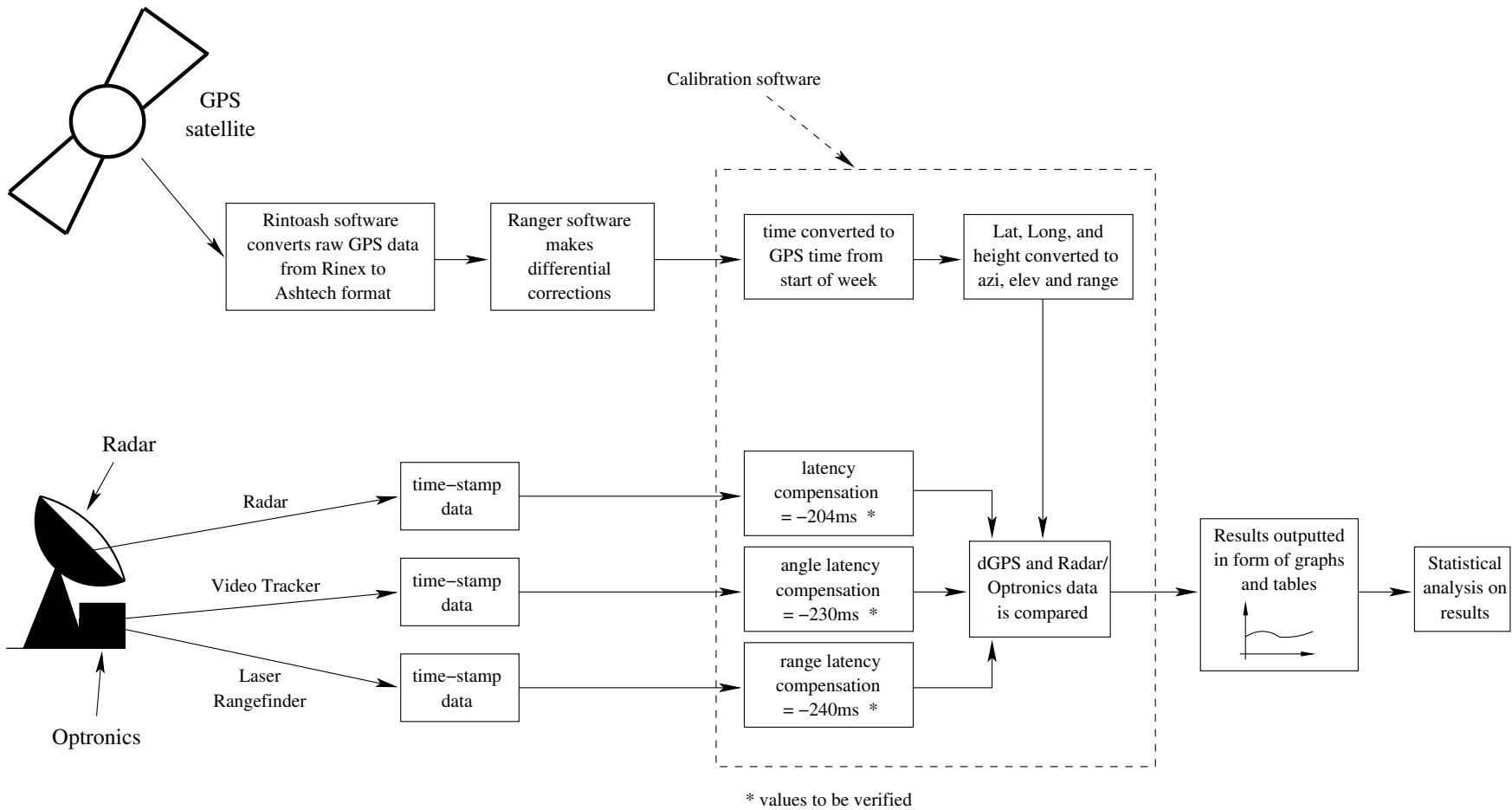


Figure 1.1: Block diagram of the calibration system.

1.4 Previous Work on the Calibration Software

Some software was written in Matlab by Oladipo Fadiran of UCT in 2001-2002, to analyse the original test data set of the Optronics and GPS system. Results of this initial test-run are found in the document written by Mr. Fadiran [6]. This software used a modified format of the Optronics test data for the comparison. The radar sensor was not yet ready at the time of writing his software. The GPS data was processed by Prof. Merry of UCT using the *Ranger* and *Rintoash*¹ software. The *Rintoash* software converts raw GPS files from the Rinex format (used in land surveying) to the Ashtech format (used in GPS applications). The *Ranger* software makes differential corrections to Ashtech files, for use by the calibration software. The comparison of data from the two data sets were matched on the time-axis using a “closest-fit”.

When new data from the Optronics and Radar System were made available, for reasons of compatibility most of the software previously written had to be rewritten. The new Radar and Optronics data formats were incompatible with the existing code. Thus the code had to be rewritten to accommodate the raw Radar and Optronics data sets. The *Ranger* and *Rintoash* software were made available by Prof. Merry for this project, to process the GPS data [24]. There were also problems with the new GPS time conversion format. The update rate was another compatibility issue as the angle and range data from the Radar originate from one sensor, whereas the Optronics data originates from two sensors (Laser and Autotracker). Both sensors of the Optronics system have different update rates. The Radar Tracking data also contains more gaps than the Optronics data. Changes and improvements made to the software are discussed further in Chapter 4.

Credit is given to Oladipo Fadiran, for writing the original software and laying the foundation upon which the final calibration software was written.

1.5 Scope and Limitations

The accuracy of the Optronics and Radar Tracker system is investigated in this project. The investigation primarily deals with obtaining the accuracy of the Optronics and Radar Tracker system by using dGPS, through comparison of data received from the Tracker and GPS system. Some practical considerations are given, but details relating to the Tracker and GPS hardware are kept to a minimum.

¹*Ranger* and *Rintoash* are software packages used in surveying to convert the raw GPS data to differential format.

1.6 Dissertation Overview

Chapter2

Chapter 2 gives a brief outline of the concepts and theory needed to write the calibration software. This chapter is divided into three sections.

Section 1 introduces the concept of differential GPS (dGPS). A more detailed description of GPS and dGPS has been left out of this dissertation, as these concepts can be found in numerous books and online websites. Many of these references are listed in Section 1 for further reading.

Section 2 describes the algorithm used to convert the GPS data time-stamp to the same format as the Tracker data time-stamp. The time-stamp of the dGPS data is given in Coordinated Universal Time (UTC), or civil time, whereas the time-stamp of the Tracker system is stamped in GPS seconds from the beginning of the week. The time-stamps need to be matched for the calibration software to compare the results at particular time-stamp values. The time-stamp of the dGPS data needs to be firstly converted from Gregorian calendar time to Julian Days. Following the conversion to Julian Days, the Julian Day is compared with the start of the GPS epoch (6 January 1980). The number of GPS seconds from the beginning of the week is calculated by a number of algorithms. Section 2 describes some of these algorithms, but makes references to standard algorithms that can be found in textbooks.

Section 3 introduces the different co-ordinate systems of the GPS and Tracker system. The World Geodetic System 1984 (WGS-84) is the (official) reference frame of GPS. The GPS data received for analysis by the calibration software was of the WGS-84 format, whereas the Tracker data was in a local level co-ordinate system. Thus a transformation from the WGS-84 (which is a geocentric system) to a local co-ordinate reference frame is required. The transformations, and references to these transformation algorithms, are mentioned in Section 3.

Chapter3

Chapter 3 gives an overview of the Optronics and Radar Tracking System, and the GPS System. The required accuracies for the Tracking system are discussed, and the GPS accuracies and system latencies are detailed. Chapter 3 is divided into four sections.

A brief description of the concept of TAMS is given in the first section.

The second section describes the RTS 6400 Optronics and Radar Tracking System [27] used for the calibration system. This 60 km range X-band combined Optronics and Radar Tracking System uses a highly stable TWT and advanced Doppler signal processing. Data needed for the analysis comes from three sensors:

- X-band radar sensor (50Hz)

- laser rangefinder (12.5Hz)
- video autotracker (TV cameras) (50Hz).

The tracking accuracy requirements for the Tracker system, to be verified by the calibration system, are listed. The calibration accuracy needs to be more accurate than the Tracker system, to verify the Tracker system. It was decided that the GPS system must be three times more accurate than the Tracker system, ie. the equivalent range accuracy (one sigma level) of the verification system should be 1.5m or better.

Section 3 details the GPS system. In this section the various field tests and methods for choosing the GPS system are very briefly described. The Ashtech Ranger GPS system was chosen as the most suitable GPS system in terms of cost and performance. The values of its performance are given, along with an explanation of the interpretation of these performance values and accuracies. The dimensions of the airplane onboard which the GPS antenna is mounted, are given.

Chapter 3 concludes with Section 4, which describes the problem of system latency for both the GPS and Tracker systems. When comparing two sets of data, it is imperative that the time-stamped data has been latency compensated. This latency compensation ensures that time delays are minimised. Mismatches in the time-stamping result in decreased accuracies in the differential comparison. Due to real life restrictions, the latency compensation measured is never exact. The latency values for the radar, optronics and GPS systems are listed, along with an explanation of each latency value.

The total latency compensation to be applied to the data is:

- –204 ms for the Radar data.
- –230 and –240 ms respectively for the Angle and Range data of the Optronics.

Chapter4

Chapter 4 details the background considerations needed to write the calibration software. A clear distinction is drawn between the original code written by Oladipo Fadiran, and the final calibration software used to make the accuracy analysis. The chapter is broken down into a number of sections, with each section highlighting important considerations taken into account when designing the calibration software.

The first section describes how the differential GPS data was obtained from the raw GPS data. The conversion from raw GPS to differential GPS involves some post-processing using the *Rintoash* and *Ranger* software packages. These software packages, supplied by Prof. Merry, are briefly described.

The format of the data tested for this dissertation is discussed. The format is significantly modified from that used for the original software. Section 2 in Chapter 4 describes these modifications and the implications for the software.

The next two sections discuss the co-ordinate systems and the time-stamp conversions. Equations referred to in this section are found in Chapter 2.

Two sections on the characteristics of the Tracker and GPS data are included. Two factors that affect the accuracy of the GPS readings are the number of space vehicles (satellites) used when taking a reading, and the Position Dilution of Precision (PDOP). The PDOP gives the measure of favourability of the satellite constellation when taking GPS readings. The values of these parameters are considered and a minimum value is chosen when considering the data. The *rule-of-thumb* value of 6 [10, pg 151], was chosen as the cut-off value. Discontinuities in both the Tracker and GPS time-stamps are also described. The reasons for these discontinuities are discussed further in Chapter 4.

Because the Tracker system outputs data at different data-rates (values mentioned in Chapter 3 overview) to the GPS system (1 Hz), the dGPS data needs to be interpolated to match the data. The concluding section describes a number of different interpolation options, from which the user of the software may choose, in interpolating the dGPS data to required data rates. The different interpolation options (including *cubic*, *spline* and *linear*) are compared. The *cubic* interpolation function is chosen as the default option, as this method gives the most suitable results on real data.

Chapter5

Chapter 5 is written to serve as a potential manual for users of the calibration software. This chapter runs briefly through the software, in an orderly way that reflects the flow and structure of the software.

The first section describes the variables and parameters that may be modified by the user in the software *setup* file. These parameters include the *latency*, *GPS data rate*, *interpolation method*, and some others.

The second section describes the data directories with respect to the working path of the calibration software. It is necessary for the user to know where the data folders for the Radar, Optronics and dGPS are located. If these directories do not exist, the software will create them. The relevant data must be located in the correct data folder for the software to function properly. The software searches the data folders for the data files, and displays a menu from which the user can choose the relevant data files to analyse.

Section 3 describes the folders that serve as a repository for the results that are produced by the calibration software. If these folders do not exist in the correct path, the software will create them. This information is necessary for a potential user who needs to know where the results produced by the software are kept. The results are stored as either figures or tables. The figures are saved in an encapsulated postscript format, and the tables are saved in a text format.

The bulk of the chapter consists of a fourth section that takes the reader through the software, from start to completion at a system level. All the user options and inputs are explained. Setup files

that can be used to modify certain system parameters are described. This allows the user to locate and change system parameters. By reading this section in parallel with the flow-diagrams found at the end of the chapter, the user can easily follow and run through the functioning of the calibration software.

The chapter concludes with a section containing a top-level flow diagram of the calibration software. Three more flow diagrams are included, which depict three function files in the calibration software. These diagrams are included to clearly describe the functioning of the software, without the need for tedious explanations.

Chapter6

Chapter 6 describes the results obtained from the calibration software. These results are analysed, with mention made of the graphs and tables that appear in this Chapter and Appendices. The latency values given in Chapter 3 are tested for accuracy. This chapter is broken down into four sections.

Sections 1 and 2 list the files and settings used to run the calibration software, for the Optronics and Radar respectively. The values of the results when running the calibration software are tabulated for clarity. Only values obtained from running the software with full latency compensation are tabulated in this Chapter. Tables for the output values, when running the software without full latency compensation, are found in the Appendices. Within each of these two sections, the results for each file that was analysed are tabulated, as well as the results for all inbound and outbound flights. A difference plot for the first analysed segment between the Radar/Optronics range, elevation and azimuth data and the dGPS range, elevation and azimuth data is included, along with a plot of the Radar/Optronics range, elevation and azimuth data. Plots for all the analysed segments are found in the Appendices.

The third section describes the output of the latency verification testing. The output results are compared with the values of the latency values given for the analysed data. Discrepancies between the listed latencies and the values that give the smallest mean errors are present for both the Radar and Optronics systems. These discrepancies are explained in this section.

The last section comments on the results from Sections 1, 2 and 3. Mention is made of the validity of the data, and some comments on the tracking accuracy are made.

Chapter7

The statistical analysis is dealt with in this chapter. The purpose of this chapter is to make a statement regarding the accuracy of the Tracker system, by comparing the calculated Tracker accuracy with the specified Tracker accuracy in Section 1.3. Chapter 7 is divided into two sections.

Section 1 aims to discover the effect of the co-ordinate transformation on the error distribution of the dGPS data. The error distributions of the dGPS input variables *longitude*, *latitude* and *height* are compared with the output variables *range*, *azimuth* and *elevation*. The distribution is simulated

using a Gaussian distribution as input. Plots and histograms of the output variables are studied, to evaluate whether the output distribution is a Gaussian distribution. To further test the output for a Gaussian distribution, an hypothesis test is performed on the output data.

The Tracker accuracy is calculated in Section 2. The variance of the dGPS data is found by fitting a polynomial to the GPS data to represent the *mean* for the data, as the range is changing with time. The covariance of the dGPS and difference data is calculated, and the Tracker accuracy is computed. The chapter concludes with a comparison of the calculated Tracker accuracy and the specified Tracker accuracy.

Chapter8

Based on the findings in Chapters 6 and 7, some conclusions are made regarding the TAMS. Recommendations for improving TAMS and future work are considered in this chapter.

Chapter 2

Theory of DGPS, radar and statistical methods

The objective of this chapter is to outline the most relevant concepts and theory used to write the calibration software. A brief outline of the concept of differential GPS (dGPS) is described, with a number of references to more comprehensive texts on the subject for the reader of this dissertation to pursue. The conversion from Universal Time Coordinated (UTC) to GPS seconds from the beginning of the week (to compare time-stamps) is discussed, with some equations that are used to write the time conversion algorithm for the calibration software. Finally, some of the co-ordinate transformations that will convert the dGPS data into a comparable format, are listed.

2.1 dGPS

The basic concept of differential GPS will be introduced in Section 2.1.1. A more detailed discussion of GPS and differential GPS is presented in the references for this section. An introductory text on differential GPS can be found in [11]. A more thorough discussion of GPS and differential GPS can be found in [1, pg 47-67] and [10, pg 136-155]. A simple tutorial on the basic functioning of GPS and dGPS can be found at [31] and [17].

2.1.1 Basic Concept

Before Selective Availability was turned off in May 2000, a civilian user of the GPS system could not expect a very high navigation accuracy (15-40 m at best [10, pg 15]). This degradation of the point positioning accuracy, due to Selective Availability, consequently led to the development of dGPS. The technique of differential GPS is based on differential measurements. Two receivers are

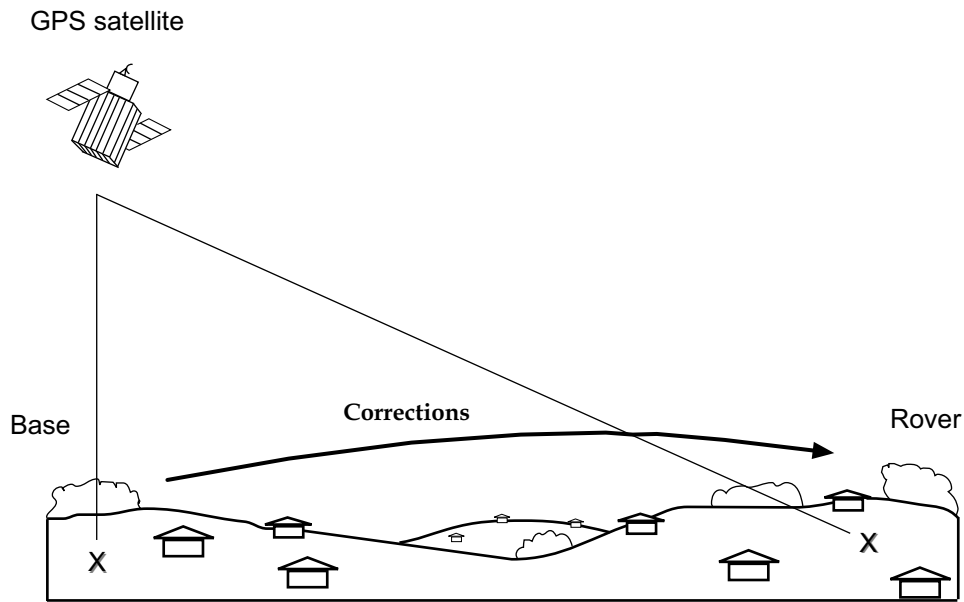


Figure 2.1: Concept of dGPS [10, pg 136].

needed, one as a reference receiver (base receiver) at a known fixed position, and the other receiver's (possibly roving) position to be determined (see Figure 2.1).

The position of the base receiver is accurately determined through use of surveying techniques. The base receiver receives transmissions from carefully selected satellites, and determines any positional errors from its known position. These errors are then relayed to the roving receiver [1, pg 50] via telemetry (ie. controlled radio link [10, pg 136-137]). The GPS receiver uses these error corrections to display a more accurate position. This higher accuracy is based on the fact that the factors of GPS errors are fairly similar over short distances (up to 500 km [10, pg 137]), and therefore the errors are virtually eliminated by the differential technique.

2.2 Time Conversion

For the calibration software to compare the data of the Tracker and the GPS system, the time-stamps need to be matched. The time-stamp of the dGPS data is given in Universal Time Coordinated (UTC), or civil time. This time-stamp needs to be converted to GPS seconds from the beginning of the week. The time-stamp of the Tracker system is stamped in GPS seconds from the beginning of the week.

The conversion of UTC to GPS seconds from the beginning of the week involves a number of complicated conversions. The time-stamp of the dGPS data needs to be firstly converted from Gregorian calendar time to Julian Days. The equation for this conversion can be found in [20], [10, pg 37-

38], [25, pg 137-178] and [14, pg 33]. Let the civil date be expressed by integer values for the year Y , month M , and day D :

$$jd = \text{fix}(365.25 \times yr) + \text{fix}(30.6001 \times (mn + 1)) + b + 1720996.5 + D$$

where fix denotes the integer part of the real number closest to zero given by:

$$\begin{aligned} yr &= Y - 1 \quad \text{and} \quad mn = M + 12 \quad \text{if} \quad M \leq 2 \\ yr &= Y \quad \quad \quad \text{and} \quad mn = M \quad \quad \quad \text{if} \quad M > 2 \end{aligned}$$

and b is given by $\text{fix}(yr/400) - \text{fix}(y/100)$.

Following the conversion to Julian Days, the Julian Day is compared with the start of the GPS epoch (6 January 1980). The number of GPS seconds from the beginning of the week is calculated by a number of calculations outlined in [10, pg 38] and [25, pg 137-178].

2.3 Co-ordinate Transformation

The World Geodetic System 1984 (WGS-84) is the (official) reference frame of GPS. The GPS data received for this analysis was of the WGS-84 format, whereas the Tracker data was in a local level co-ordinate system. Thus, a transformation from the WGS-84 (which is a geocentric system) to a local co-ordinate reference frame was required.

Figure 2.2 overleaf (which has been adapted from Figures 10.1 and 10.2 of [10, pg 280,283]) depicts the relationship between the co-ordinate systems. The diagram on the left of Figure 2.2 shows point P , with longitude λ , latitude φ and height h . It can be seen on this figure how the ellipsoidal co-ordinates relate to the Cartesian co-ordinates \mathbf{X} , \mathbf{Y} and \mathbf{Z} . The relationship between the Global and local level co-ordinate systems are seen in the figure on the right of Figure 2.2. The relationships of the different variables and transformations from one co-ordinate system to another, can be found in [10, pg 279-290], [9, pg 62], [1, pg 154-155] and [14, pg 451-485]. A collection of papers that thoroughly detail co-ordinate transformations can be found in [8].

2.4 Summary of Chapter

The concept of dGPS was discussed, detailing how known error measurements from the base station are used to increase the accuracy of the positional measurements of the GPS receivers, in the vicinity of the base station. The conversion from UTC to GPS seconds from the beginning of the week was

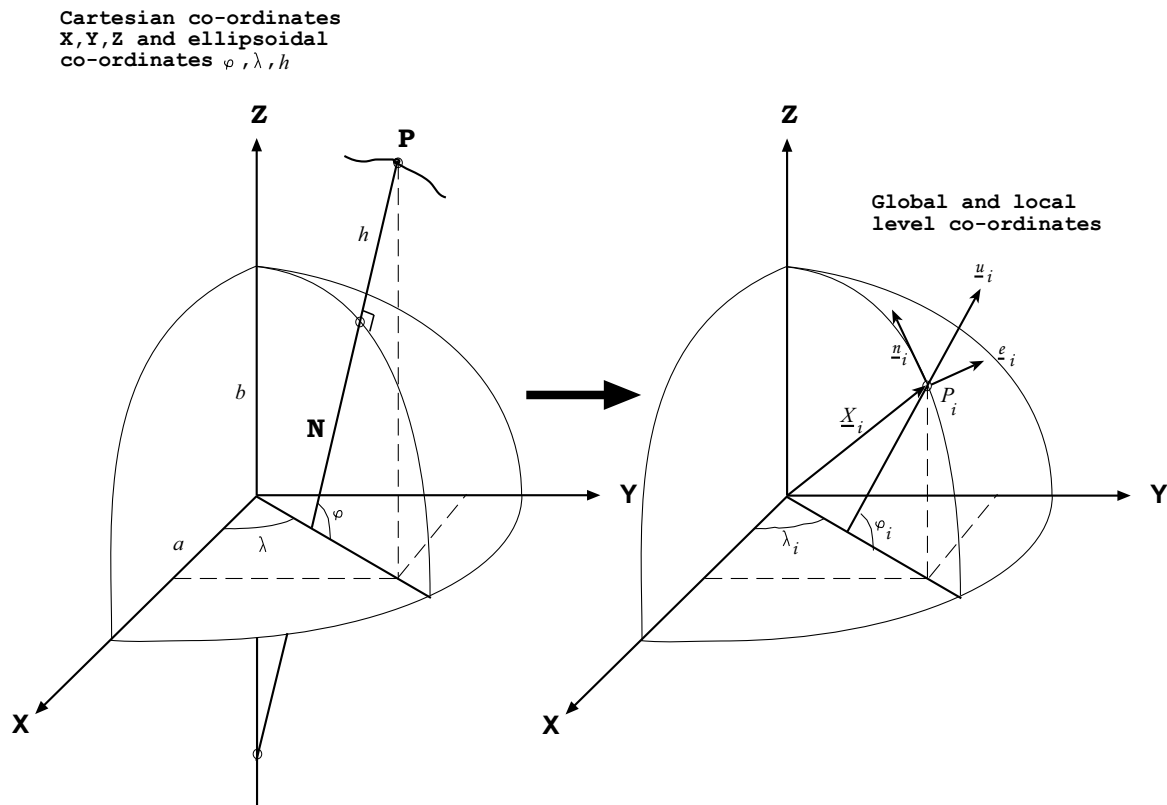


Figure 2.2: Relationships of the various co-ordinate systems.

described, with an algorithm to convert the GPS time-stamp from Gregorian calendar time to Julian days, and comparing these values with the GPS epoch to calculate the GPS seconds. Finally, the procedure to convert the GPS variables from *longitude*, *latitude* and *height* to *range*, *azimuth* and *elevation* was discussed, with the aid of a diagram depicting the different co-ordinate systems.

Chapter 3

Components of the Tracking Accuracy Measurement System (TAMS)

This chapter details the fundamental components, accuracies and latencies of the Tracker and GPS systems used in the calibration system. The chapter starts off by describing the concept of the Tracking Accuracy Measurement System. The Tracker system that needs to be calibrated, and details of the required accuracies, are described in Section 3.2. Section 3.3 describes the GPS chosen to calibrate the Tracker system, and details the accuracy of the GPS system. The chapter concludes (Section 3.4) with a list of the system latencies that influence differential comparison.

3.1 Concept of the Tracking Accuracy Measurement System

The Tracking Accuracy Measurement System (TAMS) was designed to exploit the positional accuracy of differential Global Positioning System (dGPS) technology, to qualify an Optronics Tracker System. In essence, a roving GPS receiver, capable of measuring high dynamic movement, is mounted to a target and records target position as it is tracked by the Tracker sensors. The TAMS records the sensor output and carefully time-stamps the data with GPS time.

After the data has been collected, the GPS data is differentially corrected using measurements from the base-station. The dGPS data is then translated to the sensor reference frame, using the calibration software described in this dissertation. The sensor data can then be compared to the dGPS measurements, once suitable interpolation and correction for sensor latency has taken place. A statistical study on these compared measurements allow the sensor readings to be qualified. This concept is described in the system diagram in Chapter 1.

3.2 RTS 6400 Optronics and Radar Tracking System

The Optronics/Radar system used in the calibration system was the RTS 6400, as seen in Figure 3.1. It is a 60 km range X-band combined Optronic and Radar Tracking System [27]. It uses a highly stable TWT [29] and advanced Doppler signal processing. The data for the analysis came from three of the sensors, namely the:

- X-band radar sensor (50Hz)
- laser rangefinder (12.5Hz)
- autotracker (TV cameras) (50Hz).



Figure 3.1: Picture of the RTS 6400 [27] Optronics and Radar Tracker System.

Required Tracker accuracy

The tracking accuracy performance requirements for the Tracker system, to be verified by the calibration system, are given in [23]:

1. 5m in *range*
2. 1.5mrad in *azimuth* and *elevation* angle from 500m to 25km

The accuracies stipulated in [23], do not state whether the accuracies represent the standard deviation. For the purposes of this dissertation, it is assumed that the accuracies represent the standard deviations. At a range of 25km, this angular accuracy translates to 37.5m, but at a range of 500m, 1.5mrad translates to 0.75m. This latter requirement will make most of the evaluated data unsuitable if strictly applied. The accuracy of the system needs to be more accurate than the Tracker system, in order to verify the Tracker system. It was decided that the GPS system needs to be three times more accurate than the Tracker system [19], ie. the equivalent range accuracy (one sigma level) of the verification system should be 1.5m or better.

3.3 GPS System

The choice of GPS for the calibration system involved numerous field tests, of different types of GPS with varying accuracy and price. The field tests were carried out by Prof. Merry of UCT. These tests included a static test over a *short* baseline (3.5m), tests over a *long* baseline (19.1km), and a *kinematic* test. The details of the tests and results were compiled into a document written by Prof. Merry [19].

Based on the field test results, the Ashtech Ranger receiver was used as the GPS for the calibration system. Some of the results of the chosen Ashtech Ranger GPS are reproduced below for clarity [19] (It should be noted that the GPS met manufacturer's specification when the PDOP was 4 or less than 4.):

- For the *short* baseline tests, it was concluded that there were no significant biases in the results for the three sessions, and the mean positions all agreed with one another and the known position to within 0.3 m (horizontal) and 0.2 m (vertical).
- For the *long* baseline field tests, there were again no significant biases and the results of the means agreed with one another and to the known position to within 0.3 m (horizontal) and 0.2 m (vertical).
- The errors did not increase as the baseline increased (over the reasonably short baseline of < 20 km), however, there is a larger spread in both the horizontal position and height as the baseline increases.
- The results of the *kinematic* test show that there is no material degradation in accuracy when operating in the *kinematic* mode.

The kinematic test is of particular interest in this project, as the Tracker system must be able to handle targets moving at speeds of up to 280 m/s mentioned in Section 3.2.

A summary of the results [19] for the GPS that was chosen can be described as follows:

- The Ranger system provides horizontal positioning accuracies of 1 m horizontal and vertical positioning accuracies of 2 m, provided observations are made when the PDOP is 4 or less.
- The Tracker system should be sufficient to validate the Tracker system for target ranges of 3 km to 25 km, but is not suitable to validate the Tracker for target ranges less than 3 km.

The Ashtech Ranger GPS system is capable of producing relative positions, in the WGS84 coordinate system, which can be converted to ranges, azimuths and elevation angles. These positions

are time tagged with GPS time. The GPS data analysed by the software was 1Hz. For the calibration software, this GPS data of 1Hz had to be matched to the 12.5Hz and 50Hz data of the Optronics range and Optronics/Radar azimuth and elevation. The procedure is discussed in Chapter 4 and 5.

GPS Accuracy

The GPS accuracies can be summarized as follows [23]:

“The estimated accuracies, in the WGS84 co-ordinate system are:

Mowbray base (TRGE), RRS base, Tracker origin: 5cm horizontal and vertical.

The relative accuracy of the Ranger GPS system (and hence of the Rover unit) is 1m horizontal and 2m vertical (provided the observations are made with a PDOP of 4 or less). This means that the dGPS readings in a Cartesian Co-ordinate system, should lie within an ellipsoidal shaped figure (See Figure 3.2), with a horizontal axis of 2m (on the horizontal plane), and a vertical axis of 4m, centered at the true position of the target.

Note: These accuracies are at the one sigma level, i.e. 68% confidence level (for 95% confidence, double the numbers given above. Thus the readings will lie within an ellipsoidal shaped figure, with a horizontal axis of 4m (on the horizontal plane), and a vertical axis of 8m centered at the true position of the target. This means that the accuracy with which the Tracking Error can be determined for each target position will be the same in the Cartesian CRF, but this is however not the case in a polar CRF. It should also be noted that the 68% confidence level applies to the data that is used. In each segment of data, some data was not used, and the confidence level does not apply to this data.”

As mentioned previously, the above accuracies are not influenced by movement from the receiver, and are therefore valid for the case of a moving target.

The accuracy ellipsoid described above is depicted in Figure 3.2. The position of the target, given relative to point A in the diagram, could lie anywhere within the ellipsoid.

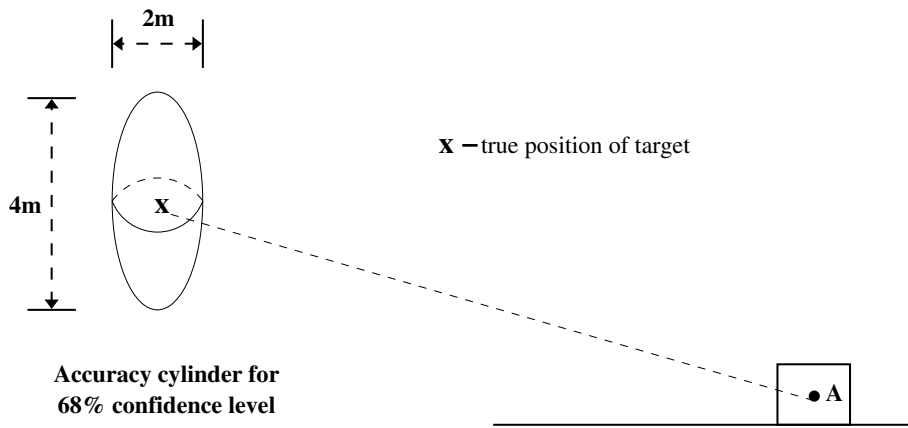


Figure 3.2: Ellipsoid of accuracy for 68% confidence level, in the Cartesian CRF.

The dGPS angle accuracies are calculated in the Polar CRF, using Figure 3.3. The accuracies are calculated in Figure 3.3 using the equation [12, pg39]:

$$s = r\theta$$

where r is the range in meters, θ is the angle in radians, and s is the length of the arc. Due to the large distance of the range, the arc can be approximated by straight lines of 1 and 2m respectively in Diagram 3.3. The range is taken at certain intervals mentioned in Section 3.2.

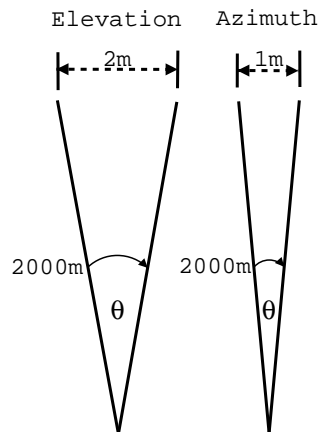


Figure 3.3: Polar CRF for azimuth and elevation, with range of 2000m.

The TAMS dGPS angle accuracies in the Polar CRF are tabulated in Tables 3.1 and 3.2, to show the variation of angle accuracy with target range.

Table 3.1: Azimuth and Elevation accuracies vs Range for 68% confidence.

Range (km)	Azimuth Accuracy (mrad)	Elevation Accuracy (mrad)
2	± 0.5	± 1
5	± 0.2	± 0.4
10	± 0.1	± 0.2
20	± 0.05	± 0.1

Table 3.2: Azimuth and Elevation accuracies vs Range for 95% confidence.

Range (km)	azimuth accuracy (mrad)	elevation accuracy(mrad)
2	± 1	± 2
5	± 0.4	± 0.8
10	± 0.2	± 0.4
20	± 0.1	± 0.2

Aircraft Dimensions

The raw GPS readings (not yet differentially corrected) used in this analysis, originate from a GPS receiver mounted onboard an airplane. The dimensions of the plane used to fly the sortie are given in Figure 3.4. Since the GPS antenna is mounted 1.6m from the nose of the aeroplane, it can be assumed that at a certain range the difference between inbound and outbound flights should be equal to or smaller than 5.1m. This means that the GPS range is 1.6m longer for inbound flights, and 5.1m longer for outbound flights, if we assume that reflections occur at the nose, tail and join of the wing and body of the aircraft, as seen in Figure 3.4.

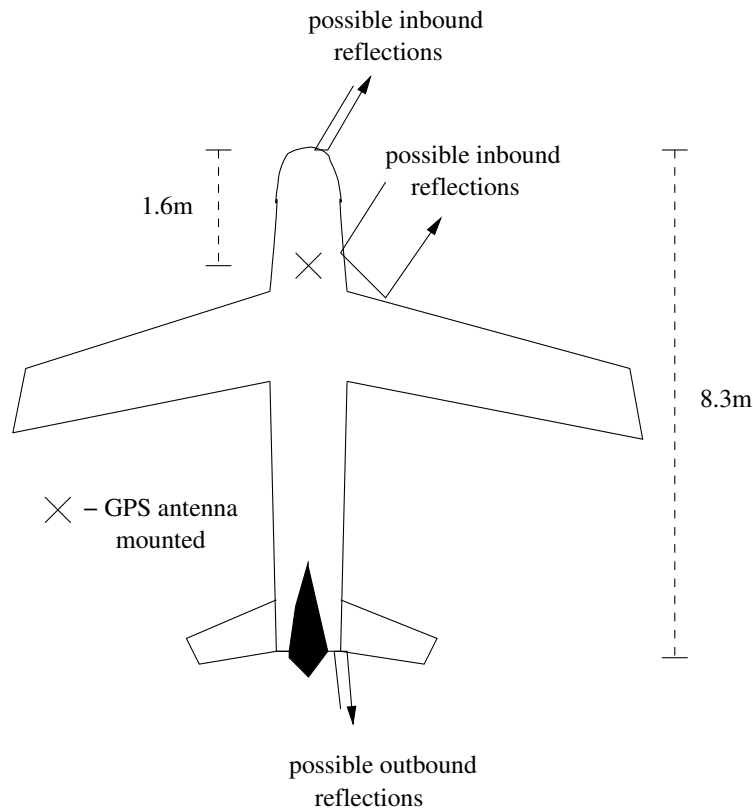


Figure 3.4: Dimensions of the aircraft used to collect the GPS data, with the GPS antenna mounted 1.6m from nose.

3.4 System Latencies

When comparing two sets of data, it is imperative that the time-stamped data has been latency compensated. This latency compensation ensures that time delays are minimised. Mismatches in the time-stamping will result in decreased accuracies in the differential comparison. Due to real life restrictions, the latency compensation measured will never be exact, but the accuracy of these measurements are investigated in Chapter 6.3.

Description of latency problem

3.4.1 Radar

A number of data latencies need to be considered (for each recorded radar target position), when calculating the Tracking error. These latencies were calculated in the system by the RRS [34] as follows:

1. Data processing time delay between transmission of the radar pulse and the receipt of the pulse, to calculate a target position estimated by the System Data Processor from the Radar Signal Processor. This delay was measured as +55 msec.
2. Data processing and data transmission time delay (from the System Data Processor to the System Environment Simulator (SES)) until the data is time stamped with the GPS time in the SES and logged. The measured delay is +10.8 msec.
3. The time delay between the GPS time stamp and the actual GPS time (inherent in the method of synchronisation of the SES with the GPS Base Station) is 270 msec. This results in a latency of -270 msec.

The **total data latency** of the Tracking data timestamps vs. true GPS time is therefore:

$$(55 + 10.8 - 270) = -204 \text{ msec.}$$

3.4.2 Optronics

The derivation of the optronics time delays, or latencies, have been done in [35] and are briefly reproduced here for clarity. The optronics latencies are split up into two components:

Latency of Angle Data

1. Data processing time delay between the video frame grabber and the receipt of the target position estimated by the System Data Processor from the Autotracker, of +30 msec.
2. Data processing and data transmission time delay (System Data Processor to SES) until the data is time stamped with GPS time in the SES and logged, of +10.8 msec.
3. The time delay between the GPS time stamp and actual GPS time (inherent in the method of synchronisation of the SES with the GPS Base Station) is 270 msec. This results in a latency of -270 msec.

The **total data latency** of the Tracking data timestamps versus true GPS time is therefore:

$$(30 + 10.8 - 270) = -230 \text{ msec.}$$

Latency of LRF Range Data

1. Data processing time delay between the transmission of the Laser pulse and the receipt of the target position estimated by the System Data Processor from the Autotracker, of +20 msec.
2. Data processing and data transmission time delay (System Data Processor to SES) until the data is time stamped with GPS time in the SES and logged, of +10.8 msec.
3. The time delay between the GPS time stamp and actual GPS time (inherent in the method of synchronisation of the SES with the GPS Base Station) is 270 msec. This results in a latency of -270 msec.

The **total data latency** of the Tracking data timestamps versus true GPS time is therefore:

$$(20 + 10.8 - 270) = -240 \text{ msec.}$$

The latencies will be incorporated into the calibration software in Chapter 5, and the results of the different latencies will be described in Chapter 6. These latencies are tested for accuracy.

3.5 Summary of Chapter

The concept of the TAMS was described, giving a detailed list of the components of the system and how they interact with one another. The combined Radar and Optronics Trackers system was discussed, with a summary of the components and data rates. The Tracker accuracy to be verified in this dissertation was stated. The GPS system chosen to collect the data for this dissertation, and the accuracy of the GPS system, was referred to in this Chapter. The dimensions of the plane, and the position of the GPS antenna onboard the airplane used to collect the data, was described. The system latencies needed for the calibration software were broken down and listed, with the total latency compensation given for each sensor.

Chapter 4

Software Background and Considerations

Some initial test calibration software was written in Matlab, by Oladipo Fadiran of UCT in 2001-2002, to compare the original test data of the Optronics and GPS system. At the time of writing his software, the radar sensor was not yet ready and testing on the radar sensor was not able to be completed. The results of the initial test-run on the Optronics and dGPS data can be found in the document written by Mr. Fadiran [6].¹

When the new data from the Optronics and Radar System was made available, for reasons of compatibility most of the software previously written had to be rewritten. The new Radar and Optronics data format was incompatible with the existing code. Thus, the code had to be rewritten to accommodate the new Radar and Optronics data sets. There were also problems with the new GPS time conversion format.

Another compatibility issue was the update rate, where the angle and range data from the Radar originate from one sensor, whereas the Optronics data originates from two sensors (Laser and Autotracker). Both sensors on the Optronics system have different update rates, as described in Chapter 3.2. The Radar Tracker data also contains more gaps than the Optronics data. The changes and improvements made to the software, along with some other considerations, are discussed further in this chapter.

4.1 Tracker and Differential GPS Data files

The Tracker and GPS data received for the accuracy analysis consisted of a number of files (the files used by the calibration software to produce the results in Chapter 6 are described in Chapter 6.1.1 and 6.2.1). The Optronics and Radar data files were split into a number of straight *inbound* and *outbound* flights. Segments of data, where the test target was performing a turning maneuver

¹The use of the “*original*” software in this dissertation refers to the code written by Oladipo Fadiran.

or flying a holding pattern, were left out, due to the fact that the polynomial interpolation methods mentioned in Section 4.7 produce very large errors. Testing was done by UCT (the details of which can be found in [7]) on the interpolation of test data with the target flying different patterns. It was found that the interpolation errors are minimal when an aircraft is flying on a fairly straight and “smooth” trajectory, and the change in acceleration over the considered period is small.

The raw GPS data received for the analysis consisted of a number of data files. These files were needed to convert the raw GPS data to the required differential format. The various data formats and the differential conversion are discussed in Section 4.1.1.

4.1.1 Obtaining differential GPS data

The GPS data for the calibration accuracy analysis was not received in a differential format. Some post-processing was required to convert the GPS data into the dGPS format. Two software packages, *Rintoash* and *Ranger*, were obtained from Prof. Merry to convert the raw GPS data to the differential format. The *Rintoash* software converts the raw GPS files from the RINEX format to the Ashtech format.

RINEX and Ashtech Format

Before post-processing of the GPS data can begin, the data has to be downloaded from the receiver. This data is stored in binary (and receiver independent) format [10, pg 203], and contains observables like the navigation message. Even though the binary data from the receiver may be converted into computer independent ASCII format during downloading, the data is still dependant on the receiver. Each different available GPS processing software program has its own format, which makes it necessary to convert the data into software independent format when processed with another type of program. This software independent format has been realised with the **Receiver Independent Exchange (RINEX)** format, which promotes data exchange. The RINEX format contains four types of ASCII files [10, pg 204]:

- observation data file
- navigation message file
- meteorological data file
- GLONASS navigation message file.

The software package *Ranger* makes differential corrections to the Ashtech files, using information from the base-station. The output of the *Ranger* software produces the differential GPS data file that is used for the accuracy software.

The details of these software packages and their usage can be found in [24].

4.2 Data Format

The original software written for the calibration system was used to test the test data from the Optronics and GPS system. The format of the data received for initial testing was significantly modified from the original processed GPS and Optronics format. The format of the Optronics data Mr. Fadiran received was clearly separated into relevant data fields containing values for time, range, azimuth and elevation. The data that was not going to be used in the calibration process was left out in the modified data file. Thus, the software written by Mr. Fadiran took into account the modified format and extracted all the data from the data fields.

When the radar sensor was ready, data from the Optronics, Radar and GPS systems were made available for testing. The format of the Optronics and Radar data differed significantly from the original test data used for testing by Mr. Fadiran's code. The new data received for processing was in its original processed format. It was decided not to modify the format of this data, but to rather modify the software, making the software more versatile for future use. By making allowance for the original data format, the user of the calibration software does not need to modify the data. In the new Optronics and Radar data sets, the significant data can be found using the data *field identification tags* and data *validity indicators*, described in [35, pg3], [19] and Section 4.6.1.

4.3 Co-ordinate system of Tracker and GPS system

The co-ordinates for the differential GPS data in the data files are given in *latitude*, *longitude* and *height*. The co-ordinates for the Tracker system are however given in *range*, *azimuth* and *elevation*. To compare the data in the calibration software, it was decided to convert the dGPS data from *latitude*, *longitude* and *height* into *range*, *azimuth* and *elevation*. This involves a number of transformations.

The dGPS data firstly needs to be converted from *longitude*, *latitude* and *height* to the X, Y and Z co-ordinate reference frame. This process uses the semi-major and semi-minor axes of the WGS-84 ellipsoid, and a number of transformations mentioned in Section 2.3. The relative position of the tracked target to the GPS base station position must be calculated by converting the base station position into the X,Y and Z co-ordinate frame. The relative position of the target is now found by using the converted X,Y and Z co-ordinates of the dGPS data. The *azimuth*, *elevation* and *range* for the dGPS data can now be calculated.

The software algorithm, written to transform the co-ordinate systems, incorporates these transformations. The linearity of these transformations will be tested in Chapter 7.

4.4 Time Conversion

The algorithms used to convert the time-stamps (covered in Chapter 2.2), used by Oladipo Fadiran in the initial software, had to be slightly modified to accommodate the new data.

When running a small segment of the test data for the first time, the time-stamps did not match up. The matching error in time-stamps was narrowed down to the fact that the equations mentioned in Chapter 2.2 did not take into account that the navigation message is set to zero every 1024 weeks, since 10 bits are used to store the week number. The standard GPS epoch began on 6 January 1980, thus the first rollover occurred at midnight 21-22 August 1999. The software therefore had to be modified by converting the 1024 weeks that were lost to days. This number is then added to the Julian Day number, calculated by the formula, to make up for the lost days. This modification corrected the time-stamp matching error.

4.5 GPS data characteristics

This section describes some important characteristics of the GPS data that were considered when developing the software for the calibration system.

4.5.1 PDOP and Space vehicles (SV's)

In order to obtain precise positioning at a particular time (a concern when using GPS), the number of satellites or space vehicles (SV's) used and the satellite geometry need to be known. Only those periods when four or more satellites are in view are considered to give suitable satellite coverage. The software thus discards any data that corresponds to time-stamps where four or less satellites (SV's) were in view.

A measurement of the favourability of the geometry of the satellites used to measure *latitude*, *longitude* and *height*, is known as the **Position Dilution of Precision (PDOP)** [1, pg 159-160], [9, pg 55] and [10, pg 151]. It is generally considered that any value for the PDOP smaller than 6 is considered acceptable [10, pg 151]. This *rule-of-thumb* value was chosen for the software. The calibration software thus needs to discard any dGPS data that corresponds to a PDOP value greater than 6. This process is described in Section 4.5.3.

4.5.2 Discontinuities in dGPS time-stamp

When analysing the dGPS data file used for the analysis, it was found that it contained many discontinuities in the time-stamp. These discontinuities had to be accounted for by the software, and are

described in Section 4.5.3.

4.5.3 Sectioning the dGPS data

Due to the discontinuities in the dGPS time-stamp described in Section 4.5.2, a method to effectively handle these discontinuities needed to be implemented. Some software was originally written by Mr. Fadiran to segment the code, but the new data files provided for the analysis meant that this software had to be rewritten. Before the dGPS data is segmented, dGPS data exceeding a PDOP value of 6 needs to be discarded. The software runs through the dGPS file and searches through the PDOP values. The data fields that correspond to a PDOP value greater than 6 are discarded. This is described in the top figure (1) of Figure 4.1.

To account for the discontinuities in the time-stamp, the software runs through the dGPS data file and marks the time-stamp where a discontinuity occurred. Data between successive discontinuities are separated into a segment of dGPS data. This process is depicted in the bottom figure (2) of Figure 4.1.

Two segments of dGPS data

		Ashtech, Inc. GPPS-2	Program:	PPDIFF	Version: 5.0.01		
		Thu Dec 05 15:57:59 2002	Differentially Corrected: Y				
		SITE MM/DD/YY HH:MM:SS	SVs	PDOP	LATITUDE	LONGITUDE	HI
discard data	}	ROVR 12/04/02 09:10:31.000000	5	5.9	S 34.06896297	E 18.84081754	835.3711
		ROVR 12/04/02 09:10:32.000000	5	5.9	S 34.06887345	E 18.84132325	835.4181
		ROVR 12/04/02 09:10:33.000000	5	5.9	S 34.06875954	E 18.84181283	834.7235
		ROVR 12/04/02 09:10:34.000000	4	15.9	S 34.06858313	E 18.84233266	844.4253
		ROVR 12/04/02 09:10:35.000000	4	15.9	S 34.06839769	E 18.84280823	847.2218
		ROVR 12/04/02 09:10:36.000000	4	15.9	S 34.06819009	E 18.84325514	847.7132
		ROVR 12/04/02 09:10:37.000000	4	15.9	S 34.06795883	E 18.84367614	847.0527
		ROVR 12/04/02 09:10:38.000000	4	15.9	S 34.06769333	E 18.84408163	847.9335
		ROVR 12/04/02 09:10:39.000000	4	15.9	S 34.06740816	E 18.84445016	846.3787
		ROVR 12/04/02 09:10:40.000000	4	15.9	S 34.06709410	E 18.84479530	846.5796
discard data	}	ROVR 12/04/02 09:10:41.000000	5	3.4	S 34.06678669	E 18.84506120	836.6515
		ROVR 12/04/02 09:10:42.000000	5	3.4	S 34.06644280	E 18.84531517	831.6733
		ROVR 12/04/02 09:10:43.000000	5	3.4	S 34.06605907	E 18.84555751	833.7017
		ROVR 12/04/02 09:10:44.000000	4	15.9	S 34.06562658	E 18.84580469	846.1068
		ROVR 12/04/02 09:10:45.000000	4	15.9	S 34.06522244	E 18.84594474	844.0964
		ROVR 12/04/02 09:10:46.000000	4	15.9	S 34.06481398	E 18.84602970	839.5787
		ROVR 12/04/02 09:10:47.000000	4	15.9	S 34.06438886	E 18.84609631	840.9230
		ROVR 12/04/02 09:10:48.000000	5	3.4	S 34.06398557	E 18.84609607	834.1685
		ROVR 12/04/02 09:10:49.000000	5	3.4	S 34.06356191	E 18.84610587	834.0199
		ROVR 12/04/02 09:10:50.000000	5	3.4	S 34.06313703	E 18.84610906	834.9211
		ROVR 12/04/02 09:10:51.000000	5	3.4	S 34.06271433	E 18.84610772	835.9555
		ROVR 12/04/02 09:10:52.000000	5	3.4	S 34.06228946	E 18.84610688	837.1897

(1) Discarding the dGPS data where the PDOP value exceeds the value of 6

		Ashtech, Inc. GPPS-2	Program:	PPDIFF	Version: 5.0.01		
		Thu Dec 05 15:57:59 2002	Differentially Corrected: Y				
		SITE MM/DD/YY HH:MM:SS	SVs	PDOP	LATITUDE	LONGITUDE	HI
segment 1	}	ROVR 12/04/02 09:05:53.000000	5	3.4	S 33.97132199	E 18.85220120	817.6365
		ROVR 12/04/02 09:05:54.000000	5	3.4	S 33.97090072	E 18.85223706	817.1879
		ROVR 12/04/02 09:05:55.000000	5	3.4	S 33.97047978	E 18.85223353	816.2178
		ROVR 12/04/02 09:05:56.000000	5	3.4	S 33.97005811	E 18.85219261	816.4394
		ROVR 12/04/02 09:05:57.000000	5	3.4	S 33.96963762	E 18.85211061	816.8015
		ROVR 12/04/02 09:05:58.000000	5	3.4	S 33.96922496	E 18.85198487	817.2852
segment 2	}	ROVR 12/04/02 09:05:59.000000	4	3.6	S 33.96881804	E 18.85181342	817.5188
		ROVR 12/04/02 09:06:13.000000	4	4.7	S 33.96578223	E 18.84570476	814.1999
		ROVR 12/04/02 09:06:14.000000	4	4.7	S 33.96582493	E 18.84517654	812.4534
		ROVR 12/04/02 09:06:15.000000	4	4.7	S 33.96590942	E 18.84464300	812.0297
		ROVR 12/04/02 09:06:16.000000	4	4.7	S 33.96603756	E 18.84410329	814.0798
		ROVR 12/04/02 09:06:17.000000	4	4.7	S 33.96619924	E 18.84357878	815.5942
		ROVR 12/04/02 09:06:18.000000	4	4.7	S 33.96638867	E 18.84307613	817.2033
		ROVR 12/04/02 09:06:19.000000	4	4.7	S 33.96660756	E 18.84259542	817.9852
		ROVR 12/04/02 09:06:20.000000	4	4.7	S 33.96685216	E 18.84213658	818.6901
		ROVR 12/04/02 09:06:21.000000	4	4.7	S 33.96711926	E 18.84169945	819.1830
		ROVR 12/04/02 09:06:22.000000	4	4.7	S 33.96740101	E 18.84128225	820.0169
		ROVR 12/04/02 09:06:23.000000	4	4.7	S 33.96769383	E 18.84087590	821.7697
ROVR 12/04/02 09:06:24.000000	5	3.7	S 33.96797988	E 18.84052263	812.8040		
ROVR 12/04/02 09:06:25.000000	6	2.9	S 33.96827110	E 18.84011452	825.1163		
ROVR 12/04/02 09:06:26.000000	6	2.9	S 33.96859268	E 18.83972417	825.1165		

GPS time-stamp

(2) Breaking the dGPS data into sections where discontinuities in the time-stamp occur

Figure 4.1: Sectioning the dGPS data.

4.6 Tracker data characteristics

A number of considerations have to be included when developing the software for the calibration system. The characteristics of the data is very important and the following considerations regarding the Tracker data had to be taken into account [34], [35].

4.6.1 Zero values for Azimuth, Elevation and Range

Due to a data throughput problem in the Radar Signal Processor, a number of messages in the data files contain zero values for Radar *azimuth*, *elevation* and *range*. These invalid messages have been tagged with a “1” within the data fields. All valid data is indicated by a “2” in the data field. Only the valid data is to be used for the tracking error analysis. In the Optronics data files, there are also some messages that contain zero values. This is inherent to the tracking process, where the Autotracker fails to resolve the target for one video frame, or a communication error occurs.

To accomodate the data tagging, the software includes a *look-up* algorithm that only matches valid data to the correct time-stamp.

4.6.2 Gaps in Time Base

The Tracker System Data Processor sends the Tracking data messages once every 20 msec. Some of the messages, however, are not recorded due to a hardware problem in the data logging system. All the recorded data is correctly GPS time-stamped. Thus there are occasionally very large gaps in the time base of the tracking files. This has been taken into account when writing the software.

4.6.3 Optronic Data Update Rate

As mentioned in Section 4.6.2, the Tracker System Processor sends Tracking data every 20 msec. The *azimuth* and *elevation* angle data is updated every 20 msec cycle by the Autotracker. Due to the limited Pulse Repetition Frequency (PRF), the Laser Range Finder only updates the Optronics *range* data every fourth 20 msec cycle. These two data rates were considered when writing the calibration software.

4.7 Interpolation of dGPS data

As mentioned in Section 3.2, the Radar and Optronics system operate at different data rates. The Radar sensor and Autotracker output data at a rate of 50 Hz, whereas the laser rangefinder outputs

data at 12.5 Hz. The Mowbray base station was used for making the differential corrections to the GPS data for the Tracking Analysis. The update rate for this data is 1 Hz. Thus the *azimuth* and *elevation* of the dGPS data needs to be interpolated at 50 Hz to compare the Tracker data at the corresponding time. The *range* data of the dGPS data needs to be interpolated at 12.5 Hz to be compared to the *range* of the Tracker data.

In the original software written by Mr. Fadiran, a starting point was chosen for comparison. A time array was produced that began with the chosen starting point. Each consecutive element of the time array was an increment of 0.02 s (50 Hz) from the previous element. The dGPS data fields for *azimuth*, *elevation* and *range* were then interpolated using a “cubic”, matched up to this time array. These interpolated values were then compared with the Tracker data by matching up the time-stamps as closely as possible to the time array of the dGPS data.

After some testing, and measuring the errors introduced by this matching of “non-exact” time-stamps, it was decided to interpolate the dGPS data using the same time-stamp values as the Tracker. Thus, when comparing the dGPS and Tracker data, data points at the same time-stamp values can be chosen for comparison. This process was simulated in *Matlab*, and it was discovered that the mean errors were minimised using the exact time-stamp method. This method was therefore used for the modified software.

To convert the 1 Hz dGPS data to the required data rate of 12.5 Hz and 50 Hz, three interpolation options are offered to the user:

1. **Cubic (default):** This method of interpolation uses a piecewise cubic hermite polynomial. The *cubic* method of interpolation preserves the shape and monotonicity of the data, but is computationally intensive. It requires the most memory of all the interpolation methods. It has the advantage of having both continuous interpolated data and continuous derivatives. The interpolated data has less oscillations than the *cubic spline* method, when using data that is not smooth.
2. **Cubic splines:** This method fits a cubic function between two successive data points, and uses a *spline* function to perform *cubic spline* interpolation on the data [2, pg 9-74] and [4, pg 40-70]. This method, as in the case of the cubic, is computationally intensive, and has the longest execution time of all the interpolation methods. This method produces the smoothest results, but can occasionally produce spurious results if the data is non-uniform, which it is in many cases.
3. **Linear:** This method fits a linear function between two successive data points. This interpolation method is the least intensive. The results are continuous, but the slope changes at the vertex points.

A comparison of the three interpolation methods can be seen in Figure 4.2. The *cubic* interpolation method has been chosen as the *default* method, because it produces the best results when tested on the real data.

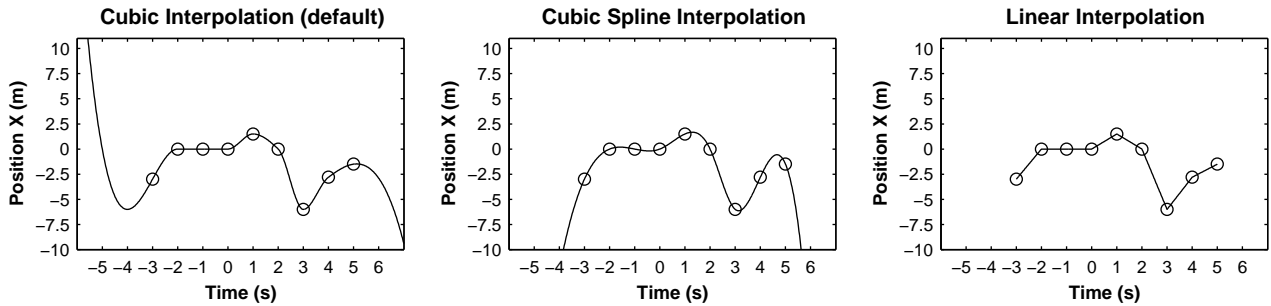


Figure 4.2: Methods of Interpolation.

4.8 Summary of Chapter

This Chapter gave an introduction to the previous software that was written for the TAMS and described the modifications that were made to the software, to accommodate the new data sets. The format of the Tracker and GPS data files were given, with an explanation of the changes in the data formats. The time conversion and co-ordinate conversion algorithms described in Chapter 2 were further explained, and the Tracker and GPS data characteristics incorporated into the software were considered. The Chapter concluded with a list of the interpolation methods that the user can choose from, to interpolate the dGPS data to the required data rate for comparison.

Chapter 5

Calibration Software

Chapter 5 is written to serve as a potential manual for users of the calibration software. This chapter runs briefly through the software in an orderly way that reflects the flow and structure of the software. The user input variables and parameters are described, as well as the relevant software directories and folders. The software is described at a top-level, with some software internals detailed in Section 5.5. By reading this chapter in parallel with the flow-diagrams (Figure 5.1 and 5.2) presented in Section 5.5, the user can follow the functionality of the calibration software.

5.1 User variables

A number of variables exist that are used by the calibration software. These can be set, or changed by the user. The variables can be accessed in the *setup* file in the program path.

The following variables and parameters can be set and changed within the setup file:

- **GPS data rate** - this value is needed for interpolation purposes. By default the software will ask the user for the GPS data rate, but this option can be turned off in the setup file.
- **Reference base-station co-ordinates** - these co-ordinates are used when converting the GPS data to the Tracker co-ordinate system.
- **Units of measurement** - the units of measurement can be changed between *mrad* and *degrees*. The time units can also be changed from *s* to *msec*.
- **Save flag** - the software outputs many figures and tables when running and these figures and tables can be saved to disk, into the folders described in Section 5.3. The program does give the user the option of saving during operation.

- **Latency** - the latency compensation for the Optronics and Radar data can be set and modified. The software will ask for these values if they have not been set in the *setup* file.
- **Interpolation method** - the user can set the interpolation method (described in Chapter 4.7) in the *setup* file. The *default* method of interpolation is the *cubic*.

5.2 dGPS, Radar and Optronics data files

When running the calibration software, the user must ensure that the dGPS, Radar and Optronics files are in their correct folders or directories. The software automatically detects the current working directory by calling a *path* function. To make the software more versatile, none of the paths and directories have been hard-coded, but have rather been set relative to the user's current working directory. Thus the user simply needs to ensure that the data files are in their correct folders in the current working directory.

The data files should be placed in their respective directories:

- differential GPS data file (method described in Section 4.1.1) in “current path”/**GPS_Data**
- Optronics data files in “current path”/**Opt_Data**
- Radar data files in “current path”/**Rad_Data**.

If the above folders do not exist in the current working directory, then they will be automatically created by the software, but the user must ensure that the data files are then placed in these folders.

5.3 Repository for Results

A number of tabulated results and figures are produced (while the software is running). These results are placed in the following folders for further analysis:

- “current path”/**Results**: The results of individual data file analysis for the Radar and Optronics data, as well as the results for the complete inbound and outbound analysis, are tabulated and placed in this folder.
- “current path”/**Figures**: Figures of azimuth, elevation and range for the Radar and Optronics data are saved in this folder (in encapsulated postscript format). The results of the comparison between the dGPS data and the Tracker data are depicted through figures found in this folder.

- “current path”/**Tables**: At the beginning of the software analysis, the dGPS data is segmented as described in Section 4.5.3. Statistics on these sections are tabulated and placed in this folder. Statistics on the individual Optronics and Radar files can also be found in this folder.

The user can access the tables and figures from the relevant directories, by opening the files in a *text editor*.

5.4 Software Structure

This section is intended to be read in parallel with Figure 5.1 and 5.2.

5.4.1 User Menu

To run the calibration software, the user needs to change the Matlab current directory to the directory where the program files are situated. By running the command ‘*tams_menu.m*’, the program begins by presenting the user with a menu. The menu options allow the user to run the calibration software, or to run a test to verify the latency values. Upon choosing the option of running the calibration software, the program searches the “/GPS_Data” directory. All the dGPS data files are displayed for the user to choose from. There is an option to manually enter the path and name of the dGPS file.

The frequency of the dGPS data is required by the user, in order to determine dGPS time-stamp errors. The precise location of the reference point of the Tracker system is also needed to correctly calculate the dGPS *range*, *azimuth* and *elevation* in the local Tracker co-ordinate system. The default co-ordinates displayed in the menu give the precise position of the Tracker system for the collected data used for the analysis of this project. These co-ordinates can be changed by the user by selecting the relevant menu option. For the results to be accurate, the co-ordinates of the Tracker origin should be recorded using land-surveying equipment, as very small inaccuracies in the positional measurement can cause very large mean errors.

The co-ordinates for the reference point need to be entered in *real number* format as follows:

```
latitude_base = 33.9514381528; (°)
longitude_base = 18.4685435861; (°)
height_base = 83.42; (m)
```

The default co-ordinates are those co-ordinates set in the *setup* file described in Section 5.1.

5.4.2 Section the Rad/Opt and dGPS data files

The software then processes the dGPS and Tracker data, and splits the data into sections with continuous time-stamps (described in Section 4.5.3). Figure 5.3 describes the segmentation of the dGPS data. Each dGPS segment is processed and the data converted into the required format for comparison. The software writes to file a number of tables, detailing information on breakpoints and relevant information for each section of the formatted dGPS and Tracker data. These tables can be found in the “/Tables” directory, once the dGPS and Tracker data has been processed. The tables were used extensively when debugging the software, as all the information on the processed data is broken down into manageable sections.

5.4.3 Radar or Optronics

The user is then required to choose between the Optronics and Radar data for processing.

A number of options are offered to the user:

1. Difference plots
2. Range plots
3. Calculating accuracy
4. Calculate all *inbound* results
5. Calculate all *outbound* results

These options can be applied to individual files, or a directory of files by choosing options (4) or (5). The latency values need to be inputted if they were not stipulated in the setup file (Section 5.1). Two latency values are required when processing the Optronics data, for the *autotracker* and *laser range-finder* respectively. If no value is entered, then no latency compensation will be applied to the data.

5.4.4 Radar/Optronics data

The Radar/Optronics data is read from the data directories into the software. Figure 5.4 outlines the algorithm for reading in the Optronics data. This algorithm also applies to the Radar data with some modifications, as all data from the radar sensor is received at the same data rate.

5.4.5 Interpolation of dGPS data

The dGPS data is interpolated (described in Chapter 4.7) to match the Radar/Optronics time-stamp. Before the dGPS data is interpolated, latency compensation (specified by user) is applied to the

Radar/Optronics data. The interpolation algorithm is described in Figure 5.5.

5.4.6 Producing Results

The Radar/Optronics and interpolated dGPS data is compared, and the resulting *min*, *max*, *mean*, *standard deviation (std)* and *root-mean-square (RMS)* of the differential data are written to file. These results can be found in “current path”/**Results**. The results found in this folder, along with the statistical distributions, are used in statistically analysing the data to verify the system accuracy. These details are found in Chapter 7.

5.5 Software Internals

To illustrate the software more clearly, five flow-diagrams are presented at the end of this section. Figure 5.1 and 5.2 describe the top-level flow-diagram of the calibration software. These two top-level flow diagrams are broken down further, by describing important functions and processes within the software. Blocks in Figure 5.1 and 5.2 that are marked with a large letter: **A**, **B** or **C**, represent the functions that are further broken down and can be seen in Figures 5.3, 5.4 and 5.5. Important information regarding these diagrams are described below.

GPS segmentation (see Figure 5.3)

note: marked by A in Figure 5.1

- The PDOP value of 6 is the *rule-of-thumb* value chosen in Chapter 4.5.1 from [10, pg 151].
- Where there are breakpoints in the GPS time-stamp, the data is separated into segments.
- Occasionally, some spurious results occur in the GPS data file and these data points are discarded. These spurious results are found by comparing the individual data points to the *mean* of the surrounding data points.

Optronics and Radar data input (see Figure 5.4)

note: marked by B in Figure 5.2

- The validity indicator mentioned in this flow-diagram is described clearly in Chapter 4.6.1, where a value of '1' denotes *invalid* data, and a value of '2' denotes *valid* data.

dGPS data interpolation (see Figure 5.5)

note: marked by C in Figure 5.2

- This flow-diagram applies to the dGPS and Optronics data, where the data from the Optronics comes from two sensors [27], with different data rates. The dGPS data is also interpolated to the Radar time (not shown in Figure 5.5, but visible in Figure 5.2), using the same process as described by Figure 5.5, but using 1 interpolation time.
- The *cubic* interpolation method is chosen as *default*, for the reasons described in Chapter 4.7.

5.6 Summary of Chapter

The TAMS software was described at a top level, with the Chapter serving as a potential manual for the user. The variables that can be set in the TAMS setup file, were listed and briefly described. The directories that contain the data used by the software was explained, to aid the user when processing the data. The folders used to store the outputs of the software, were clearly defined. A brief run-through of the software from start to finish was aided with the use of a top level flow chart.

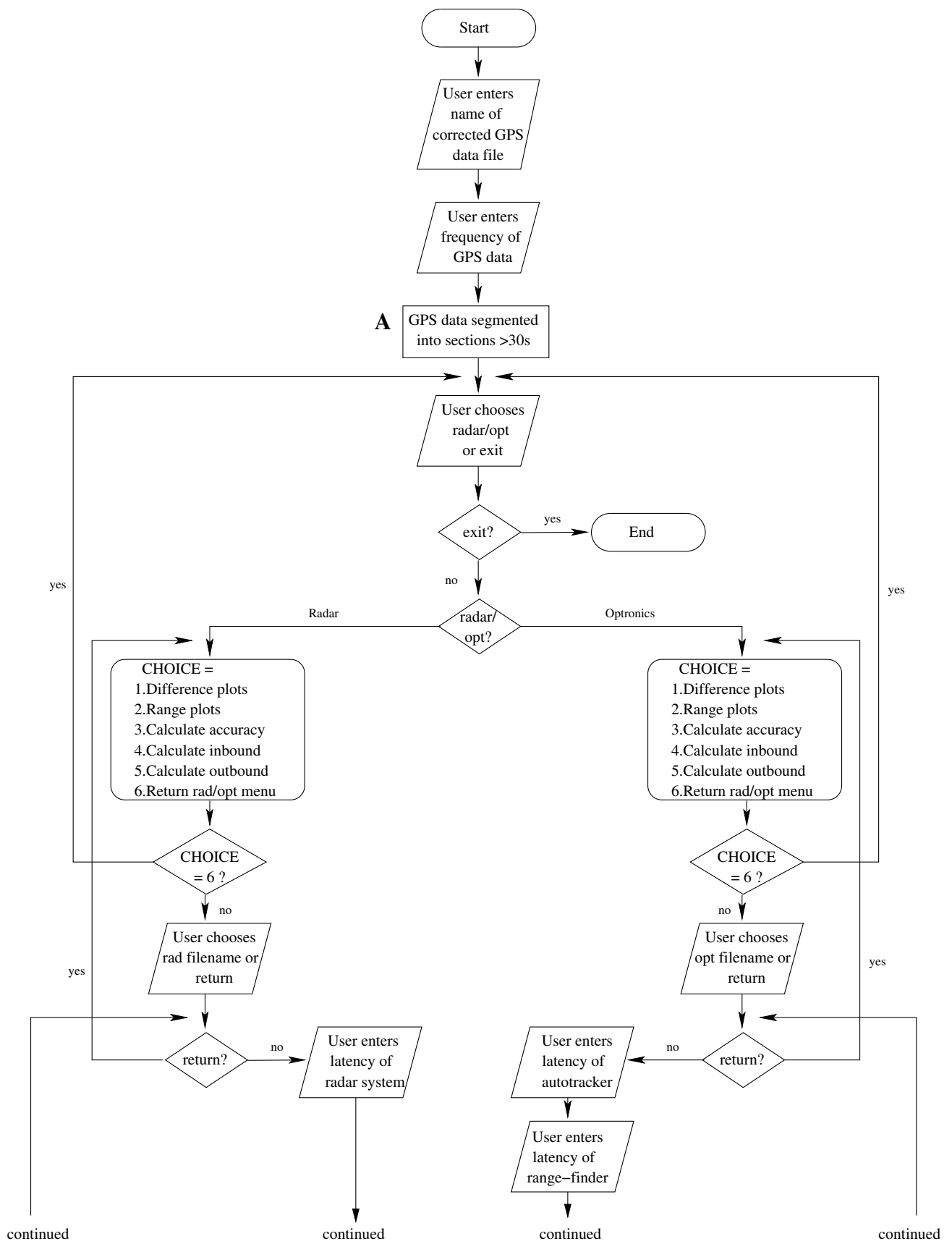


Figure 5.1: System level flow-diagram of TAMS software (1st part).

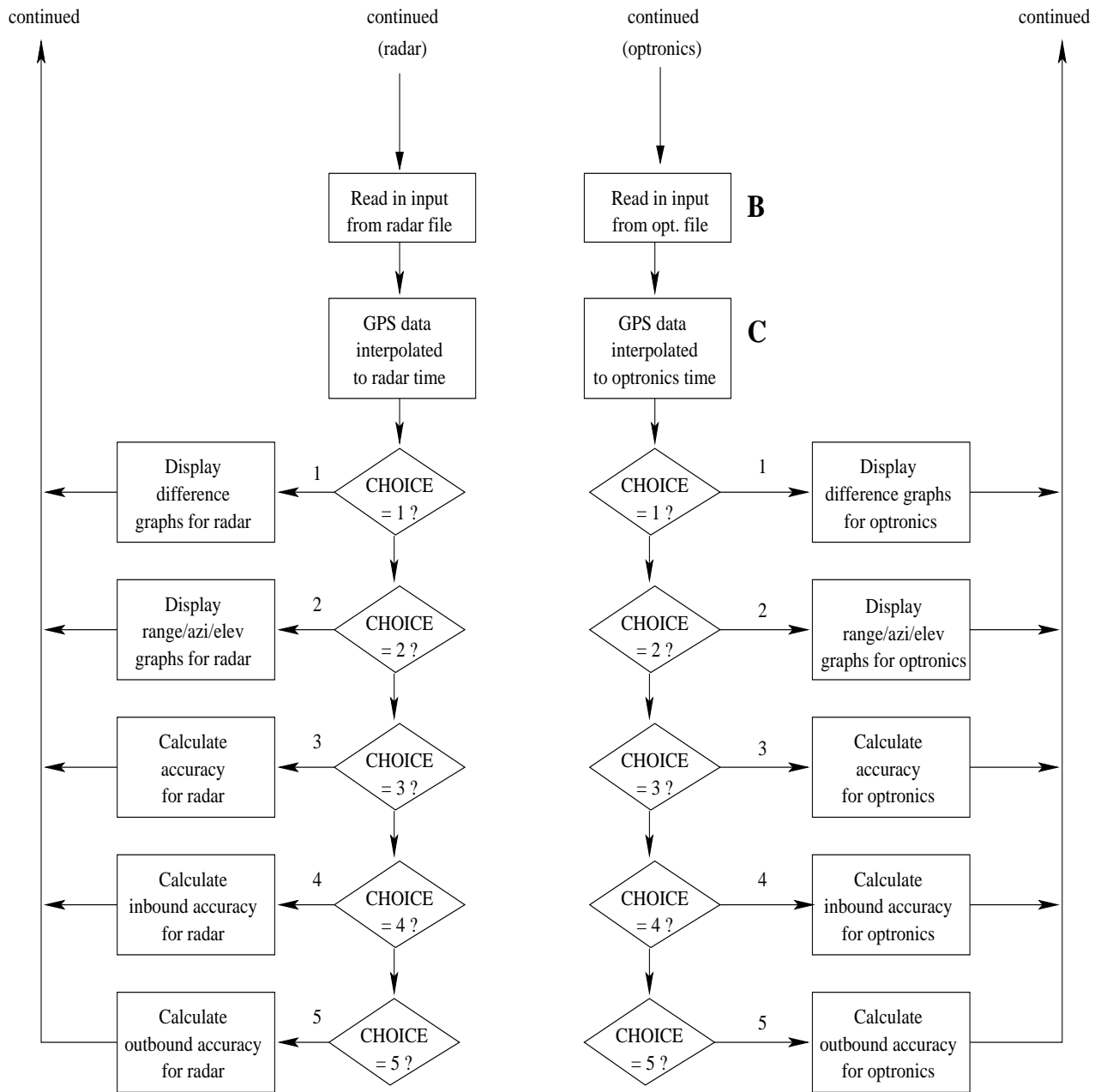


Figure 5.2: System level flow-diagram of TAMS software (2nd part).

A

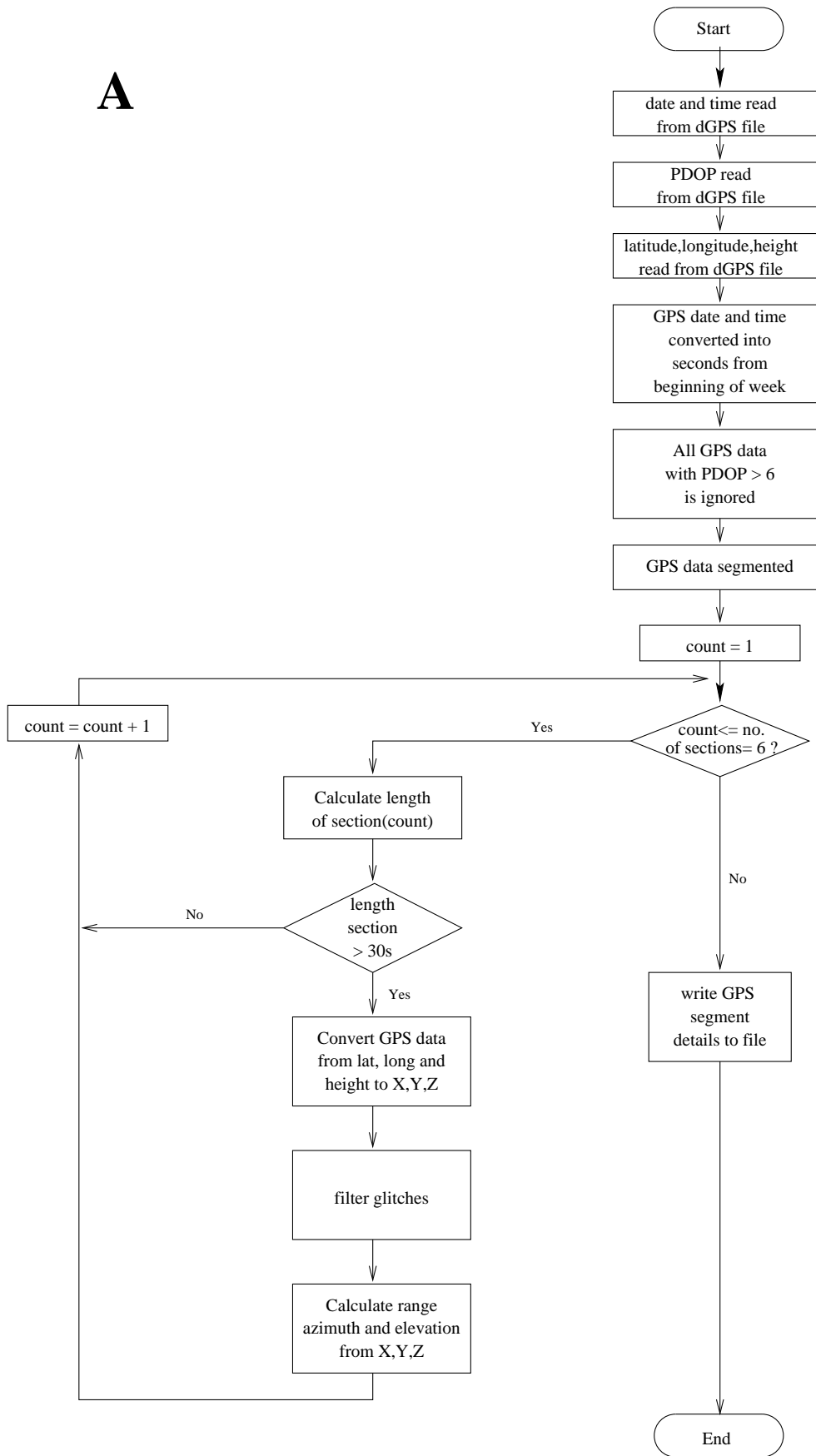


Figure 5.3: Flow-diagram of GPS segmentation.

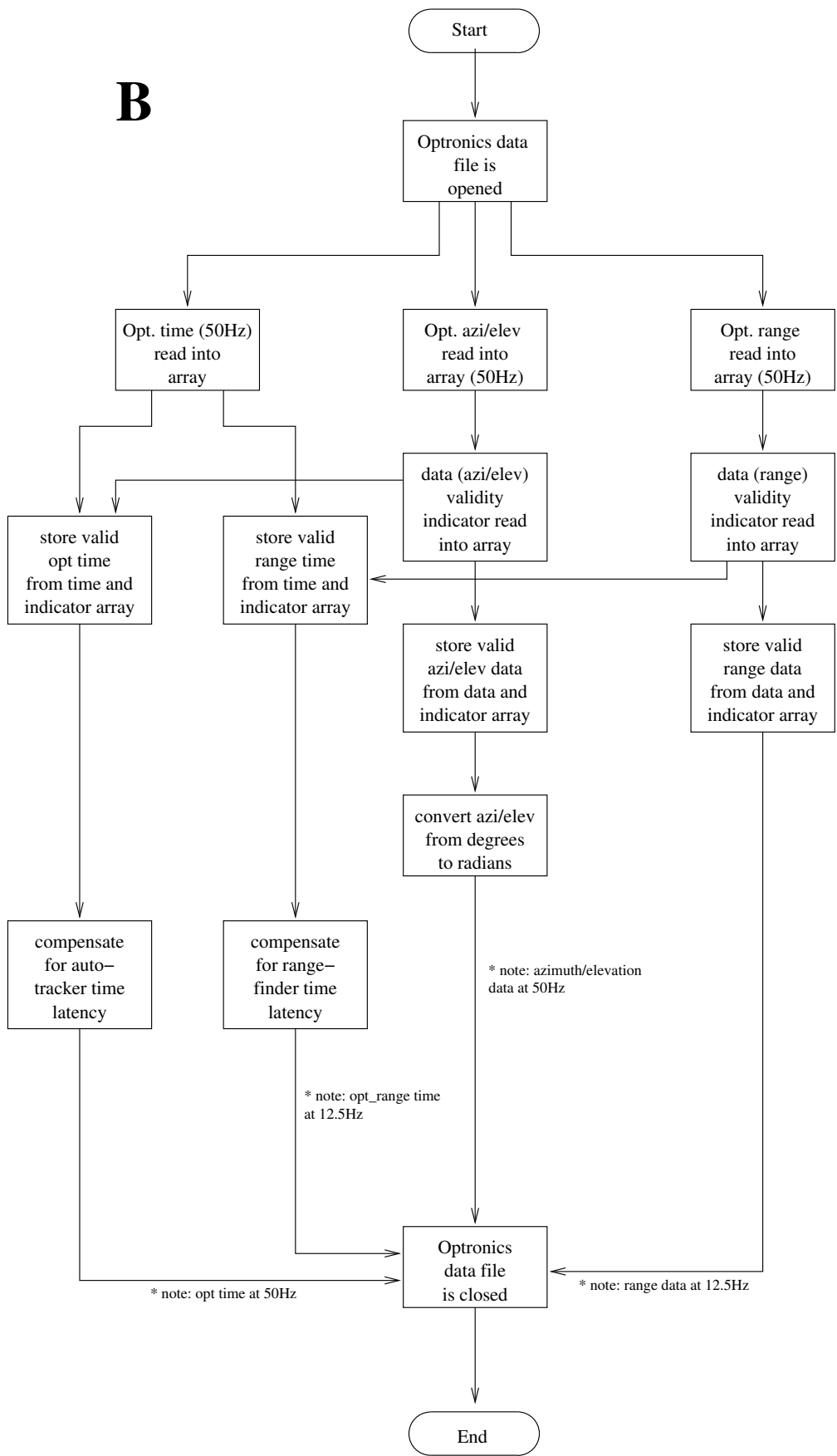


Figure 5.4: Flow-diagram of Optronics input.

C

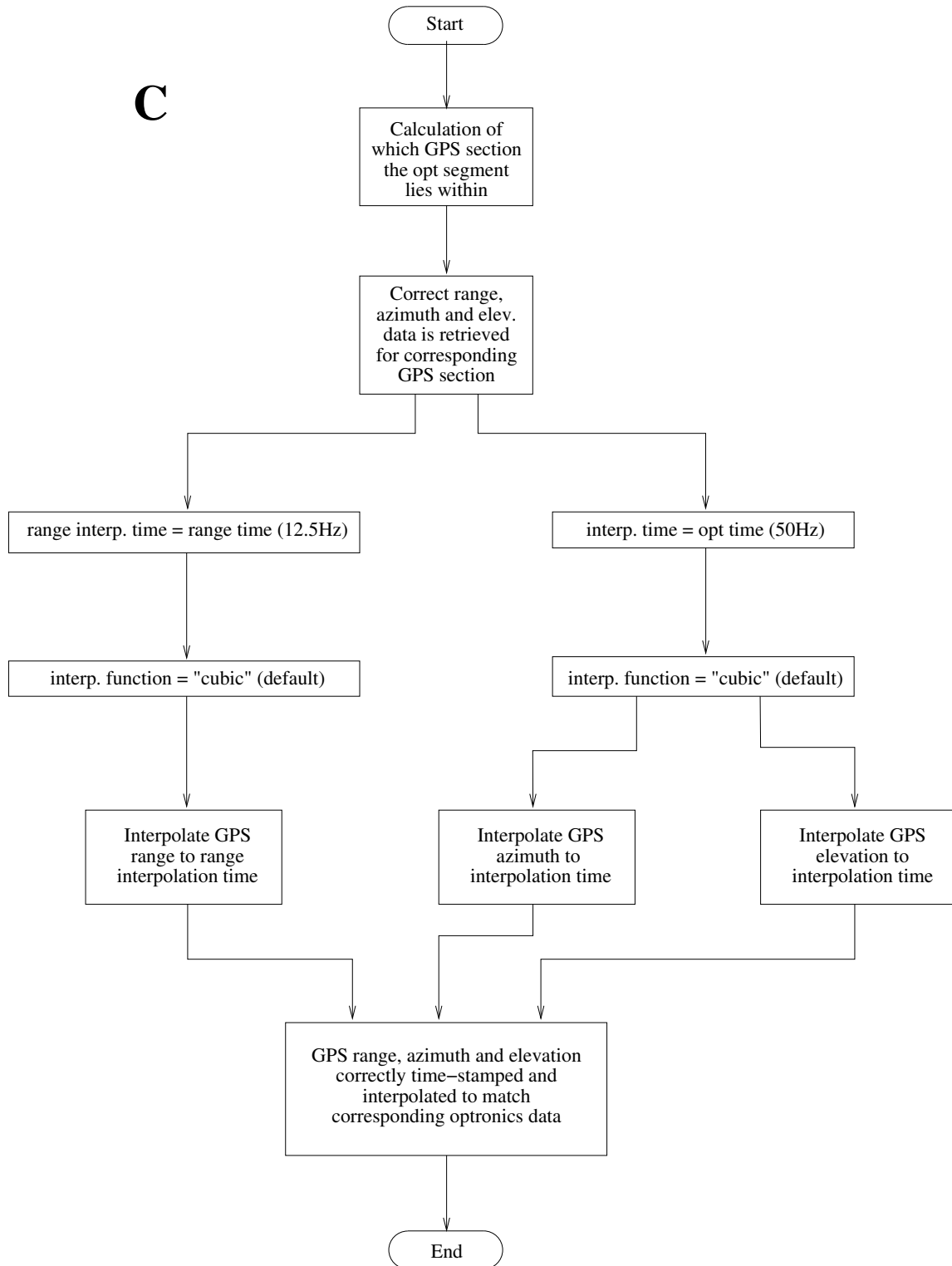


Figure 5.5: Flow-diagram of GPS data interpolated to optronics time.

Chapter 6

Results

This Chapter describes the results for the dGPS versus Optronics and Radar respectively. The data files used in the analysis are listed, and plots representing the data in these files are presented. The results from the comparison of the dGPS and Tracker data are plotted. A summary of results with full latency compensation is tabulated. The test on the system latency is described in the third section. The Chapter ends with some comments regarding the results.

6.1 Optronics vs dGPS

The results from running the calibration software for the Optronics and GPS data can be found in their respective directories, described in Chapter 5.3.

6.1.1 Overview of Optronics Data

This section gives a brief description of the Optronics files that were used by the calibration system. These Optronics files can be found in the Optronics directory on the CD attached to the back of this dissertation. A plot of the optronics range, elevation and azimuth data for the *first* analysed Optronics segment is shown as an example (Figure 6.1 overleaf). Plots of all the analysed segments can be found in Appendix A.1. The GPS derived range data is also plotted for comparison. The source of the optronics data is split into range and angle data. The angle data (consisting of azimuth and elevation), comes from the autotracker. The Laser on the optronics system measures the range.

The following data files have been examined:

1. ITB FAT 10_32_WPN_Wed_12_09_22_1.csv (Segment 1, inbound)
2. ITB FAT 10_32_WPN_Wed_12_11_36_1.csv (Segment 2, outbound)

3. ITB FAT 10_32_WPN_Wed_12_17_04_1.csv (Segment 3, inbound)
4. ITB FAT 10_32_WPN_Wed_12_18_48_1.csv (Segment 4, outbound)
5. ITB FAT 10_32_WPN_Wed_12_24_59_1.csv (Segment 5, inbound)
6. ITB FAT 10_32_WPN_Wed_12_27_09_1.csv (Segment 6, outbound)
7. ITB FAT 10_32_WPN_Wed_12_29_28_1.csv (Segment 7, inbound)

Originally nine files were made available to be analysed, but one file represented a holding pattern and the other file data recording only commenced in the middle of the leg. Thus, it was decided not to include these two files in the analysis.

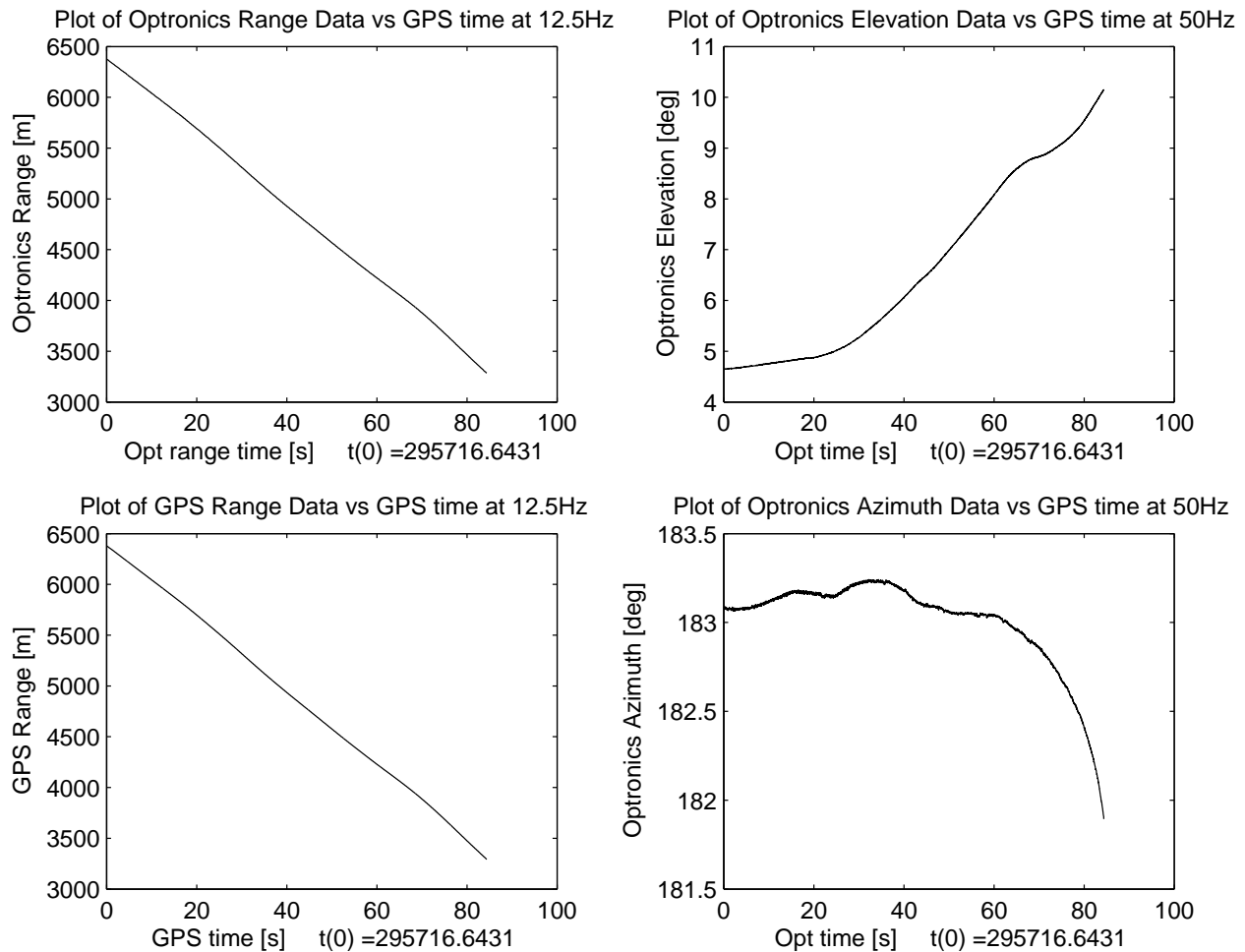


Figure 6.1: Optronics Segment 1 (ITB_FAT_WPN_Wed_12_09_22_1): Plots of optronics range, elevation and azimuth data. The GPS-derived range data is also shown for comparison.

6.1.2 Results Overview

This section presents a differential plot between the optronics range, elevation and azimuth data and the dGPS range, elevation and azimuth data, for the *first* analysed Optronics segment (Figure 6.2 overleaf). Plots of all the analysed segments can be found in Appendix A.2. No data latency compensation was applied to the data.

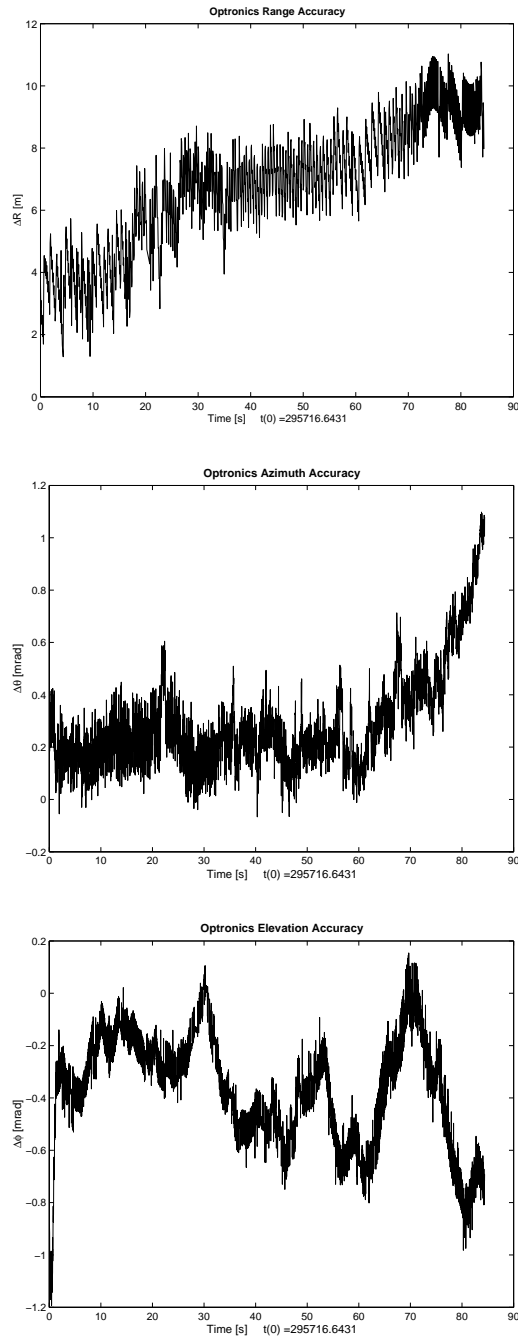


Figure 6.2: Optronics Segment 1: Difference between optronics data and GPS-derived data for range, azimuth and elevation measurements (no latency compensation).

6.1.3 Calibration software results

The tables extracted from the results directory contain information about the calibration process for the Optronics and GPS data. Information on the *min*, *max*, *mean*, *standard deviation (std)* and *root-mean-square (RMS)* are tabulated below. All tabulated results are found in the Appendices.

Optronics tracking accuracies for optronics angle and range data latency compensation of -230 and -240 ms respectively

Table 6.1: Accuracy of azimuth data, optronics angle time delay = -230 ms, optronics range time delay = -240 ms.

<i>Segment</i>	<i>min</i> [mrad]	<i>max</i> [mrad]	<i>mean</i> [mrad]	<i>std</i> [mrad]	<i>RMS</i> [mrad]	<i>Invalid Data</i> [%]
1 (inbound)	-0.142	0.634	0.235	0.110	0.259	0.427
2 (outbound)	-0.057	1.092	0.293	0.251	0.386	0.00
3 (inbound)	-0.382	0.573	0.097	0.157	0.184	0.882
4 (outbound)	0.079	0.836	0.323	0.094	0.337	0.00
5 (inbound)	-0.167	0.519	0.193	0.106	0.220	0.464
6 (outbound)	-0.113	0.644	0.203	0.126	0.239	0.00
7 (inbound)	-0.148	0.687	0.268	0.122	0.294	0.299

Table 6.2: Accuracy of elevation data, optronics angle time delay = -230 ms, optronics range time delay = -240 ms.

<i>Segment</i>	<i>min</i> [mrad]	<i>max</i> [mrad]	<i>mean</i> [mrad]	<i>std</i> [mrad]	<i>RMS</i> [mrad]	<i>Invalid Data</i> [%]
1 (inbound)	-1.162	0.369	-0.108	0.16	0.198	0.427
2 (outbound)	-1.197	0.692	-0.372	0.337	0.502	0.00
3 (inbound)	-0.622	1.138	0.252	0.321	0.408	0.882
4 (outbound)	-0.719	0.204	-0.342	0.144	0.371	0.00
5 (inbound)	-0.788	0.166	-0.293	0.180	0.343	0.464
6 (outbound)	-0.521	0.503	-0.137	0.229	0.267	0.00
7 (inbound)	-0.714	0.180	-0.284	0.184	0.339	0.299

Table 6.3: Accuracy of range data, optronics angle time delay = -230 ms, optronics range time delay = -240 ms.

<i>Segment</i>	<i>min</i> [m]	<i>max</i> [m]	<i>mean</i> [m]	<i>std</i> [m]	<i>RMS</i> [m]	<i>Invalid Data</i> [%]
1 (inbound)	-6.814	1.805	-2.006	1.735	2.651	0.427
2 (outbound)	-3.288	7.836	2.502	2.067	3.245	0.00
3 (inbound)	-8.063	1.087	-2.621	1.707	3.127	0.882
4 (outbound)	-4.290	5.453	0.980	1.756	2.010	0.00
5 (inbound)	-7.694	-0.101	-3.112	1.354	3.393	0.464
6 (outbound)	-1.362	6.576	2.858	1.524	3.000	0.00
7 (inbound)	-6.165	0.027	-3.123	1.173	3.335	0.299

All Inbound flight Results

Table 6.4: Accuracies over all inbound flights, optronics angle time delay = -230 ms, optronics range time delay = -240 ms.

<i>Measurement</i>	<i>min</i> [mrad, m]	<i>max</i> [mrad, m]	<i>mean</i> [mrad, m]	<i>std</i> [mrad, m]	<i>RMS</i> [mrad, m]
Azimuth	-0.382	0.687	0.196	0.139	0.240
Elevation	-1.162	1.138	-0.095	0.308	0.323
Range	-8.063	1.805	-2.634	1.620	3.092

All Outbound flight Results

Table 6.5: Accuracies over all outbound flights, optronics angle time delay = -230 ms, optronics range time delay = -240 ms.

<i>Measurement</i>	<i>min</i> [mrad, m]	<i>max</i> [mrad, m]	<i>mean</i> [mrad, m]	<i>std</i> [mrad, m]	<i>RMS</i> [mrad, m]
Azimuth	-0.113	1.092	0.273	0.183	0.328
Elevation	-1.197	0.692	-0.286	0.276	0.397
Range	-4.290	7.836	2.062	1.946	2.835

6.2 Radar vs dGPS

The results from running the calibration software for the Radar and GPS data can be found in their respective directories, described in Chapter 5.3.

6.2.1 Overview of Radar Data

The Radar files used for the calibration software can be found in the relevant directory on the CD attached to the back of this dissertation. The Radar files examined by the calibration software are listed in this Section. A plot of the radar range, elevation and azimuth data for the *first* analysed Radar segment is shown in Figure 6.3 overleaf. Plots of all the analysed segments can be found in Appendix B.1. These plots give an overview of the quality of the data. It can be seen that the radar data contains many gaps, which makes the tracking accuracy analysis task more difficult. The GPS data also contains gaps.

The following data files have been examined:

1. ITB FAT 10_31_WPN_Wed_10_07_23_SMS.csv (Segment 1, outbound)
2. ITB FAT 10_31_WPN_Wed_10_11_13_SMS.csv (Segment 2+3, both inbound)
3. ITB FAT 10_31_WPN_Wed_10_15_54_SMS.csv (Segment 4, outbound)
4. ITB FAT 10_31_WPN_Wed_10_19_56_SMS.csv (Segment 5+6+7, all inbound)
5. ITB FAT 10_31_WPN_Wed_10_25_04_SMS.csv (Segment 8, outbound)
6. ITB FAT 10_31_WPN_Wed_10_33_47_SMS.csv (Segment 9, inbound — not used)
7. ITB FAT 10_31_WPN_Wed_10_43_27_SMS.csv (Segment 10, inbound)
8. ITB FAT 10_31_WPN_Wed_10_48_28_SMS.csv (Segment 11, outbound)
9. ITB FAT 10_31_WPN_Wed_10_53_19_SMS.csv (Segment 12, inbound)

The 6th data file was not analysed because the data was corrupted.

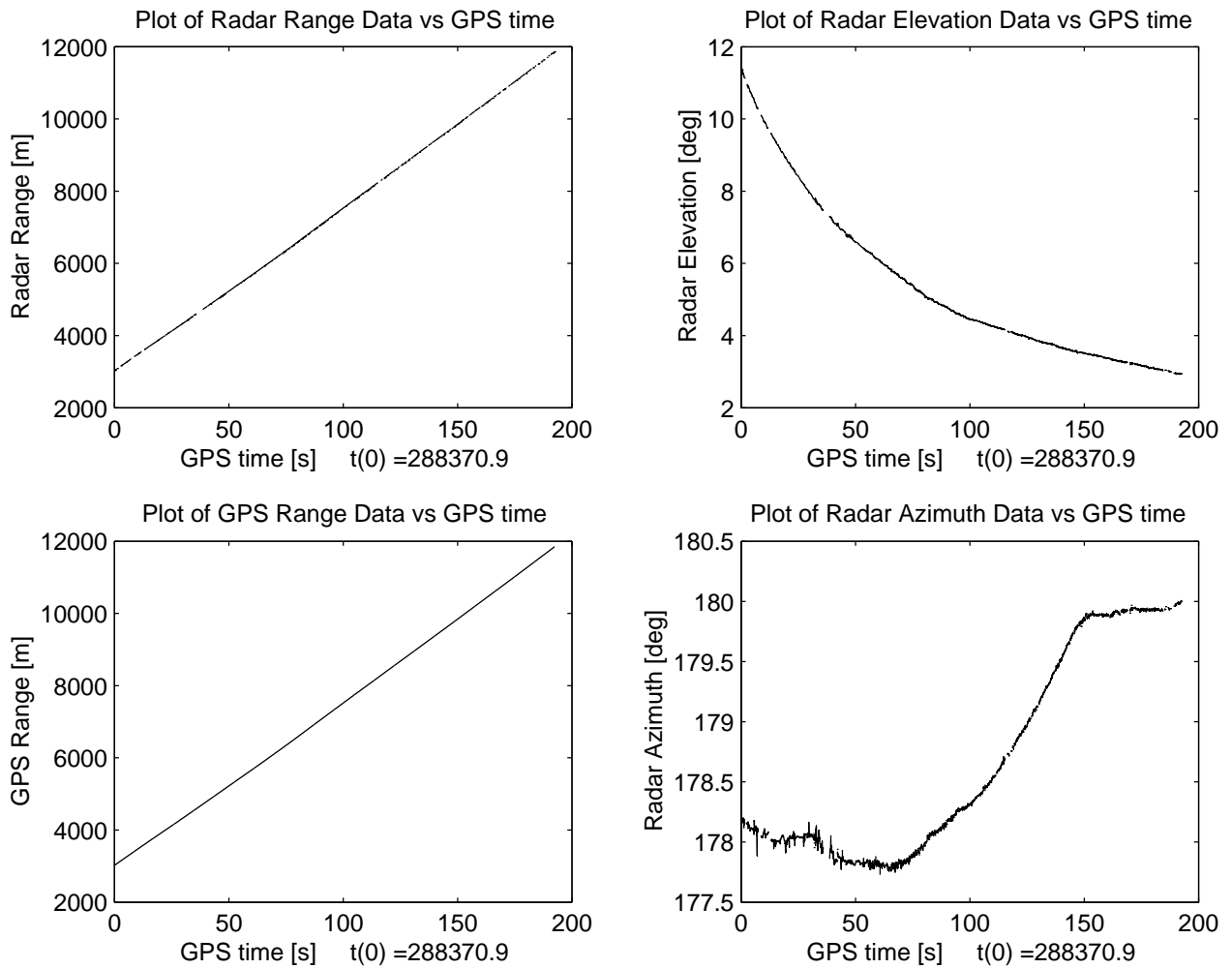


Figure 6.3: Radar Segment 1 (ITB_FAT_WPN_Wed_10_07_23): Plots of radar range, elevation and azimuth data. The GPS-derived range data is also shown for comparison.

6.2.2 Results Overview

This section presents a differential plot between the radar range, elevation and azimuth data and the dGPS range, elevation and azimuth data for the *first* analysed Radar segment (Figure 6.4). Plots of all the analysed segments can be found in Appendix B.2. No data latency compensation was applied to the data.

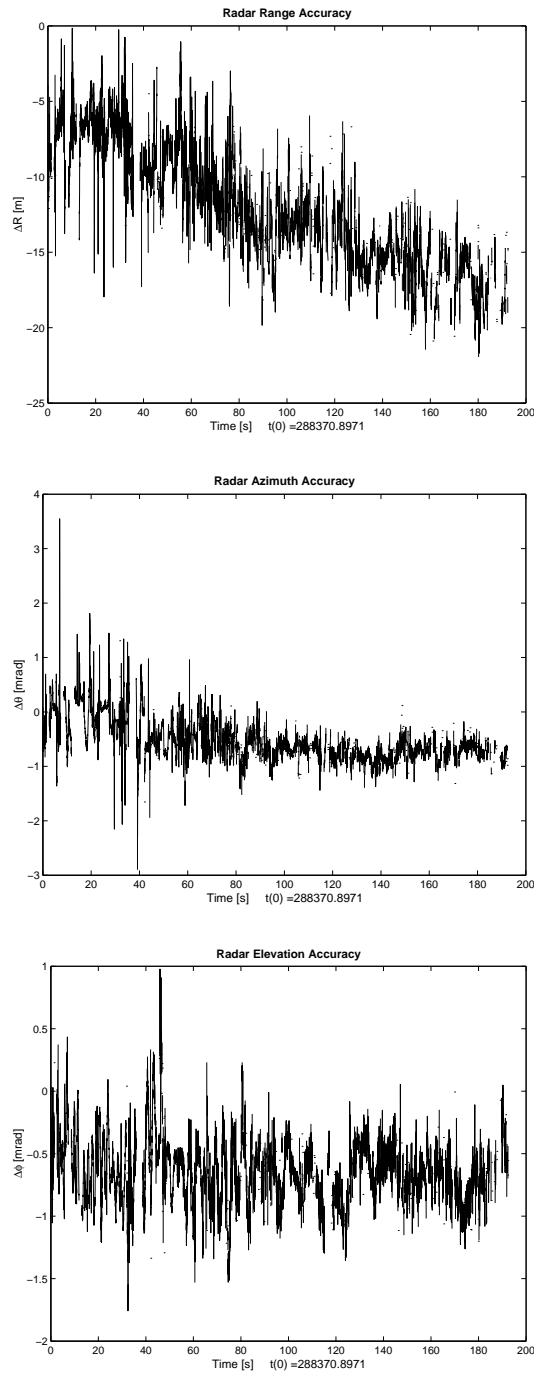


Figure 6.4: Radar Segment 1: Difference between radar data and GPS-derived data for range, azimuth and elevation measurements (no latency compensation).

6.2.3 Calibration software results

The tables extracted from the results directory contain information about the calibration process for the Radar and GPS data. Information on the *min*, *max*, *mean*, *std* and *RMS* are tabulated below. All tabulated results are found in the Appendices.

Radar tracking accuracies for radar data latency compensation of -204 ms

Table 6.6: Accuracy of azimuth data, radar time delay = -204 ms.

<i>Segment</i>	<i>min</i> [mrad]	<i>max</i> [mrad]	<i>mean</i> [mrad]	<i>std</i> [mrad]	<i>RMS</i> [mrad]	<i>Invalid data</i> [%]
1 (outbound)	-2.969	3.502	-0.482	0.369	0.607	24.672
2 (inbound)	-1.797	0.312	-0.697	0.246	0.739	14.301
3 (inbound)	-6.375	2.811	-0.308	0.687	0.753	32.144
4 (outbound)	-5.699	3.222	-0.669	0.330	0.746	33.460
5 (inbound)	-1.729	0.324	-0.667	0.237	0.708	26.902
6 (inbound)	-2.119	0.327	-0.600	0.333	0.686	34.084
7 (inbound)	-3.739	0.806	-0.660	0.515	0.837	20.209
8 (outbound)	-2.013	2.108	-0.492	0.388	0.626	25.150
9 (not used)	n/a					
10 (inbound)	-3.193	3.172	-0.643	0.394	0.754	13.027
11 (outbound)	-3.785	4.720	-0.719	0.537	0.898	30.529
12 (inbound)	-3.937	3.425	-0.699	0.474	0.845	10.201

Table 6.7: Accuracy of elevation data, radar time delay = -204 ms.

<i>Segment</i>	<i>min</i> [mrad]	<i>max</i> [mrad]	<i>mean</i> [mrad]	<i>std</i> [mrad]	<i>RMS</i> [mrad]	<i>Invalid data</i> [%]
1 (outbound)	-2.054	0.753	-0.811	0.268	0.854	24.672
2 (inbound)	-1.508	0.194	-0.708	0.239	0.748	14.301
3 (inbound)	-2.072	3.015	-0.244	0.308	0.393	32.144
4 (outbound)	-2.252	1.373	-0.488	0.383	0.621	33.460
5 (inbound)	-1.416	0.089	-0.698	0.234	0.736	26.902
6 (inbound)	-1.489	-0.367	-0.832	0.235	0.865	34.084
7 (inbound)	-1.870	0.289	-0.725	0.328	0.796	20.209
8 (outbound)	-2.605	0.281	-0.984	0.260	1.018	25.150
9 (not used)	n/a					
10 (inbound)	-2.042	1.272	-0.532	0.387	0.658	13.027
11 (outbound)	-2.406	1.157	-0.759	0.311	0.820	30.529
12 (inbound)	-2.272	3.257	-0.588	0.445	0.738	10.201

Table 6.8: Accuracy of range data, radar time delay = -204 ms.

<i>Segment</i>	<i>min</i> [m]	<i>max</i> [m]	<i>mean</i> [m]	<i>std</i> [m]	<i>RMS</i> [m]	<i>Invalid data</i> [%]
1 (outbound)	-12.180	8.833	-2.583	3.722	4.530	24.672
2 (inbound)	-11.759	7.253	-2.537	1.787	3.102	14.301
3 (inbound)	-6.370	8.615	1.825	1.737	2.519	32.144
4 (outbound)	-12.568	11.455	-2.855	2.778	3.984	33.460
5 (inbound)	-12.909	2.440	-3.580	2.033	4.116	26.902
6 (inbound)	-6.445	6.728	0.043	1.358	1.357	34.084
7 (inbound)	-9.252	11.932	1.406	2.151	2.569	20.209
8 (outbound)	-10.835	11.668	-3.008	3.215	4.402	25.150
9 (not used)	n/a					
10 (inbound)	-11.024	9.114	-0.503	2.847	2.891	13.027
11 (outbound)	-13.484	9.431	-4.684	3.519	5.858	30.529
12 (inbound)	-10.453	12.726	0.326	2.295	2.318	10.201

All Inbound flight Results

Table 6.9: Accuracies over all inbound flights, radar time delay = -204 ms.

<i>Measurement</i>	<i>min</i> [mrad, m]	<i>max</i> [mrad, m]	<i>mean</i> [mrad, m]	<i>std</i> [mrad, m]	<i>RMS</i> [mrad, m]
Azimuth	-6.375	3.425	-0.645	0.428	0.774
Elevation	-2.272	3.257	-0.590	0.381	0.702
Range	-12.909	12.726	-0.667	2.823	2.901

All Outbound flight Results

Table 6.10: Accuracies over all outbound flights, radar time delay = -204 ms.

<i>Measurement</i>	<i>min</i> [mrad, m]	<i>max</i> [mrad, m]	<i>mean</i> [mrad, m]	<i>std</i> [mrad, m]	<i>RMS</i> [mrad, m]
Azimuth	-5.699	4.720	-0.580	0.426	0.720
Elevation	-2.605	1.373	-0.778	0.349	0.852
Range	-13.484	11.668	-3.254	3.453	4.744

6.3 Verification of Latency values

This section details the process used to verify the latency values used by the calibration software, detailed in Chapter 3.4.

6.3.1 Latency test

The test was split up into four parts. These included tests on the *inbound* and *outbound* segments of the Radar and Optronics respectively. Only the values for *range* were included in this dissertation, but the study of *elevation* and *azimuth* produced similar conclusions.

For each test, the data was run through the calibration software, and the latency values were incremented about the given latency value. The data was written to file, and plots were produced comparing the latency value (s) and mean range value (m). The latency value which corresponds to the smallest value for the mean bias would be assumed the correct latency value.

The plots for the Radar *inbound* and *outbound* results can be seen in Figure 6.5 and 6.6 respectively. The plots for the Optronics *inbound* and *outbound* results can be seen in Figure 6.7 and 6.8 respectively.

For the tested data, the speed of the aircraft varied in most cases between 50m/s and 100m/s. Remembering that $velocity = distance/time$, and calculating the time between the stated full latency compensation, and the calculated lowest mean value (from Figures 6.5, 6.6, 6.7 and 6.8), the distance in meters can be measured. Table 6.11 lists the difference in range measurements for the airplane speed.

Because the scattering pattern is different for the Radar and Optronics sensors, any difference in the time delays will be different, which is clear in the Figures. The mean values (see Tables B.9 and B.10) for the inbound and outbound flights of the radar, show us that there is a bias for the difference readings. These biases are expected, due to the dimensions of the airplane, and could possibly account for the latency difference. By using the calculated values of latency, giving a minimum mean difference in the analysis, the mean difference error approaches zero.

Table 6.11: Range differences for Optronics and Radar.

	Opt (inbound)	Opt (outbound)	Radar (inbound)	Radar (outbound)
range difference (m)	3-6	2.25-4.5	0.7-1.4	3.55-7.1

For the case of the Radar sensor, the mean bias of the inbound flights from the differential comparison can be explained by remembering that the GPS is mounted at a fixed position on the airplane,

whereas the readings from the Radar sensor originate from different reflections from the front of the airplane. This difference will be smaller than the outbound flights, as the GPS antenna is mounted near the front of the airplane. This mean bias will thus translate to a mean latency bias (remembering $velocity = distance/time$), which can be seen in the Figures. Conclusions regarding the Optronics follows similar reasoning, with data originating from different parts of the airplane.

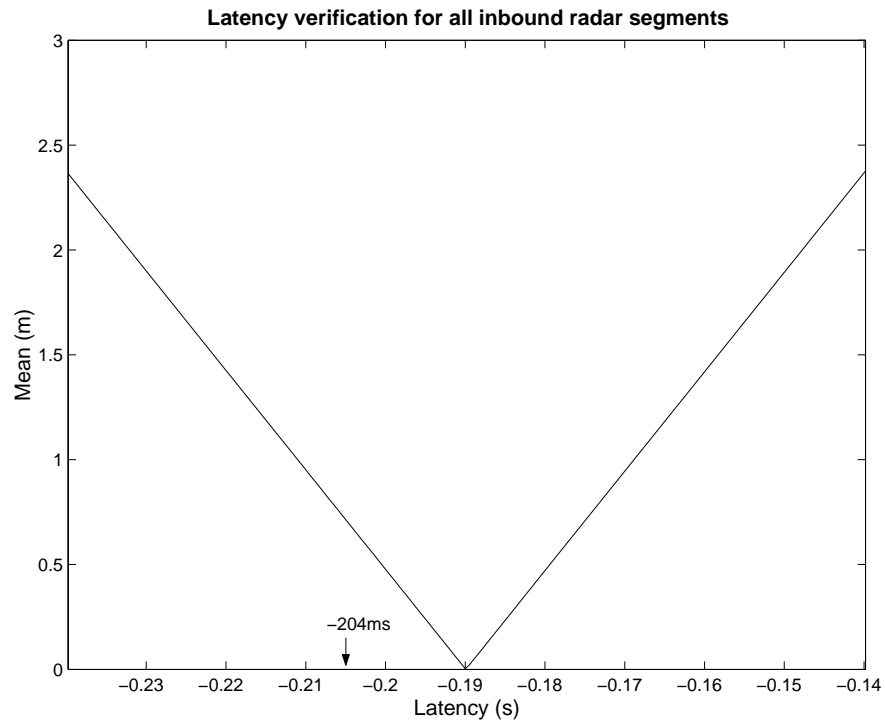


Figure 6.5: Plot of latency (s) vs. mean range (m), to verify the latency value of -204ms (radar inbound).

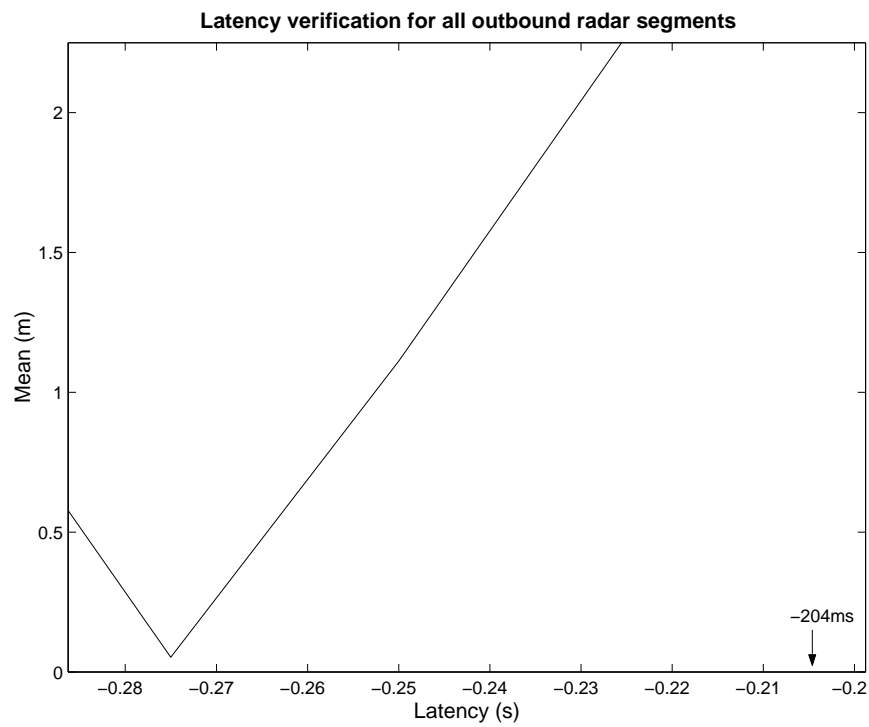


Figure 6.6: Plot of latency (s) vs. mean range (m), to verify the latency value of -204ms (radar outbound).

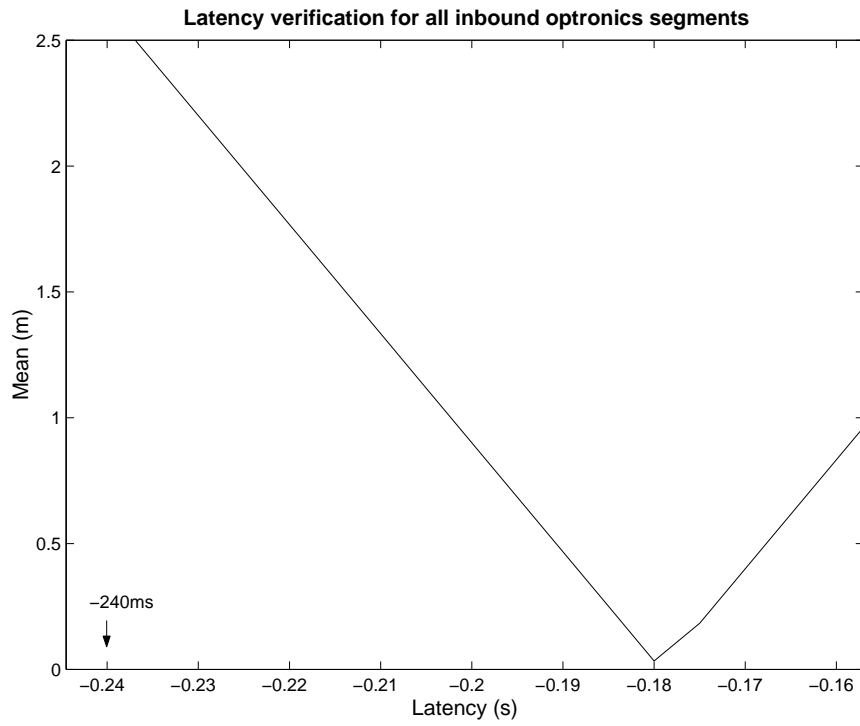


Figure 6.7: Plot of latency (s) vs. mean range (m), to verify the latency value of -240ms (optronics inbound).

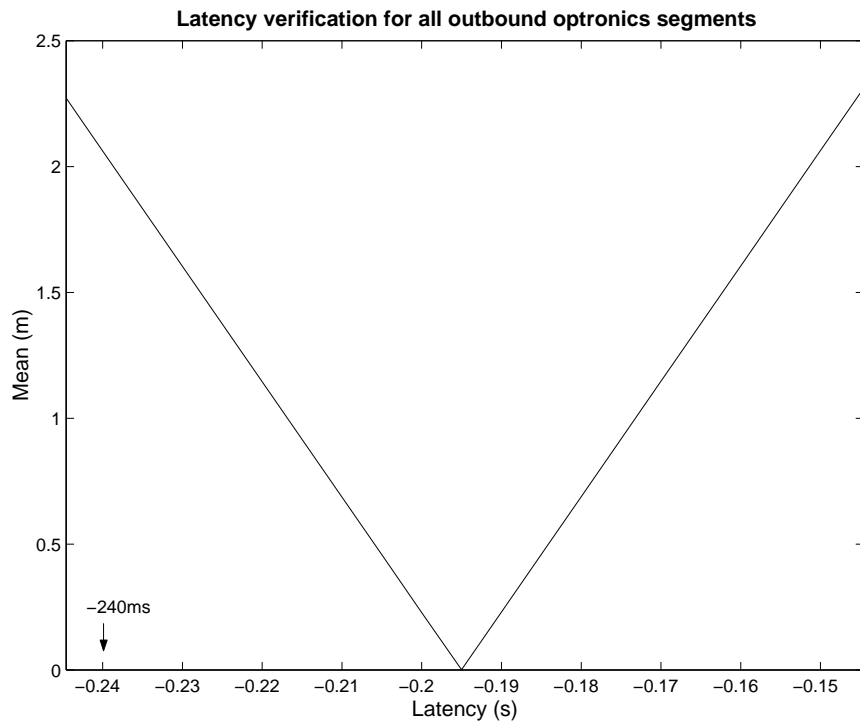


Figure 6.8: Plot of latency (s) vs. mean range (m), to verify the latency value of -240ms (optronics outbound).

6.4 Comments on Results

With the results from Section 6.1 and 6.2 in mind, the following observations and comments can be made:

1. As can be seen from the results in the tables, a very small percentage of the data from the Optronics' sensors is invalid, whereas between 10–34% of the data from the Radar sensor is invalid.
2. Data is taken of a target at various ranges. Since the GPS coordinates have to be converted to the polar coordinate system of the radar, there is a small error in the statistical calculation, as the underlying GPS error statistics will change due to the changing range (see Tables 3.1 and 3.2 in Chapter 3.3).
3. The underlying statistical error distributions have not yet been incorporated, but are dealt with in Chapter 7.
4. The true tracking accuracy should be better than has been measured here using the TAMS because:
 - There is an inherent inaccuracy in the dGPS system, which contributes to the measured error.
 - The GPS antenna is mounted about 1/3 of the length of the aircraft from the nose, while the *range* measured by the Tracker could be from reflections from the nose (inbound) or tail (outbound) of the aircraft, for both the Radar and the Laser range-finder.

Results from the test in Section 6.3 produced the following observations:

1. The latency values for both the Optronics and Radar sensors used for the analysis in this dissertation, were shown to be slightly incorrect. This could be explained by the readings for both the Radar and Optronics originating from different parts of the airplane for inbound and outbound flights. The mean bias using the given latency values, translates to a latency bias, which is evident in the Figures in Section 6.3.
2. This mean bias could explain the trend shown by the difference data to drift from the mean, as seen in the Figures in Section 6.1.1, 6.2.2 and the Appendices.

6.5 Summary of Chapter

The objective of this Chapter was to present the results after running the data through the calibration software. The results for the Optronics and Radar sensors for the inbound and outbound flights were very good. The mean biases visible in the tables can be explained by the dimensions of the airplane, with reflections from the target occurring from different parts of the aircraft, depending on which

sensor was used to track the target. The results obtained could be even better considering that the GPS has an inherent inaccuracy. The latency values used by the software were tested, and some discrepancies were discovered. The possible causes for these discrepancies were examined in this chapter.

Chapter 7

Statistical Analysis

The objective of this Chapter is to comment on the effect of the co-ordinate transformation on the dGPS error distribution, and to calculate the Tracker accuracy and hence qualify the Tracker, by comparing the Tracker specifications with the calculated Tracker accuracy.

The system described in Figure 7.1 (overleaf), depicts the first statistical problem to be analysed, and gives a basic overview of Section 7.1. The importance of the effect of the transformations on the error distribution is visible. The statistical analysis continues by calculating the Tracker accuracy in Section 7.2. A flow diagram for the steps involved can be found at the end of Chapter 7.2. The computed Tracker accuracy will be compared to the required Tracker accuracy in Chapter 3.2, to validate the Tracker's specifications.

7.1 Effect of Co-ordinate transformation on GPS error distribution

The original GPS data received to be processed by the calibration software, had to undergo numerous co-ordinate transformations to convert the GPS data from latitude, longitude and height into range, azimuth and elevation (see Chapter 2.3 and 4.3 and Figure 7.2). The effect of these transformations on the error distribution of the GPS data is the primary focus of this section.

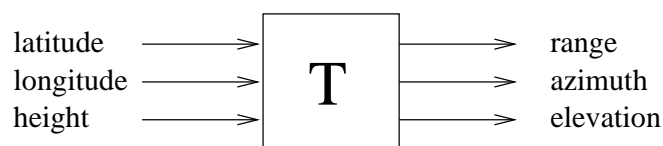


Figure 7.2: Input and Output variables of the Transformation.

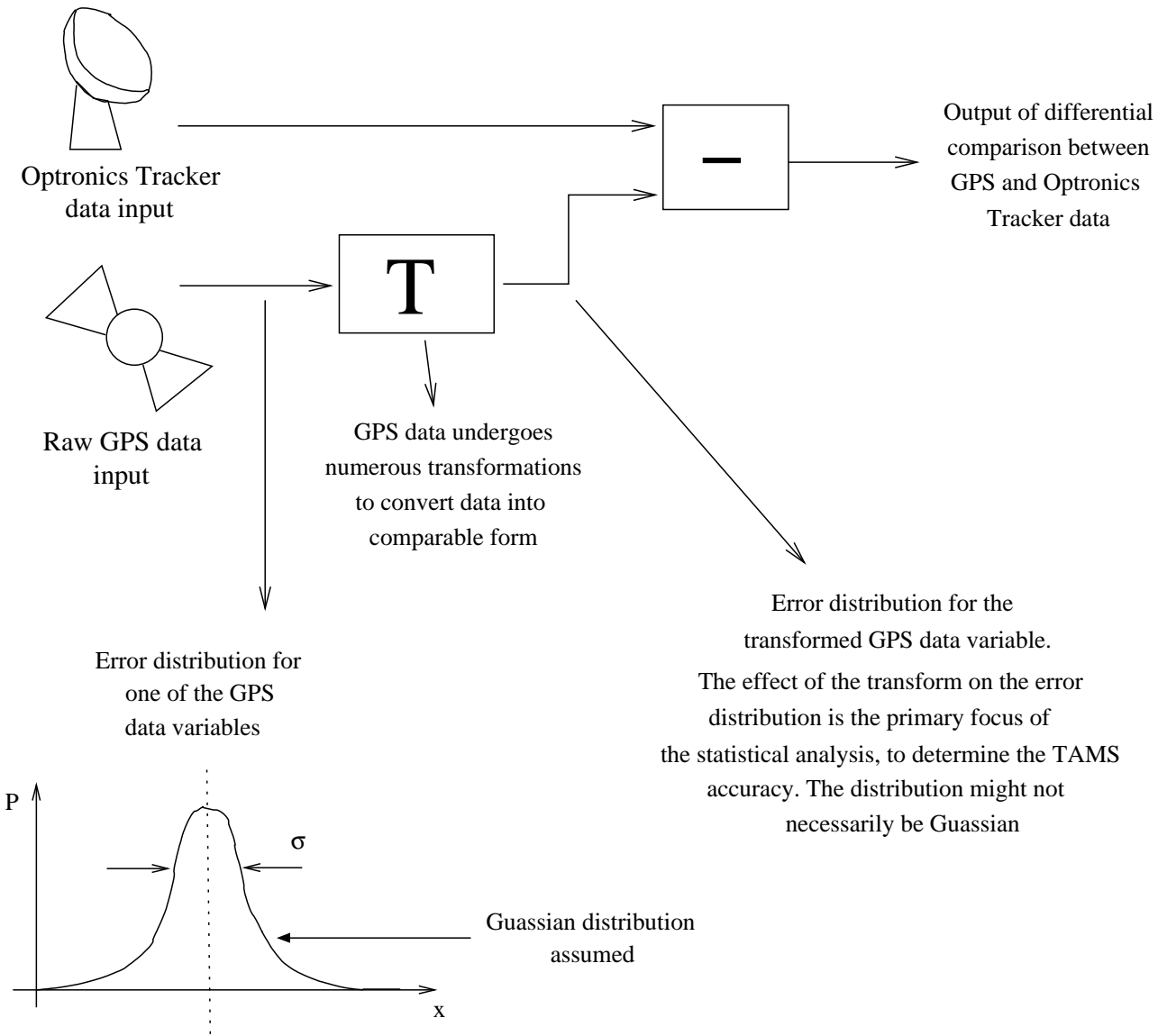


Figure 7.1: Diagram depicting the effect of the Transformation on the GPS distribution.

A number of simulations, written in *Matlab*, were performed on the statistical distribution of the GPS data. Although the exact distribution of the raw GPS data was not known, because the errors were mostly random it was assumed that the distribution is normal, based on the *central limit theorem* [13, pg 304-337], [26, pg 109-113]. The *central limit theorem* states that the *mean* of any set of variates with any distribution having a finite *mean* and *variance* tends to a normal distribution. Thus the GPS error distribution chosen to analyse was assumed to be a *Gaussian* distribution with a probability function of ([28, pg 417] , [30, pg 482] and [21, pg 109-118]):

$$f_x(x) = \frac{e^{-(x-\mu)^2/2\sigma^2}}{\sqrt{2\pi\sigma^2}}$$

where μ is the mean, and σ^2 is the variance.

For the simulation, the ellipsoidal error distribution (described in Chapter 3.3) was used to calculate the standard deviation σ . The standard deviations of $1m$ for latitude and longitude were converted to degrees. $2m$ was used as the standard deviation for height. The GPS data was analysed, and the maximum and minimum ranges were chosen as starting points for the mean μ . The mean range was also used for the simulations. A normal distribution was simulated, using these values of μ and σ , for the latitude, longitude and height. These were fed into the transformation, and the output was carefully analysed.

The simulations were written to investigate the graphical effect on the error distribution. The *Statistics Toolbox* in Matlab was used for some of the simulations.

To aid with the clear presentation of the transformation effect, a *normal plot* was used on the transformed data. A normal probability plot [16], was used on the transformed GPS data, as it gives a good indication of whether the data comes from a *normal* distribution. The normal probability plot has three graphical elements (see Figures 7.3, 7.4 and 7.5). The *plus signs* show the empirical probability versus the data value for each point in the sample. A linear fit connects the 25th and 75th percentiles of the data, and can be seen by the *solid line* in the diagram. The *dashed line* seen in the diagram extends the solid line to the ends of the sample. The probabilities from zero to one make up the y-axis. If all the data points fall near the line, then it can be assumed that the data comes from a *normal* distribution.

The *solid lines* in the normal range plots of Figures 7.3, 7.4 and 7.5 appear to be linear, thus implying that the transformed distribution is a normal distribution. The normal plots for azimuth and elevation are also linear in all cases, but these plots were not included in this dissertation.

A histogram of GPS distribution, after undergoing the co-ordinate transformation, is also visualised in these plots. The distribution in all cases looks like a normal distribution, but this assumption is tested further. A *Matlab* function analyses this GPS distribution, computes the mean and standard deviation of the fitted normal distribution, and computes a value for mean and standard deviation.

The final test on the assumption that the distribution is normal involves an hypothesis test, using the 'Lilliefors' [15] test for 'goodness of fit' to a normal distribution. This test evaluates the hypothesis that the GPS data has a normal distribution with unspecified mean and variance, against the alternative that the GPS data does not have a normal distribution. The empirical distribution of the data is compared with a normal distribution of the same mean and variance as the data. The result of this test was that the GPS data does have a normal distribution.

After the testing, the distributions of the range, azimuth and elevation can safely be considered normal distributions, with means and standard deviations calculated for the normal distributions, based on the fitted normal distribution. By varying the standard deviation of the input distribution and studying the output, it is concluded that the transformations are linear over the ranges tested in this dissertation.

Figures 7.3, 7.4 and 7.5 list the standard deviations, and it can be seen that, as expected, the standard deviation decreases as the range increases. When the value for elevation was varied, the distribution maintained its Gaussian distribution, but the standard deviation increased dramatically as the elevation angle increased.

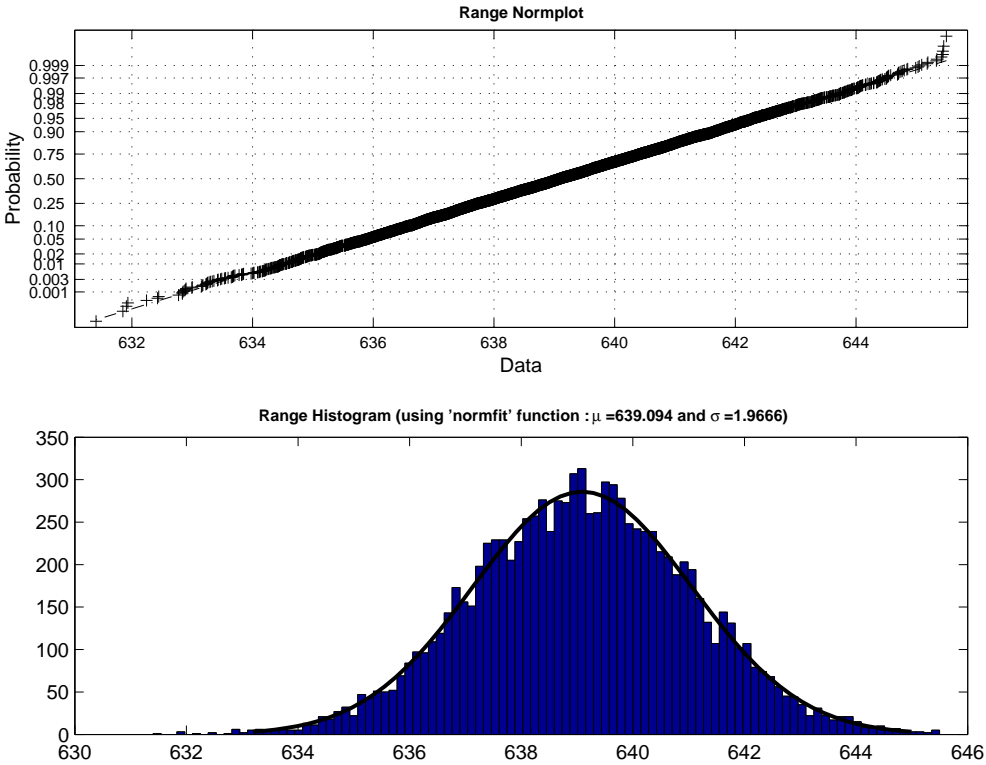


Figure 7.3: Normal plot and histogram for closest range bin (639.09m).

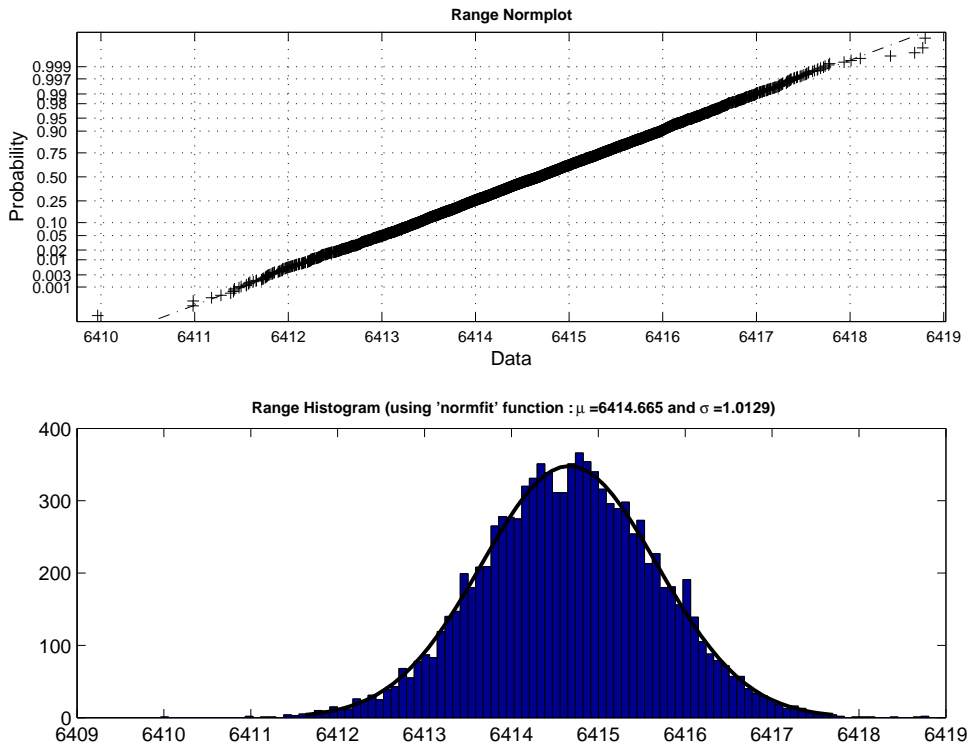


Figure 7.4: Normal plot and histogram for mean range bin (6414.68m).

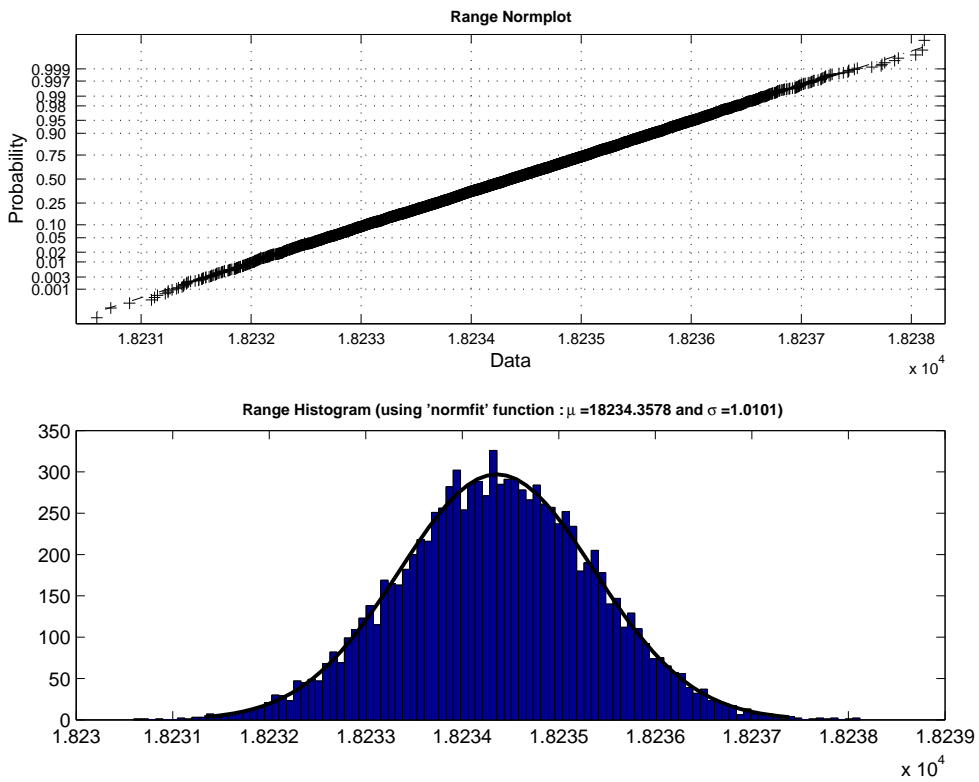


Figure 7.5: Normal plot and histogram for furthest range bin (18234.357m).

7.2 Calculating Tracker *variance* and *standard deviation*

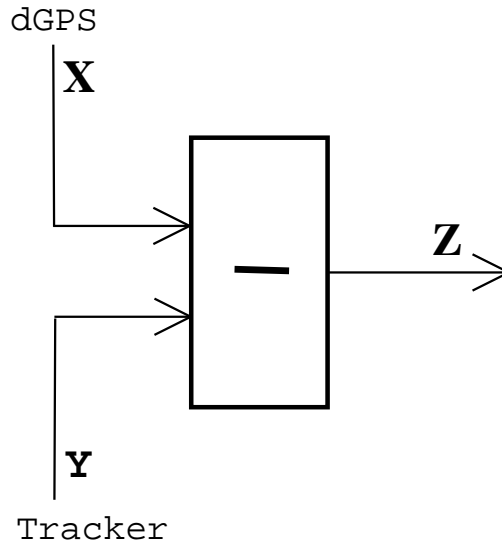


Figure 7.6: Diagram of differential data Z computed from the dGPS and Tracker Data.

To verify the Tracker accuracy specified in Chapter 3.2, the Tracker standard deviation must be calculated. This is computed by first calculating the Tracker variance from the difference (Z) and dGPS (X) data.

As seen in Figure 7.6, $Z = X - Y$, where X and Y are two *independent* normally distributed random variables with means of μ_X and μ_Y , and variances of σ_X^2 and σ_Y^2 respectively. Z has a mean of μ_Z and a variance of σ_Z^2 . To compute the *mean* and *variance* of Y , we consider the equation $Y = X - Z$. X and Z are not statistically *independent* in this case, as Z depends on X . The *variance* of Y (σ_Y^2), is computed as follows [30, pg 457-532], [22, pg 230-321], [5, pg 143-248], [26, pg 75-123] :

$$\begin{aligned}
 Var\{Y\} &= E\{Y^2\} - (E\{Y\})^2 = E\{(Y - E\{Y\})^2\} \\
 &= E\{X^2 - 2XZ + Z^2\} - (E\{X - Z\})^2 \\
 &= E\{X^2\} - 2E\{XZ\} + E\{Z^2\} - (E\{X\}^2 - 2E\{X\}E\{Z\} + E\{Z\}^2) \\
 &= E\{X^2\} - E\{X\}^2 + E\{Z^2\} - E\{Z\}^2 - 2(E\{XZ\} - E\{X\}E\{Z\}) \\
 &= Var\{X\} + Var\{Z\} - 2\underbrace{(E\{XZ\} - E\{X\}E\{Z\})}_{(a)} \tag{7.1}
 \end{aligned}$$

but *covariance* is defined in [5, pg 216] :

$$\sigma_{XZ} = Cov\{X, Z\} = E\{XZ\} - E\{X\}E\{Z\}$$

but this result is equal to that of **(a)**. Therefore Equation 7.1 becomes :

$$\begin{aligned} \text{Var}\{Y\} &= \text{Var}\{X\} + \text{Var}\{Z\} - 2\text{Cov}\{X, Z\} \\ &= \sigma_X^2 + \sigma_Z^2 - 2\text{Cov}\{X, Z\} \end{aligned} \quad (7.2)$$

To calculate the *variance* of the Tracker, the covariance of the *difference* and *dGPS* data needs to be computed. When computing this variance, the *mean* of the dGPS data has to be calculated. Because the GPS antenna mounted onboard the aircraft is moving with time, so the dGPS data readings increase and decrease with time. A curve fitting the trend of the data for the GPS variables thus needs to be found for use as the *mean*. This scenario is depicted in Figure 7.7. Thus, the new dGPS data incorporates the fitted polynomial as its *mean* value.

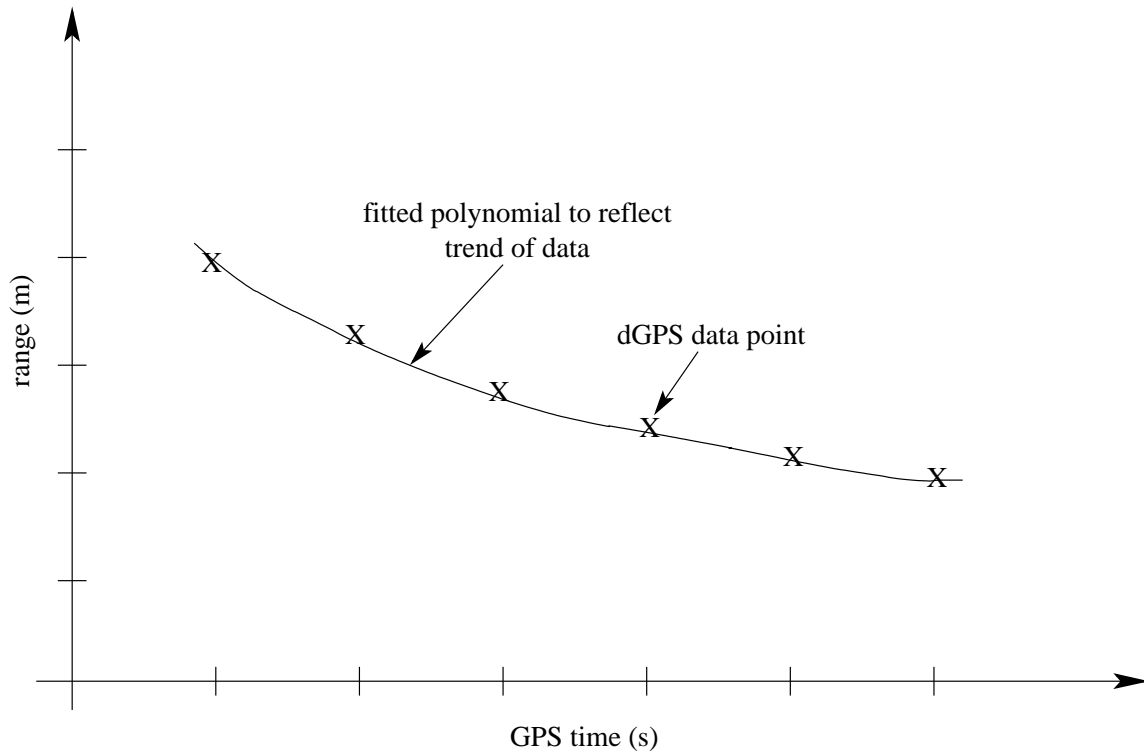


Figure 7.7: Fitted mean curve to reflect data trend.

To compute the polynomial to represent the dGPS data trend, the coefficients of the polynomial must be computed. 1st and 2nd order polynomials are investigated, and the coefficients compared.

The general equation for a polynomial of degree n :

$$y = a_1t^n + a_2t^{n-1} + \dots + a_nt + a_{n+1} \quad (7.3)$$

can be simplified to give the equation of a 1st order polynomial (order $n = 1$):

$$y = a_1t + a_2 \quad (7.4)$$

A polynomial of 1st degree was fitted to the dGPS data, using *Matlab*, and the coefficients (a_1 and a_2) of the polynomial were calculated.

The dGPS data was also fitted with a 2nd order polynomial, to compare the coefficients of the 1st order polynomial. The equation of the 2nd order polynomial (order $n = 2$) is:

$$y = a_1t^2 + a_2t + a_3 \quad (7.5)$$

Coefficients a_1 , a_2 and a_3 were also computed using a fitted polynomial in *Matlab*.

Because the data received for this dissertation only included flight ranges of between 3 and 6km for the Optronics sensor, and between 3 and 11km for the Radar sensor, only the range bins of 5km and 10km could be considered.

The values of the coefficients for the dGPS fitted range polynomials are tabulated in Tables 7.1, 7.2 and 7.3. Table 7.1 gives the coefficients of the 1st and 2nd order polynomials to fit the dGPS range data, when comparing the dGPS range data to the Optronics range data at the 5km range bin. Tables 7.2 and 7.3 give the 1st and 2nd order coefficients of the polynomial intended to fit the dGPS range data, when comparing the dGPS range data to the Radar range data at the 5km and 10km range bins. The values for the azimuth and elevation coefficients are found in the Appendices.

Table 7.1: Coefficients of dGPS **range** data for Optronics 5km range bin.

order of polynomial	a_1	a_2	a_3
1	-4.554	1.35×10^7	0
2	5.965×10^{-2}	-3.544×10^4	5.265×10^9

Table 7.2: Coefficients of dGPS **range** data for Radar 5km range bin.

order of polynomial	a_1	a_2	a_3
1	-48.474	1.4×10^7	0
2	9.713×10^{-3}	-5.659×10^3	8.421×10^8

Table 7.3: Coefficients of dGPS **range** data for Radar 10km range bin.

order of polynomial	a_1	a_2	a_3
1	-48.841	1.411×10^7	0
2	-9.68×10^{-3}	5.54×10^3	-7.927×10^8

When comparing the 1st and 2nd order coefficients, and the graphs of the dGPS data and the fitted 1st and 2nd order polynomials, it was found that the 2nd order polynomial most closely fits the trend of the data. The 2nd order polynomial was therefore chosen to represent the fitted curve for the dGPS data, for range, azimuth and elevation.

The polynomial equations in 7.4 and 7.5 are solved using the calculated 2nd order coefficients, and the new dGPS data is found by evaluating the polynomial at the original time intervals.

The covariance for the difference data and the new dGPS data is calculated as follows [21, pg 172]:

$$cov(x, z) = E[(x - \mu_x)(z - \mu_z)] \quad (7.6)$$

Equation 7.6 is used to calculate the covariance matrix:

$$\begin{bmatrix} \sigma_x^2 & cov_{xz} \\ cov_{zx} & \sigma_z^2 \end{bmatrix}$$

where cov_{xz} and cov_{zx} ($cov_{xz} = cov_{zx}$) represent the covariance between the *difference* and *dGPS* data, and σ_x^2 and σ_z^2 represents the variance of the *difference* and *dGPS* data respectively.

The **covariance** of X and Z, $cov\{X, Z\}$, and the **variance** of the X and Z data, σ_x^2 and σ_z^2 , is used to compute the **Tracker variance**, σ_y^2 , using Equation 7.2. The **standard deviation** of the Tracker (σ_y) is calculated from the variance, and these values are compared to the stated accuracies in Chapter 3.2.

Table 7.4: Optronics standard deviations (σ_y).

Range bin (km)	Azimuth (mrad)	Elevation (mrad)	Range (m)
5	0.108	0.124	1.071

Table 7.5: Radar standard deviations (σ_y).

Range bin (km)	Azimuth (mrad)	Elevation (mrad)	Range (m)
5	0.455	0.311	1.551
10	0.153	0.174	1.322

By comparing the results in Tables 7.4 and 7.5 to the required accuracy values in Chapter 3.2, it is seen that the Tracker meets specification over the range of 3km to 11km.

7.3 Summary of Chapter

The final Chapter in this dissertation laid out the statistical analysis performed on the data. Examining the effect of the co-ordinate transformation on the dGPS data proved that the Guassian error distribution of the dGPS input data maintained its Guassian distribution, and that the transformation was linear for the ranges tested in this dissertation. The accuracy of the Tracker was calculated by computing the covariance of the dGPS and difference data. The original dGPS data was fitted with a polynomial of 2nd degree, to compute the moving average. The new dGPS data (original dGPS data with the trend removed) was used in the calculations. The Tracker accuracy was compared with the specified Tracker accuracy, and the Tracker was qualified for the tested range bins.

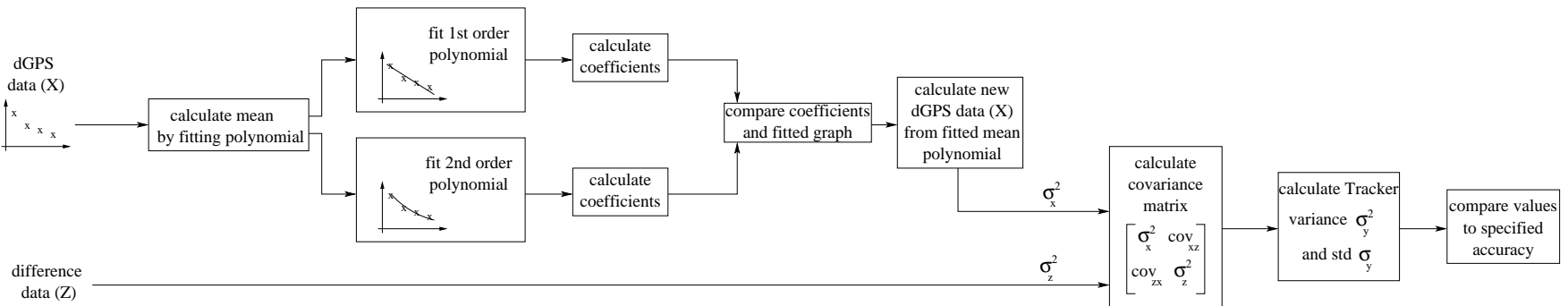


Figure 7.8: Flow diagram to compute Tracker Accuracy.

Chapter 8

Conclusions and Recommendations

This Chapter comments on the conclusions with regards to the results of Chapter 6 and 7, and lists some recommendations for consideration.

8.1 Conclusions

8.1.1 Tracker system meets specification

Based on the comparison of the results obtained in Chapter 7.2 and the specified accuracies in Chapter 3.2, the Tracker system meets the required specification of:

- 5m in *range*
- 1.5mrad in *azimuth* and *elevation* angle

for target ranges of between 3km and 11km. The actual accuracy of the Tracker should be slightly better than calculated, due to the inherent inaccuracy of the dGPS system.

8.1.2 Minimal Tracker data limits analysis

The data received for this dissertation from the Optronics and Radar sensor consisted of data for range bins between 3km and 11km. Thus, the Tracker required accuracy could not be qualified outside these range bins.

8.1.3 Insufficient data at particular range bins

When performing the statistical analysis on the data, there was very limited data at particular range bins. Due to this lack of data, a degradation in the accuracy resulted.

8.1.4 Latency values

When the latency compensation values specified for the analysed data were tested, it was found that there was a slight mis-match in time for the lowest *mean* value. Using the values received for the analysis could decrease the calculated Tracker accuracy, because when tested, they do not represent the lowest *mean* value. This factor could also explain the trend of the data in the difference plots in Chapter 6 to gradually drift from the mean.

8.2 Recommendations

8.2.1 Test software by simulating data in radar simulator

The software used for this dissertation was tested as thoroughly as possible. However, by simulating Tracker and dGPS data using a radar simulator, the software can be thoroughly tested under all conditions. The expected outputs can be tested against the software results and hence qualify the software.

8.2.2 Collect data at all range bins to qualify Tracker

To qualify the Tracker from 500m to 25km as stipulated in Chapter 3.2, data from the Radar and Optronics sensors at all these range bins should be collected.

8.2.3 Perform radial test flights to increase data at particular range bins

By collecting data from radial test flights at a particular radius, sufficient data at particular range bins can be collected. This increase in data will improve the accuracy of the statistical analysis.

Bibliography

- [1] N. Ackroyd and R. Lorimer, "Global Navigation: A GPS user's guide", Lloyd's of London Press LTD, 2nd edition, 1994.
- [2] J. H. Ahlberg and E. N. Nilson, "The Theory of Splines and Their Applications", Academic Press, 1967.
- [3] Army Technology, "The Website for the Defense Industries - Army" www.army-technology.com/projects/avenger, Website for Defense Industries - Army, 2003.
- [4] R. E. Bellman and R. S. Roth, "Methods in Approximation", D. Reidel Publishing Company, 1986.
- [5] J. L Devore "Probability and Statistics", Thomson Learning, Probability handbook, 2000 - 5th edition, pg 143 - 248.
- [6] O. Fadiran, "Results of Optronics data", technical report, July 2002.
- [7] O. Fadiran and M. R. Inggs, "Tracking Accuracy Measurement Systems (TAMS) Phase 2", Interim Report, 17 June 2002.
- [8] E. M. Gaposchkin and B. Kolaczek (editors), "Reference Co-ordinate Systems for Earth Dynamics", Astrophysics and Space Science library, Volume 86, Proceedings of the 56 th Colloquium of the International Astronomical, 1981.
- [9] GPS World, "GPS World's Big Book of GPS 2000", Advanstar Communications, 1999.
- [10] B. Hofmann-Wellenhof and H. Lichtenegger, "GPS : Theory and Practice", SpringerWien-NewYork, 5th edition, 2001.
- [11] J. Hurn, "Differential GPS Explained", textbook, Trimble, 1993.
- [12] S. Kingsley and S. Quegan, "Understanding Radar Systems", Scitech, 2nd edition, 1999.

- [13] I. H. LaVelle, "An Introduction to Probability, Decision, and Inference", Holt Rinehart and Winston, Inc., 1970.
- [14] A. Leick, "GPS Satellite Surveying", John Wiley and Sons, 2nd edition, 1995.
- [15] Mathworks, "mathworks help" www.mathworks.com/access/helpdesk/help/toolbox/stats/, The Mathworks, Inc., 2004.
- [16] The Mathworks, Inc, "Matlab Help", Mathworks - online documentation, 1994 -2004.
- [17] S. McElroy, "Getting started with GPS surveying", GPSCO, 1993.
- [18] Merriam-Webster Dictionary, "Merriam-Webster dictionary" www.m-w.com, Merriam-Webster Unabridged Online Dictionary, 2003.
- [19] C.L. Merry, "Interim Report — Assessment of the suitability of using GPS to verify the accuracy of the tracker system", technical report, 2 February 2002.
- [20] O. Montenbruck, "Practical Ephemeris Calculations", Springer-verlag, 1989.
- [21] D. Montgomery and G. Runger, "Applied Statistics and Probability for Engineers", John Wiley and Son, Inc., 3rd edition, 2003.
- [22] D. S. Moore, "The Basic Practice of Statistics ", Freeman, Statistics handbook, 1995.
- [23] A.N. Mountain, "Accuracy Analysis for TAMS Radar/Optronics Data: Final Report", technical report, 27 May 2003.
- [24] A.N. Mountain, "GPS Data Conversion", technical report, January 2003.
- [25] I. I. Mueller and H. Eichhorn, "Spherical and Practical Astronomy as Applied to Geodesy", Frederick Ungar Publishing Co., 2nd edition, 1977.
- [26] L. Ott, "An Introduction to Statistical Methods and Data Analysis", PWS-Kent Publishing Company, 3rd edition, 1988.
- [27] Reutech Radar Systems, "Reutech Radar Systems website" www.rrs.co.za/rts6400.html, RRS, 2003.
- [28] M. Schwartz, "Information, Transmission, Modulation, and Noise", McGraw-Hill Publishing Company, 4th edition, 1990.
- [29] M. Skolnik, "Radar Handbook", Mcgraw-Hill, 2nd edition, 1990, 4.15 - 4.17.
- [30] F. G. Stremmer, "Communication Systems", Addison-Wesley Publishing Company, 3rd edition, 1990.

- [31] Trimble, "trimble" www.trimble.com/gps/index.html, Trimble Navigation Limited, 2003.
- [32] University of New South Wales, "University of South Wales" www.gmat.unsw.edu.au, School of Surveying and Spatial Information Systems, 2001.
- [33] U.S. Coast Guard, "U.S. Coast Guard" www.navcen.uscg.gov, U.S. Coast Guard - Navigation Center, 30 July 2003.
- [34] G. van der Merwe, "Memorandum — ITB FAT Radar Tracking Data", Reutech Radar Systems, 14 January 2003.
- [35] G. van der Merwe, "Memorandum — ITB FAT Optronics Tracking Data", Reutech Radar Systems, 4 February 2003.

Appendix A

Optronics Results

A.1 Overview of Optronics Data

This appendix presents plots of the Optronics range, elevation and azimuth data for each of the analysed segments. The segments analysed are listed in Chapter 6.1.1. The dGPS-derived range data is also plotted for comparison. The source of the Optronics data is split into range and angle data. The angle data (consisting of azimuth and elevation), comes from the autotracker. The Laser on the optronics system measures the range.

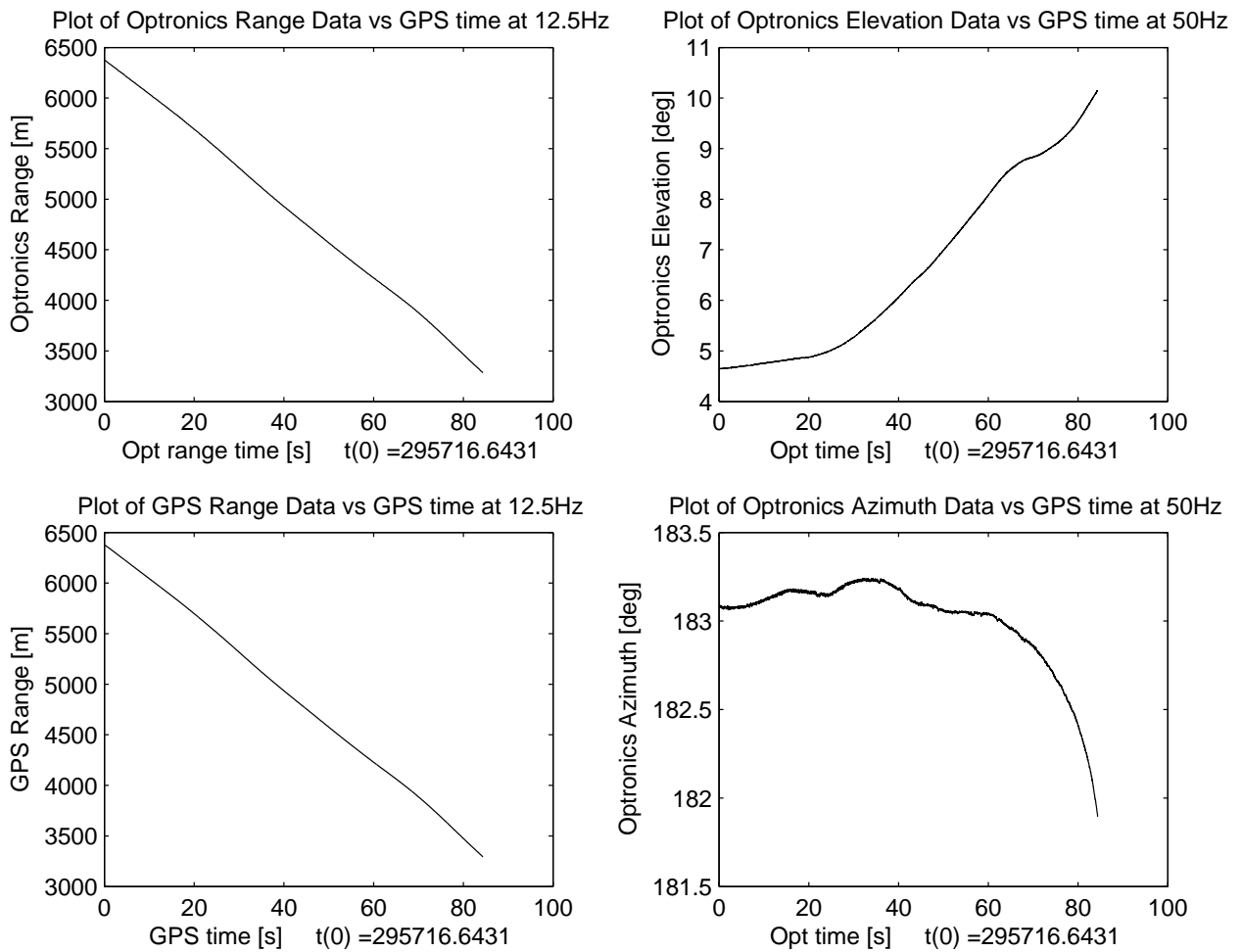


Figure A.1: Optronics Segment 1 (ITB_FAT_WPN_Wed_12_09_22_1): Plots of optronics range, elevation and azimuth data. The GPS-derived range data is also shown for comparison.

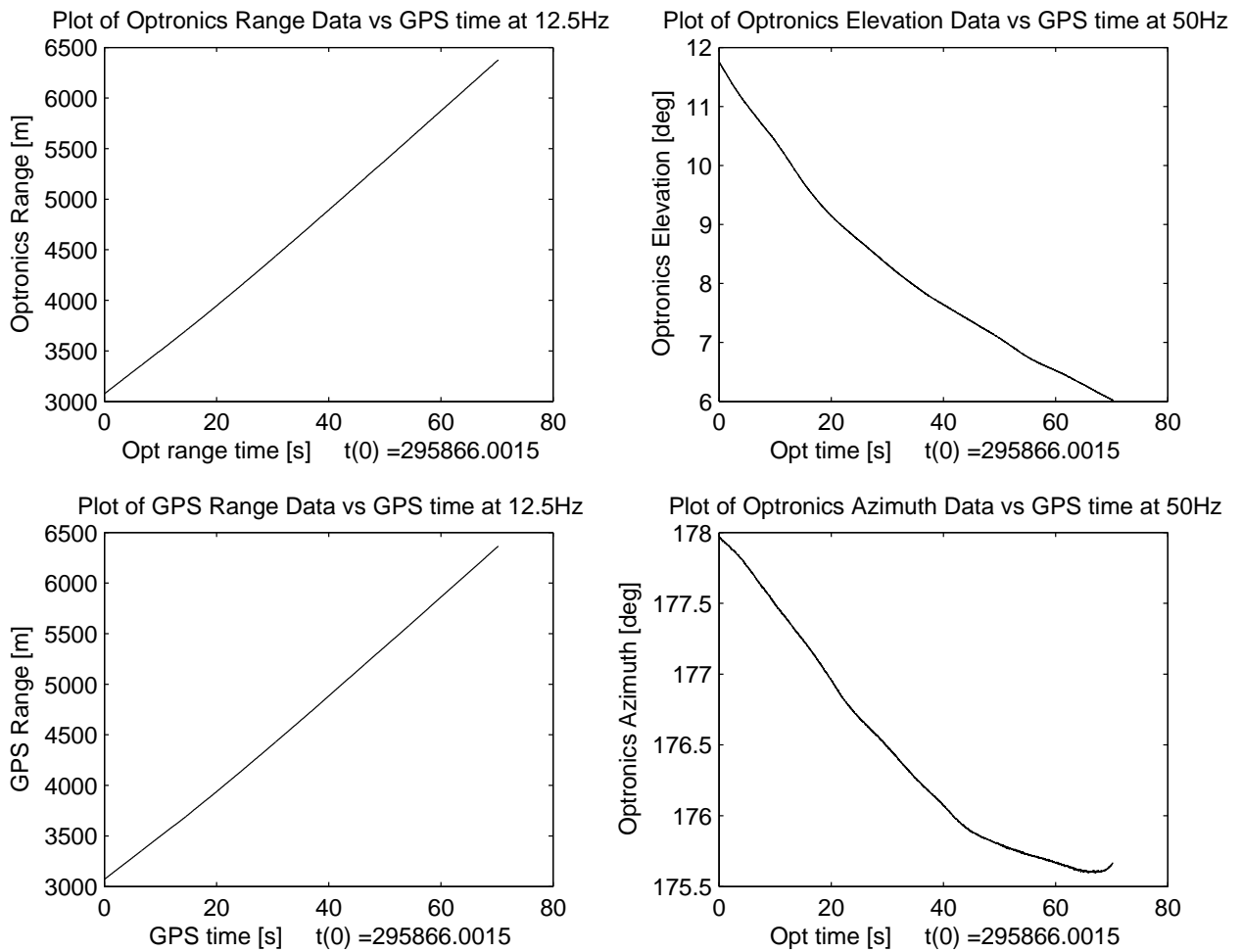


Figure A.2: Optronics Segment 2 (ITB_FAT_WPN_Wed_12_11_36_1): Plots of optronics range, elevation and azimuth data. The GPS-derived range data is also shown for comparison.

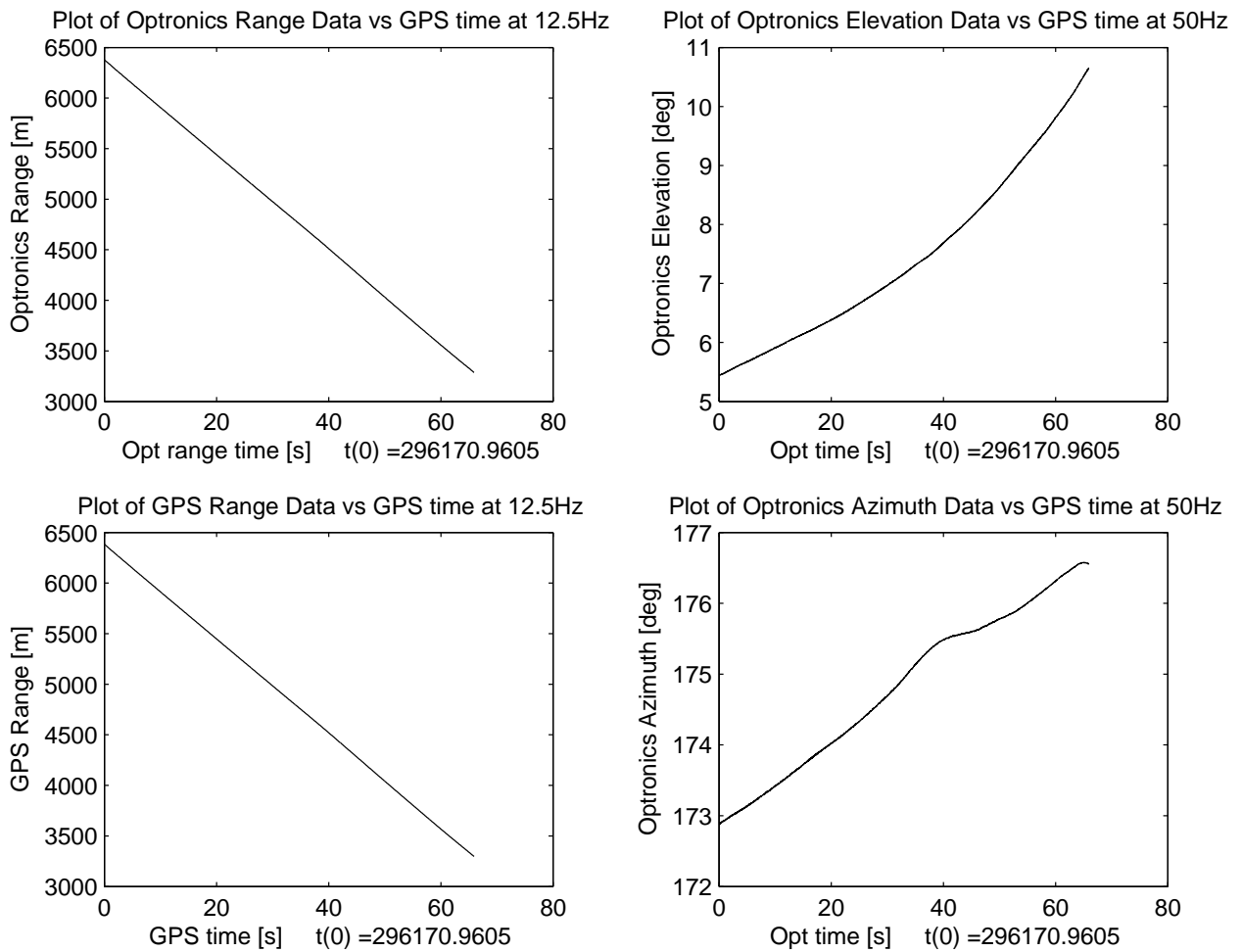


Figure A.3: Optronics Segment 3 (ITB_FAT_WPN_Wed_12_17_04_1): Plots of optronics range, elevation and azimuth data. The GPS-derived range data is also shown for comparison.

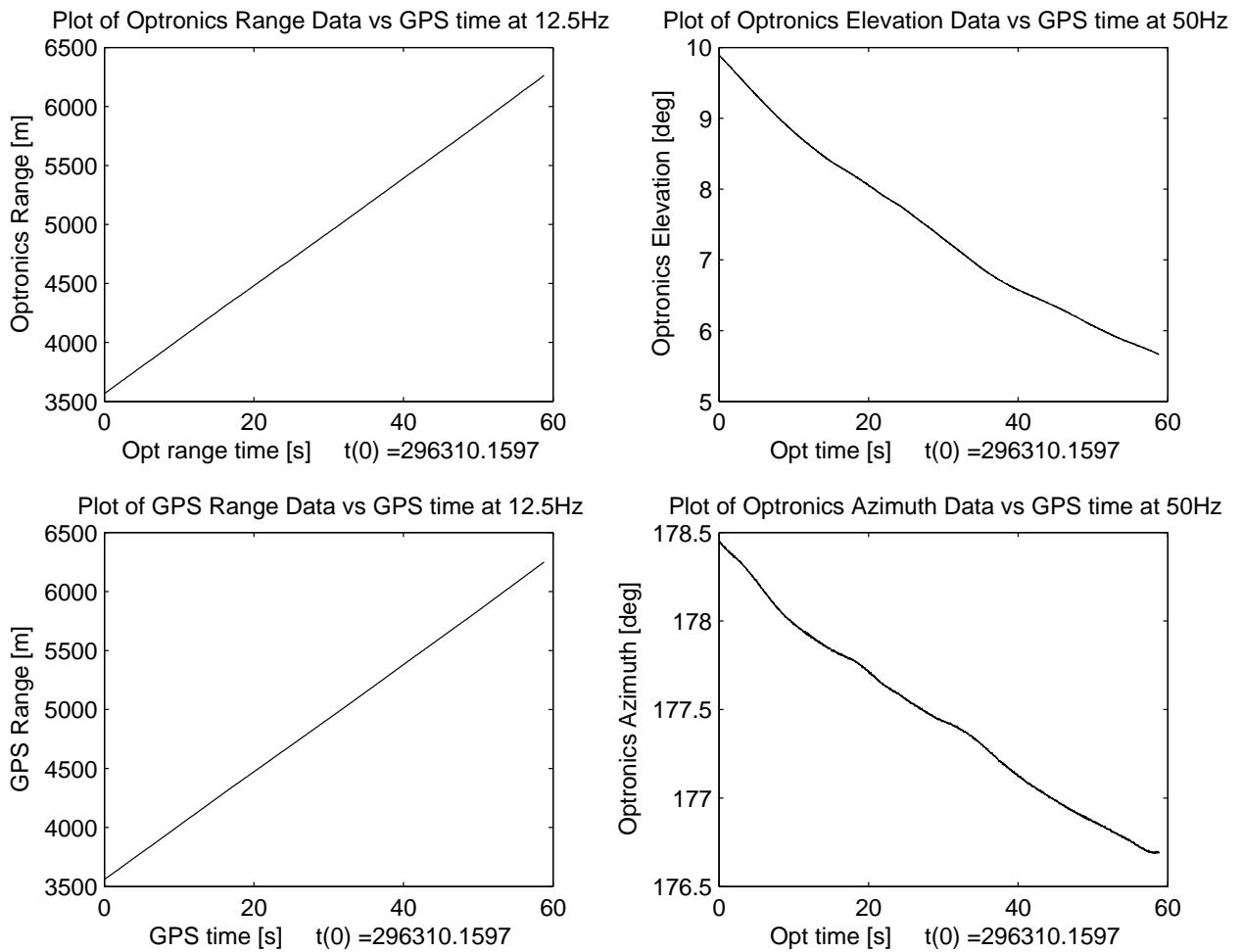


Figure A.4: Optronics Segment 4 (ITB_FAT_WPN_Wed_12_18_48_1): Plots of optronics range, elevation and azimuth data. The GPS-derived range data is also shown for comparison.

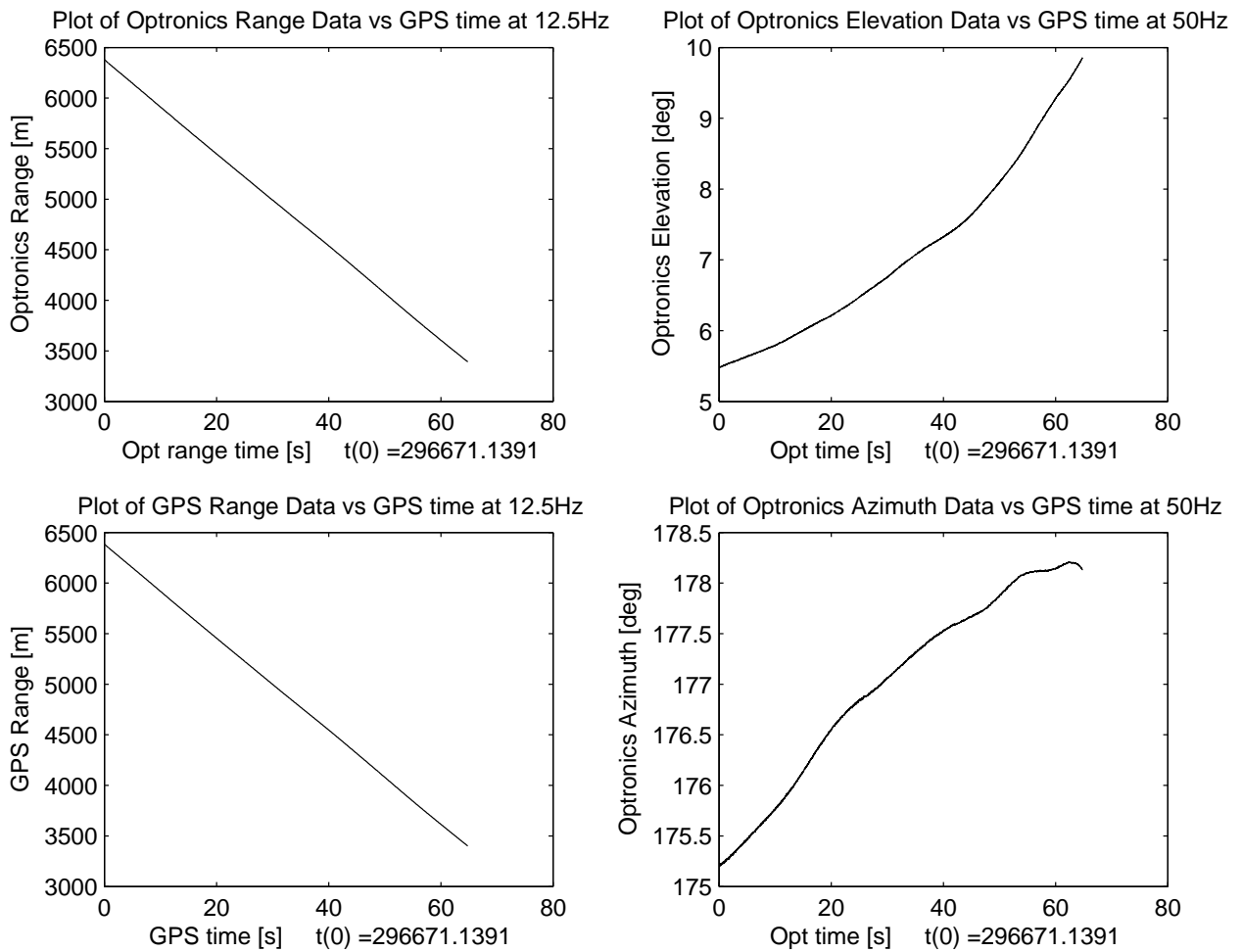


Figure A.5: Optronics Segment 5 (ITB_FAT_WPN_Wed_12_24_59_1): Plots of optronics range, elevation and azimuth data. The GPS-derived range data is also shown for comparison.

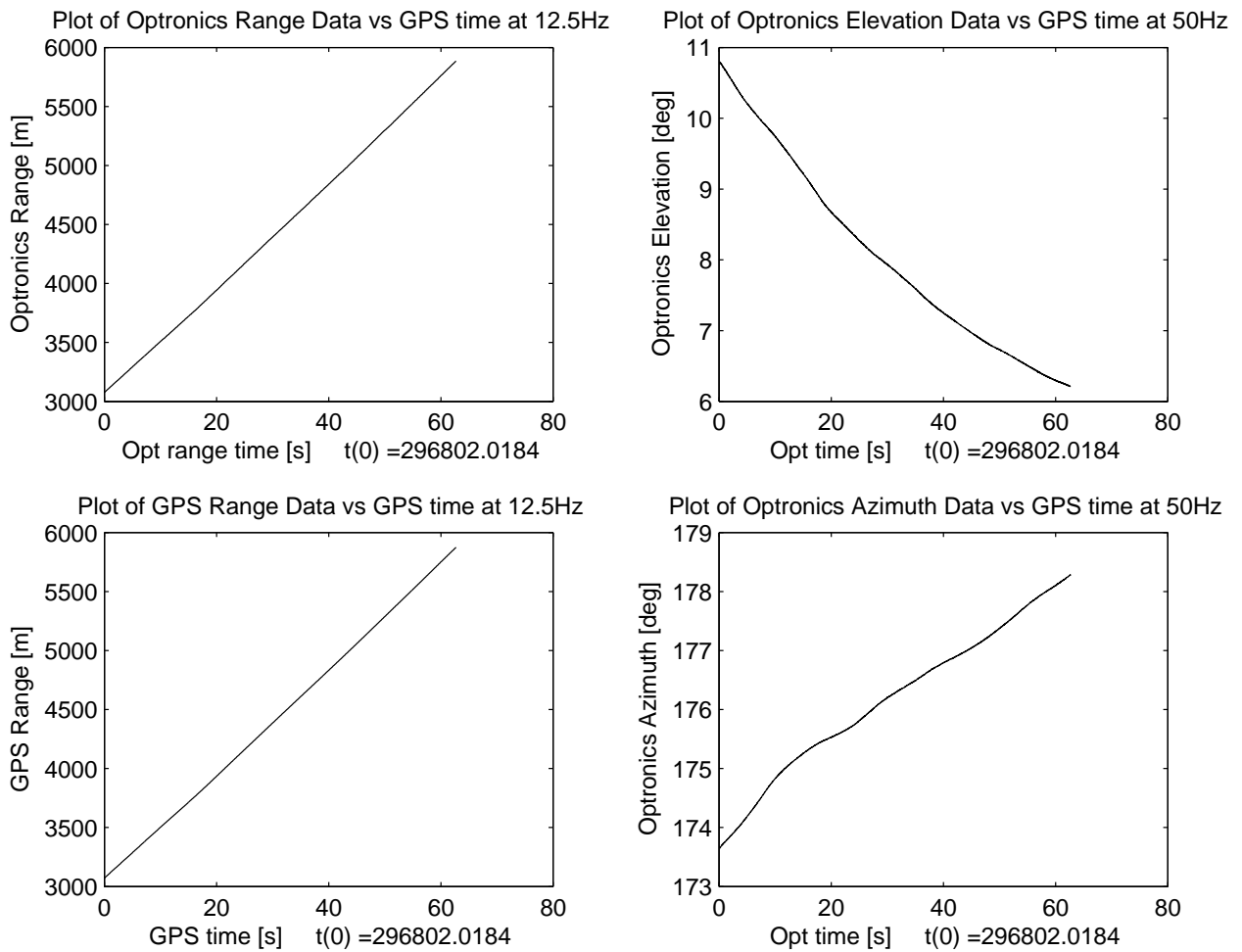


Figure A.6: Optronics Segment 6 (ITB_FAT_WPN_Wed_12_27_09_1): Plots of optronics range, elevation and azimuth data. The GPS-derived range data is also shown for comparison.

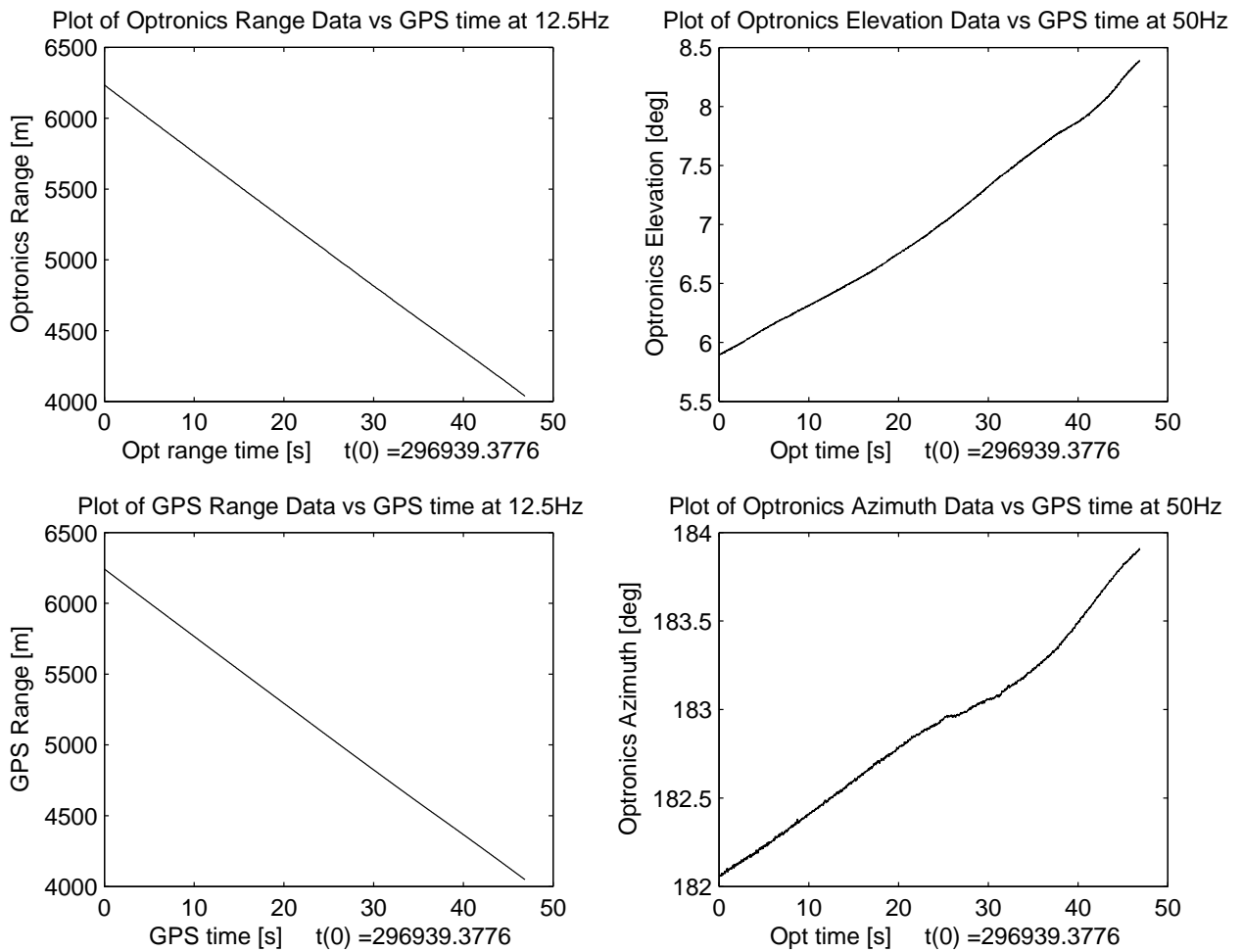


Figure A.7: Optronics Segment 7 (ITB_FAT_WPN_Wed_12_29_28_1): Plots of optronics range, elevation and azimuth data. The GPS-derived range data is also shown for comparison.

A.2 Results Overview

This appendix presents difference plots between the Optronics range, elevation and azimuth data and the dGPS range, elevation and azimuth data, for each of the analysed segments. No data latency compensation was applied to the data. Refer to Chapter 6.1.2.

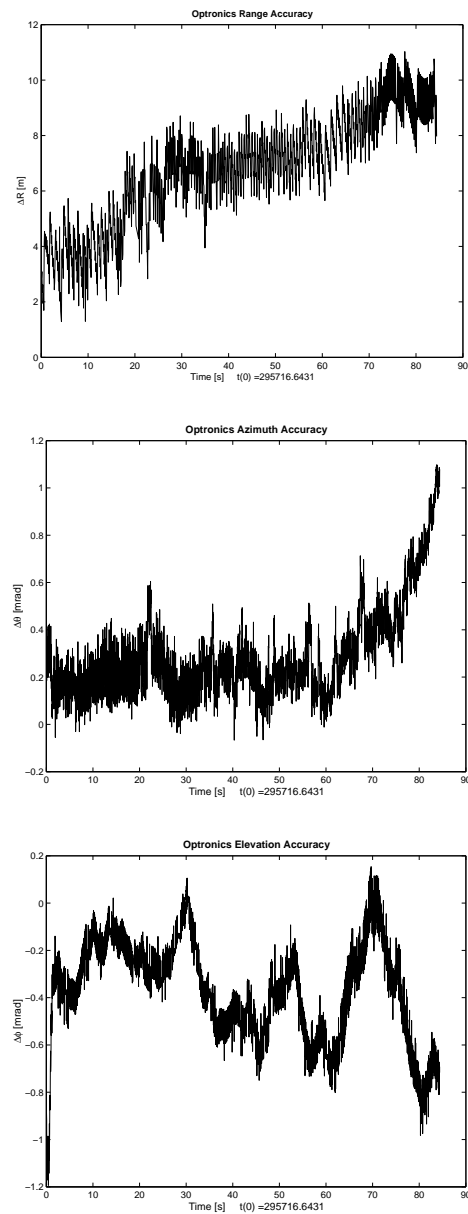


Figure A.8: Optronics Segment 1: Difference between optronics data and GPS-derived data for range, azimuth and elevation measurements (no latency compensation).

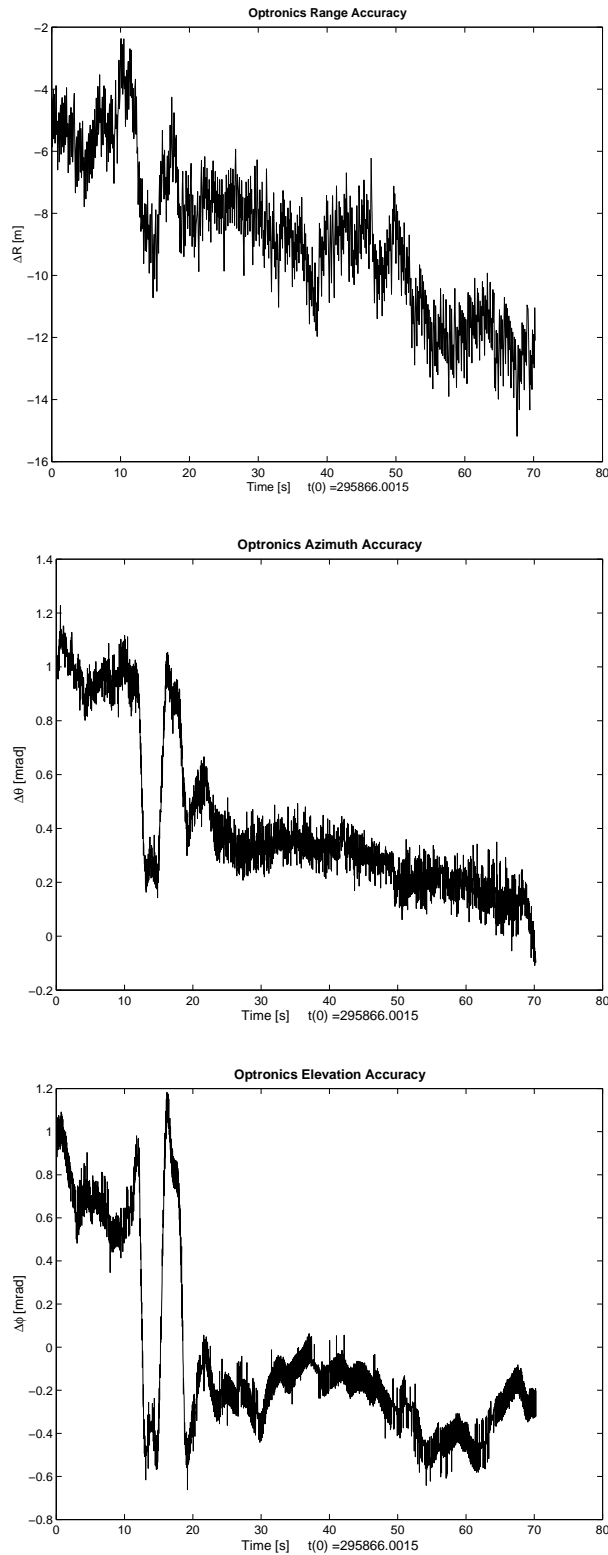


Figure A.9: Optronics Segment 2: Difference between optronics data and GPS-derived data for range, azimuth and elevation measurements (no latency compensation).

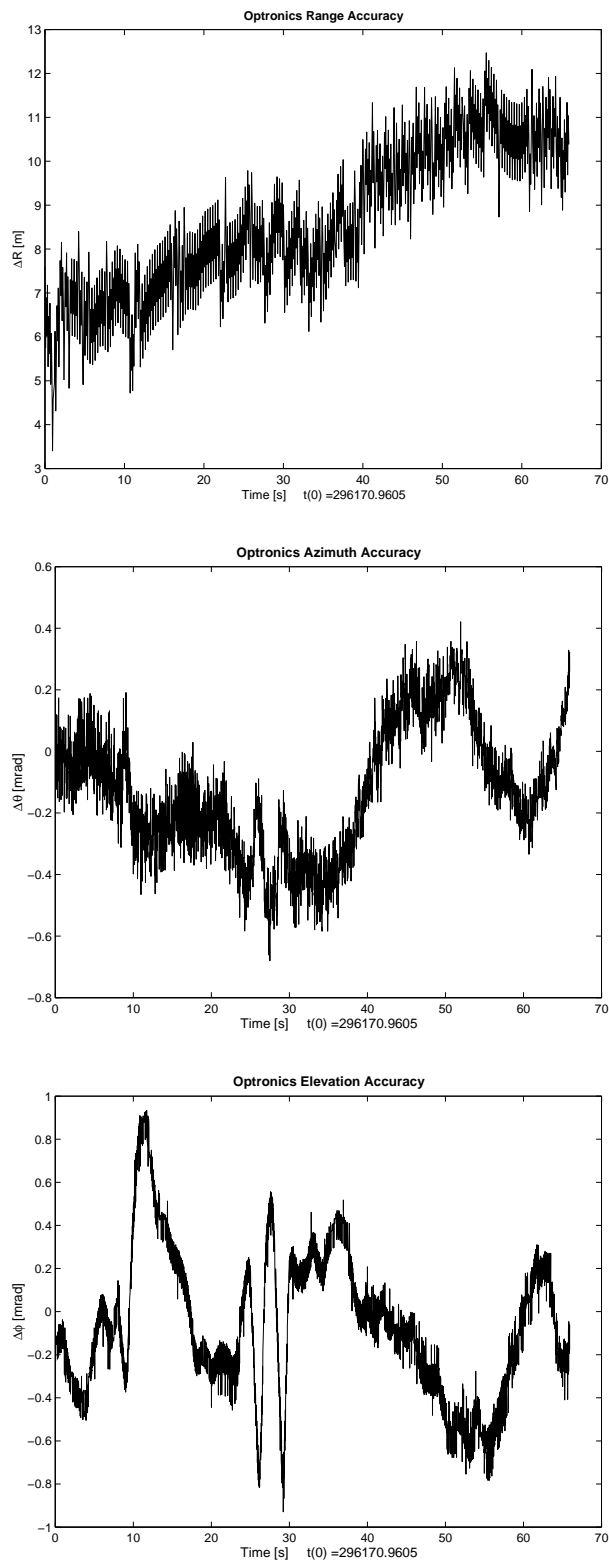


Figure A.10: Optronics Segment 3: Difference between optronics data and GPS-derived data for range, azimuth and elevation measurements (no latency compensation).

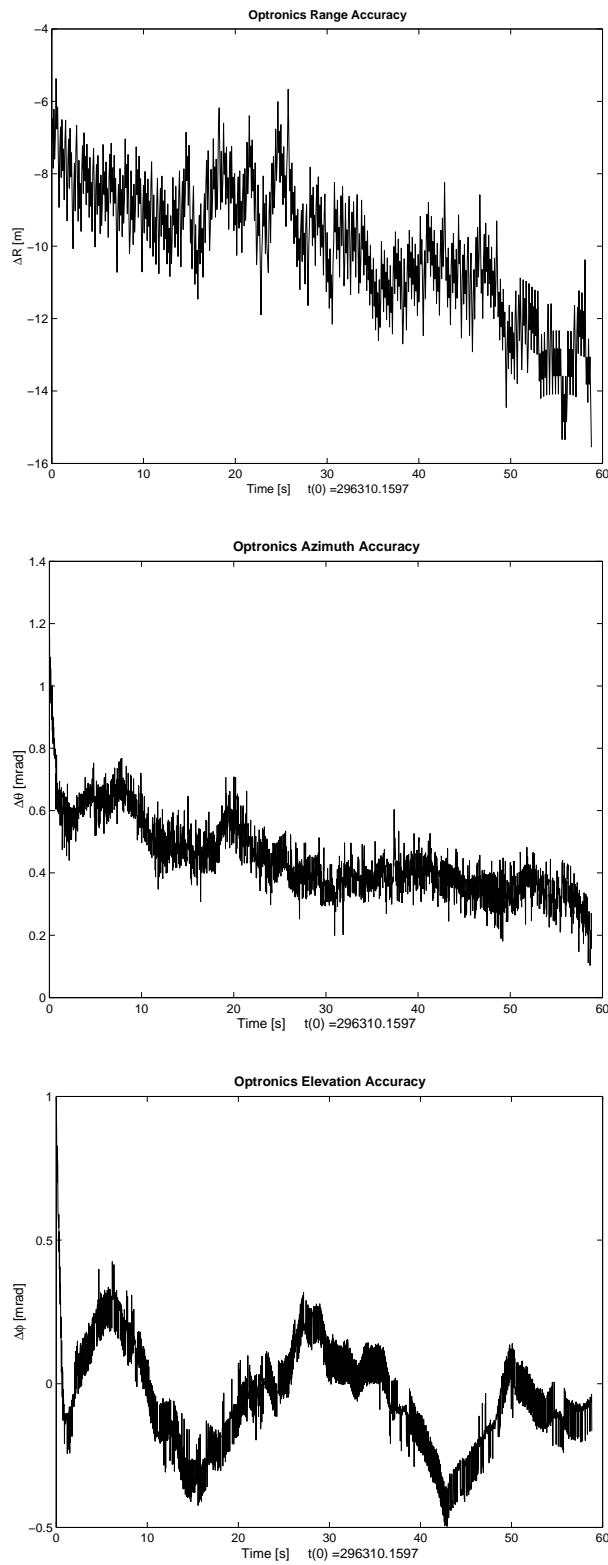


Figure A.11: Optronics Segment 4: Difference between optronics data and GPS-derived data for range, azimuth and elevation measurements (no latency compensation).

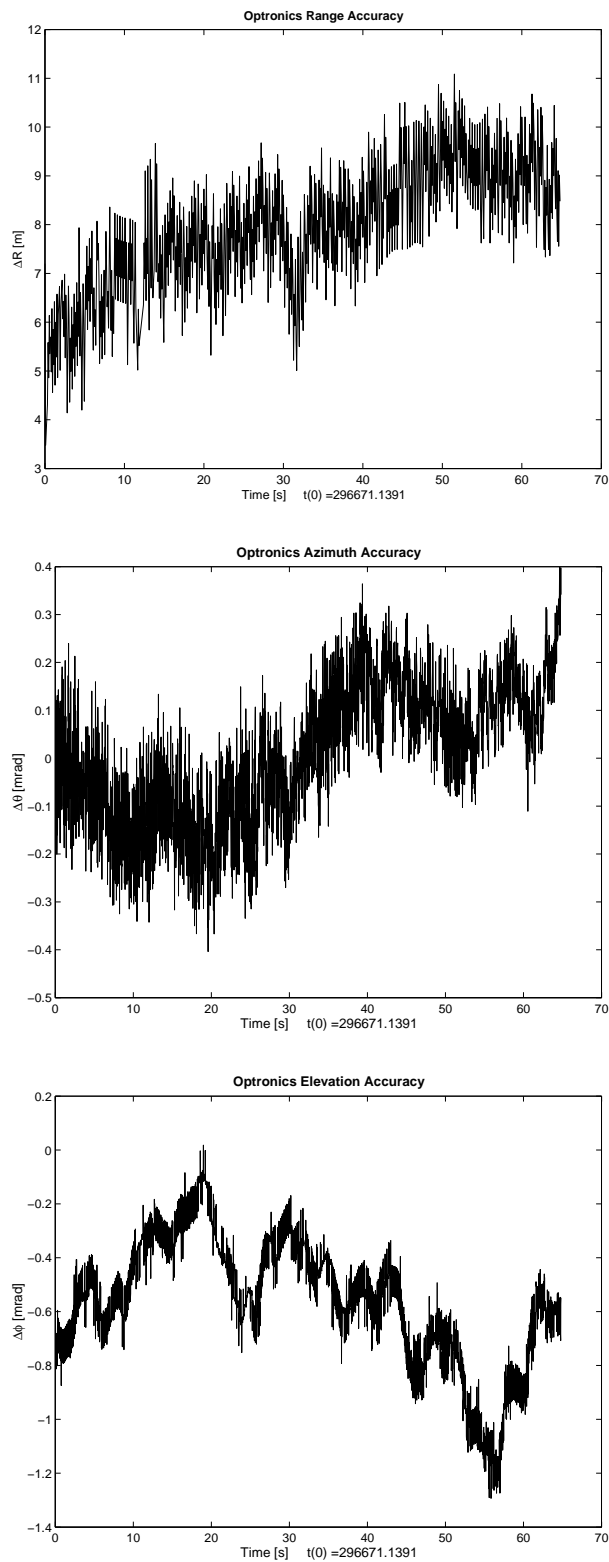


Figure A.12: Optronics Segment 5: Difference between optronics data and GPS-derived data for range, azimuth and elevation measurements (no latency compensation).

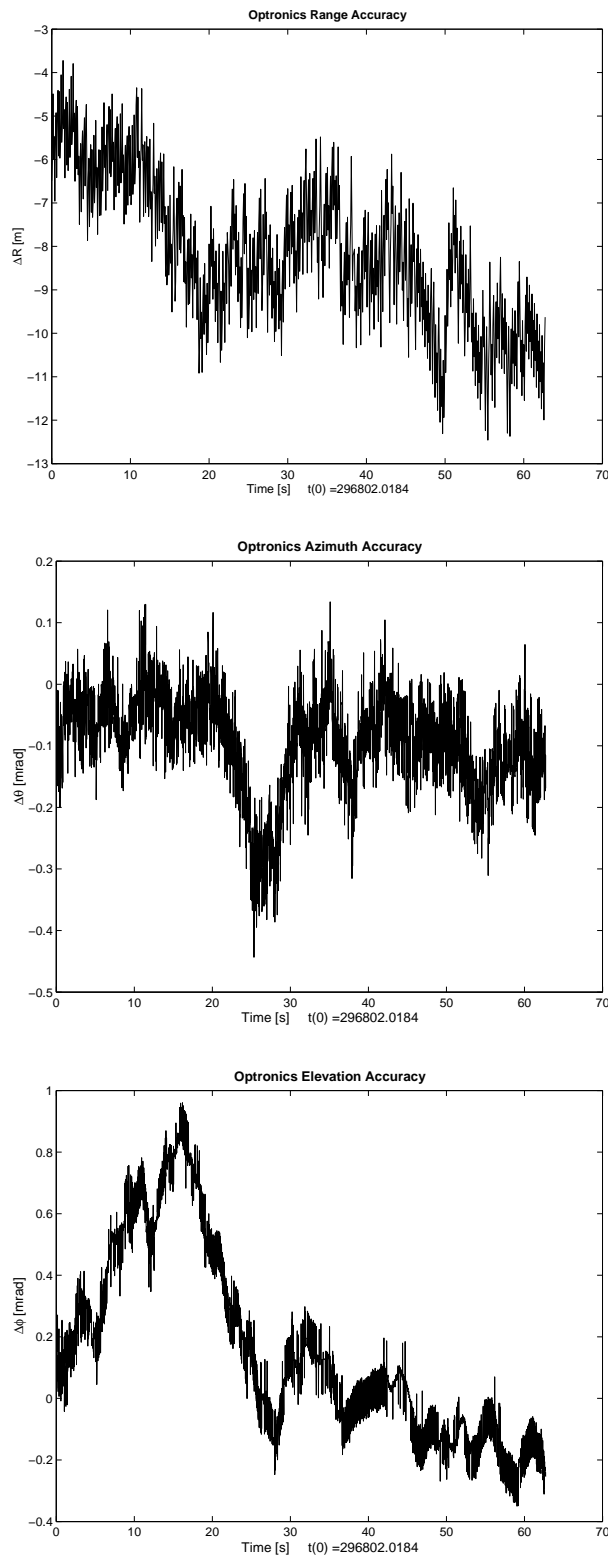


Figure A.13: Optronics Segment 6: Difference between optronics data and GPS-derived data for range, azimuth and elevation measurements (no latency compensation).

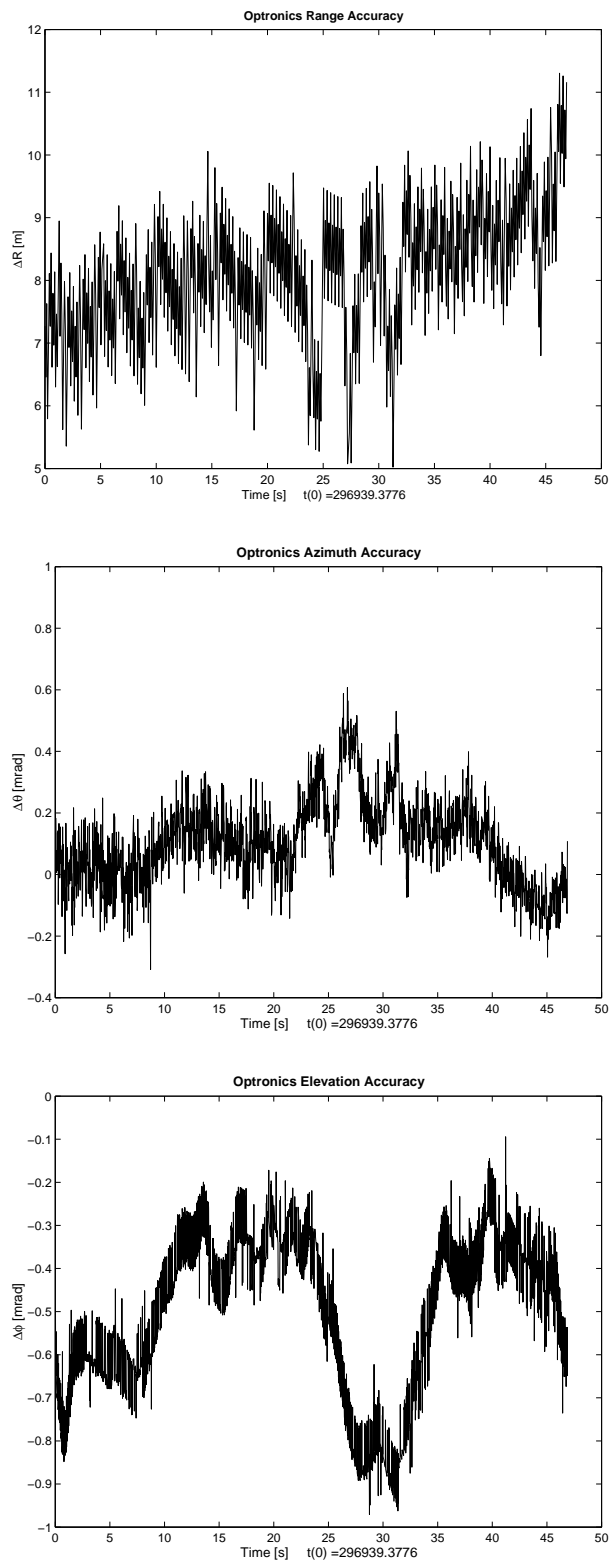


Figure A.14: Optronics Segment 7: Difference between optronics data and GPS-derived data for range, azimuth and elevation measurements (no latency compensation).

A.3 Results for ITB FAT - TAMS using LL data

Refer to Chapter 6.1.3.

A.3.1 Optronics tracking accuracies for optronics data latency compensation of 0 ms

Table A.1: Accuracy of azimuth data, optronics time delay = 0 ms.

<i>Segment</i>	<i>min</i> [mrad]	<i>max</i> [mrad]	<i>mean</i> [mrad]	<i>std</i> [mrad]	<i>RMS</i> [mrad]	<i>Invalid Data</i> [%]
1 (inbound)	-0.067	1.098	0.291	0.193	0.349	0.427
2 (outbound)	-0.109	1.228	0.428	0.298	0.521	0.00
3 (inbound)	-0.680	0.421	-0.128	0.210	0.246	0.882
4 (outbound)	0.103	1.156	0.446	0.125	0.463	0.00
5 (inbound)	-0.404	0.398	0.012	0.0142	0.143	0.464
6 (outbound)	-0.443	0.134	-0.095	0.082	0.125	0.00
7 (inbound)	-0.308	0.607	0.110	0.137	0.176	0.299

Table A.2: Accuracy of elevation data, optronics time delay = 0 ms.

<i>Segment</i>	<i>min</i> [mrad]	<i>max</i> [mrad]	<i>mean</i> [mrad]	<i>std</i> [mrad]	<i>RMS</i> [mrad]	<i>Invalid Data</i> [%]
1 (inbound)	-1.194	0.154	-0.373	0.214	0.430	0.427
2 (outbound)	-0.662	1.183	-0.040	0.430	0.432	0.00
3 (inbound)	-0.929	0.934	-0.067	0.337	0.344	0.882
4 (outbound)	-0.496	0.924	-0.050	0.184	0.191	0.00
5 (inbound)	-1.293	0.018	-0.565	0.239	0.614	0.464
6 (outbound)	-0.350	0.960	0.158	0.306	0.344	0.00
7 (inbound)	-0.971	-0.094	-0.499	0.182	0.531	0.299

Table A.3: Accuracy of range data, optronics time delay = 0 ms.

<i>Segment</i>	<i>min</i> [m]	<i>max</i> [m]	<i>mean</i> [m]	<i>std</i> [m]	<i>RMS</i> [m]	<i>Invalid Data</i> [%]
1 (inbound)	1.298	11.026	6.779	2.034	7.077	0.427
2 (outbound)	-15.182	-2.369	-8.755	2.252	9.112	0.00
3 (inbound)	3.405	12.470	8.618	1.733	8.790	0.882
4 (outbound)	-15.552	-5.373	-9.999	1.851	10.169	0.00
5 (inbound)	3.477	11.087	7.935	1.344	8.048	0.464
6 (outbound)	-12.459	-3.723	-8.149	1.740	8.332	0.00
7 (inbound)	5.022	11.303	8.110	1.104	8.184	0.299

Table A.4: Accuracies over all inbound flights, optronics time delay = 0 ms.

<i>Measurement</i>	<i>min</i> [mrad, m]	<i>max</i> [mrad, m]	<i>mean</i> [mrad, m]	<i>std</i> [mrad, m]	<i>RMS</i> [mrad, m]
Azimuth	-0.680	1.098	0.084	0.241	0.255
Elevation	-1.293	0.934	-0.366	0.314	0.483
Range	1.289	12.470	7.767	1.810	7.975

Table A.5: Accuracies over all outbound flights, optronics time delay = 0 ms.

<i>Measurement</i>	<i>min</i> [mrad, m]	<i>max</i> [mrad, m]	<i>mean</i> [mrad, m]	<i>std</i> [mrad, m]	<i>RMS</i> [mrad, m]
Azimuth	-0.443	1.228	0.263	0.319	0.413
Elevation	-0.662	1.183	0.022	0.343	0.344
Range	-15.552	-2.369	-8.939	2.221	9.211

A.3.2 Optronics tracking accuracies for optronics angle and range data latency compensation, of -230 and -240 ms respectively

These are shown in Tables A.6 to A.10.

Table A.6: Accuracy of azimuth data, optronics angle time delay = -230 ms, optronics range time delay = -240 ms.

<i>Segment</i>	<i>min</i> [mrad]	<i>max</i> [mrad]	<i>mean</i> [mrad]	<i>std</i> [mrad]	<i>RMS</i> [mrad]	<i>Invalid Data</i> [%]
1 (inbound)	-0.142	0.634	0.235	0.110	0.259	0.427
2 (outbound)	-0.057	1.092	0.293	0.251	0.386	0.00
3 (inbound)	-0.382	0.573	0.097	0.157	0.184	0.882
4 (outbound)	0.079	0.836	0.323	0.094	0.337	0.00
5 (inbound)	-0.167	0.519	0.193	0.106	0.220	0.464
6 (outbound)	-0.113	0.644	0.203	0.126	0.239	0.00
7 (inbound)	-0.148	0.687	0.268	0.122	0.294	0.299

Table A.7: Accuracy of elevation data, optronics angle time delay = -230 ms, optronics range time delay = -240 ms.

<i>Segment</i>	<i>min</i> [mrad]	<i>max</i> [mrad]	<i>mean</i> [mrad]	<i>std</i> [mrad]	<i>RMS</i> [mrad]	<i>Invalid Data</i> [%]
1 (inbound)	-1.162	0.369	-0.108	0.16	0.198	0.427
2 (outbound)	-1.197	0.692	-0.372	0.337	0.502	0.00
3 (inbound)	-0.622	1.138	0.252	0.321	0.408	0.882
4 (outbound)	-0.719	0.204	-0.342	0.144	0.371	0.00
5 (inbound)	-0.788	0.166	-0.293	0.180	0.343	0.464
6 (outbound)	-0.521	0.503	-0.137	0.229	0.267	0.00
7 (inbound)	-0.714	0.180	-0.284	0.184	0.339	0.299

Table A.8: Accuracy of range data, optronics angle time delay = -230 ms, optronics range time delay = -240 ms.

<i>Segment</i>	<i>min</i> [m]	<i>max</i> [m]	<i>mean</i> [m]	<i>std</i> [m]	<i>RMS</i> [m]	<i>Invalid Data</i> [%]
1 (inbound)	-6.814	1.805	-2.006	1.735	2.651	0.427
2 (outbound)	-3.288	7.836	2.502	2.067	3.245	0.00
3 (inbound)	-8.063	1.087	-2.621	1.707	3.127	0.882
4 (outbound)	-4.290	5.453	0.980	1.756	2.010	0.00
5 (inbound)	-7.694	-0.101	-3.112	1.354	3.393	0.464
6 (outbound)	-1.362	6.576	2.858	1.524	3.000	0.00
7 (inbound)	-6.165	0.027	-3.123	1.173	3.335	0.299

Table A.9: Accuracies over all inbound flights, optronics angle time delay = -230 ms, optronics range time delay = -240 ms.

<i>Measurement</i>	<i>min</i> [mrad, m]	<i>max</i> [mrad, m]	<i>mean</i> [mrad, m]	<i>std</i> [mrad, m]	<i>RMS</i> [mrad, m]
Azimuth	-0.382	0.687	0.196	0.139	0.240
Elevation	-1.162	1.138	-0.095	0.308	0.323
Range	-8.063	1.805	-2.634	1.620	3.092

Table A.10: Accuracies over all outbound flights, optronics angle time delay = -230 ms, optronics range time delay = -240 ms.

<i>Measurement</i>	<i>min</i> [mrad, m]	<i>max</i> [mrad, m]	<i>mean</i> [mrad, m]	<i>std</i> [mrad, m]	<i>RMS</i> [mrad, m]
Azimuth	-0.113	1.092	0.273	0.183	0.328
Elevation	-1.197	0.692	-0.286	0.276	0.397
Range	-4.290	7.836	2.062	1.946	2.835

Appendix B

Radar Appendices

B.1 Overview of Radar Data

This appendix presents plots of the radar range, elevation and azimuth data for each of the analysed segments. The segments analysed are listed in Chapter 6.2.1. The dGPS-derived range data is also plotted for comparison. These plots give an overview of the quality of the data. It can be seen that the radar data contains many gaps, which makes the tracking accuracy analysis task more difficult. The GPS data also contains gaps.

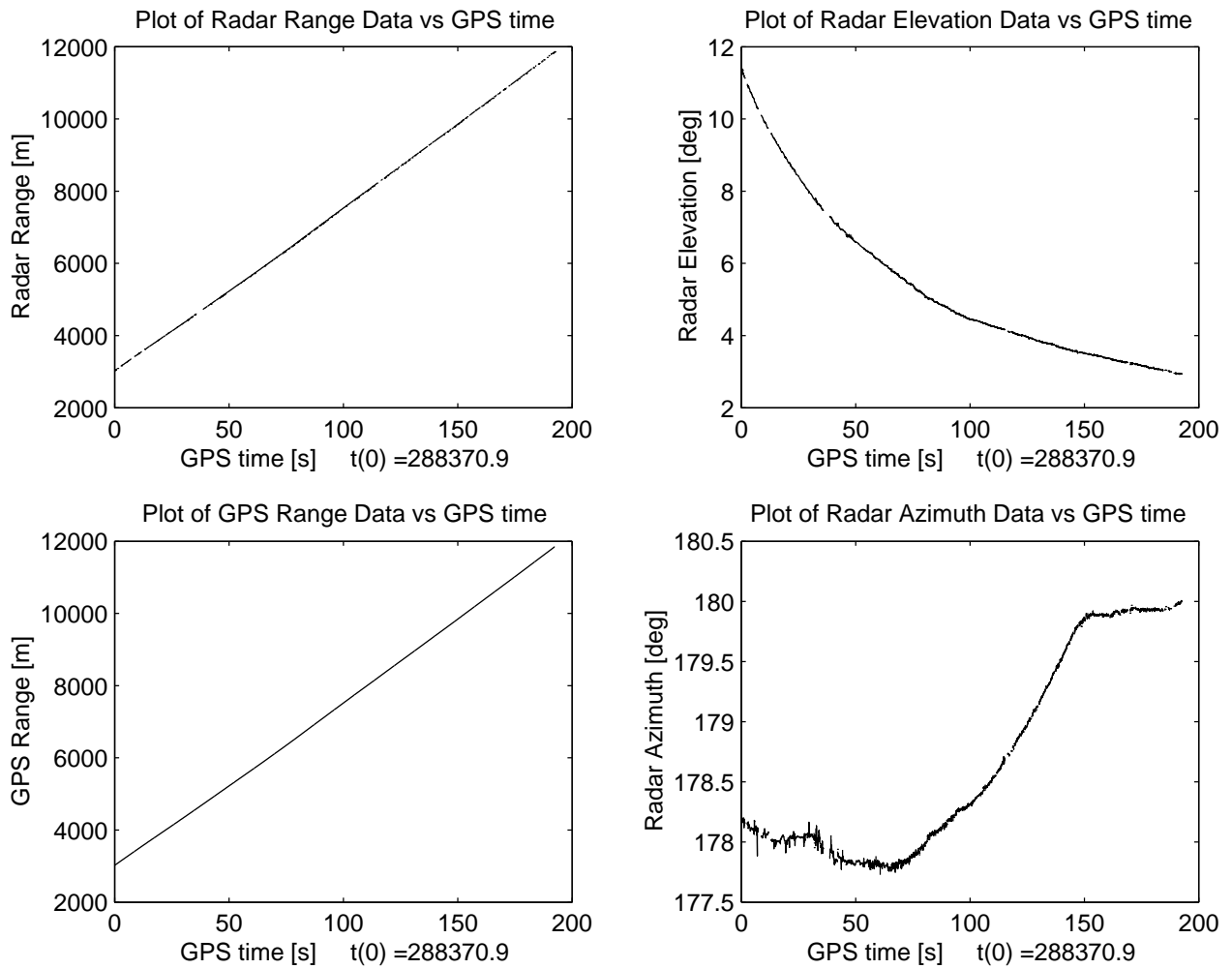


Figure B.1: Radar Segment 1 (ITB_FAT_WPN_Wed_10_07_23): Plots of radar range, elevation and azimuth data. The GPS-derived range data is also shown for comparison.

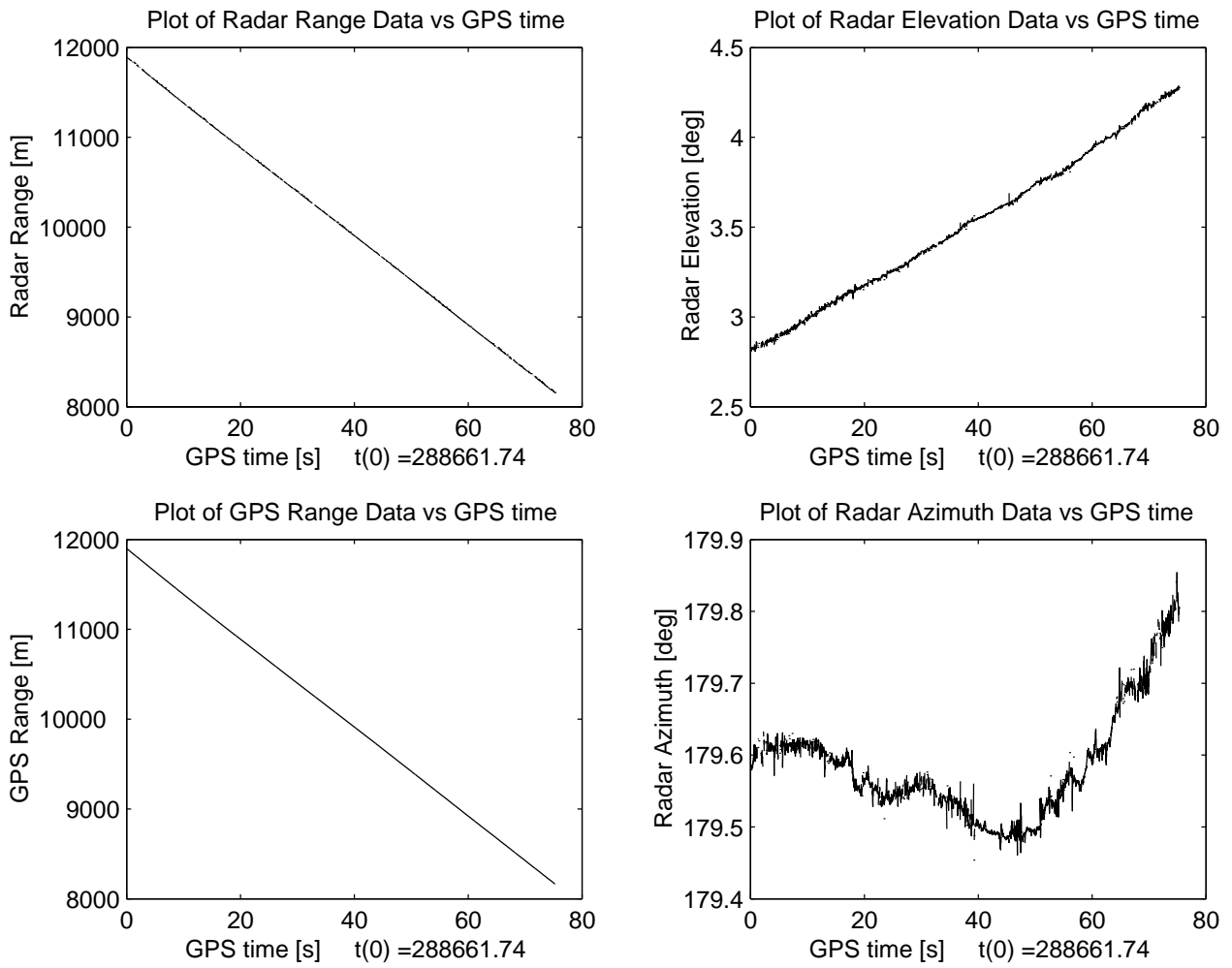


Figure B.2: Radar Segment 2 (ITB_FAT_WPN_Wed_10_11_13): Plots of radar range, elevation and azimuth data. The GPS-derived range data is also shown for comparison.

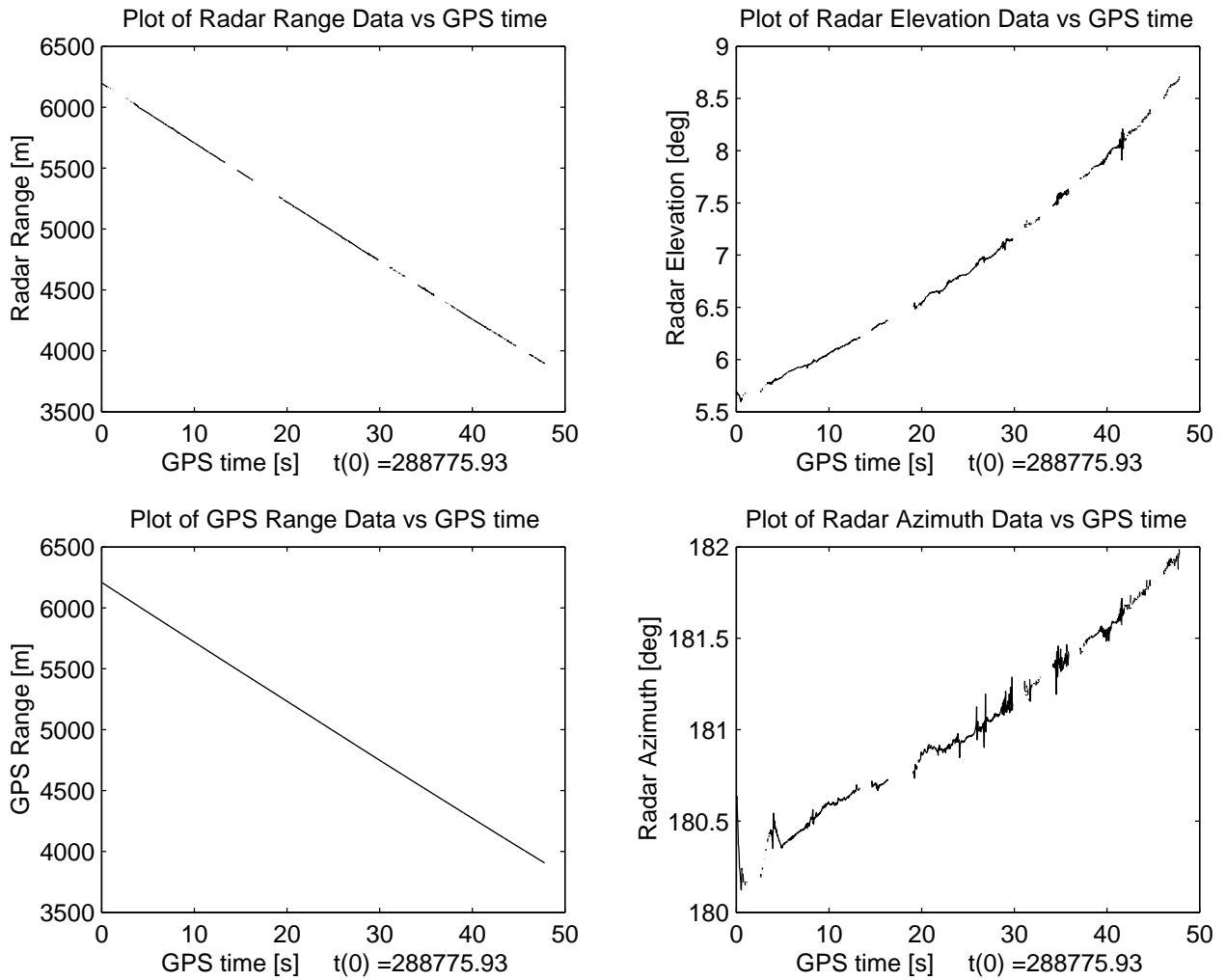


Figure B.3: Radar Segment 3 (ITB_FAT_WPN_Wed_10_11_13): Plots of radar range, elevation and azimuth data. The GPS-derived range data is also shown for comparison.

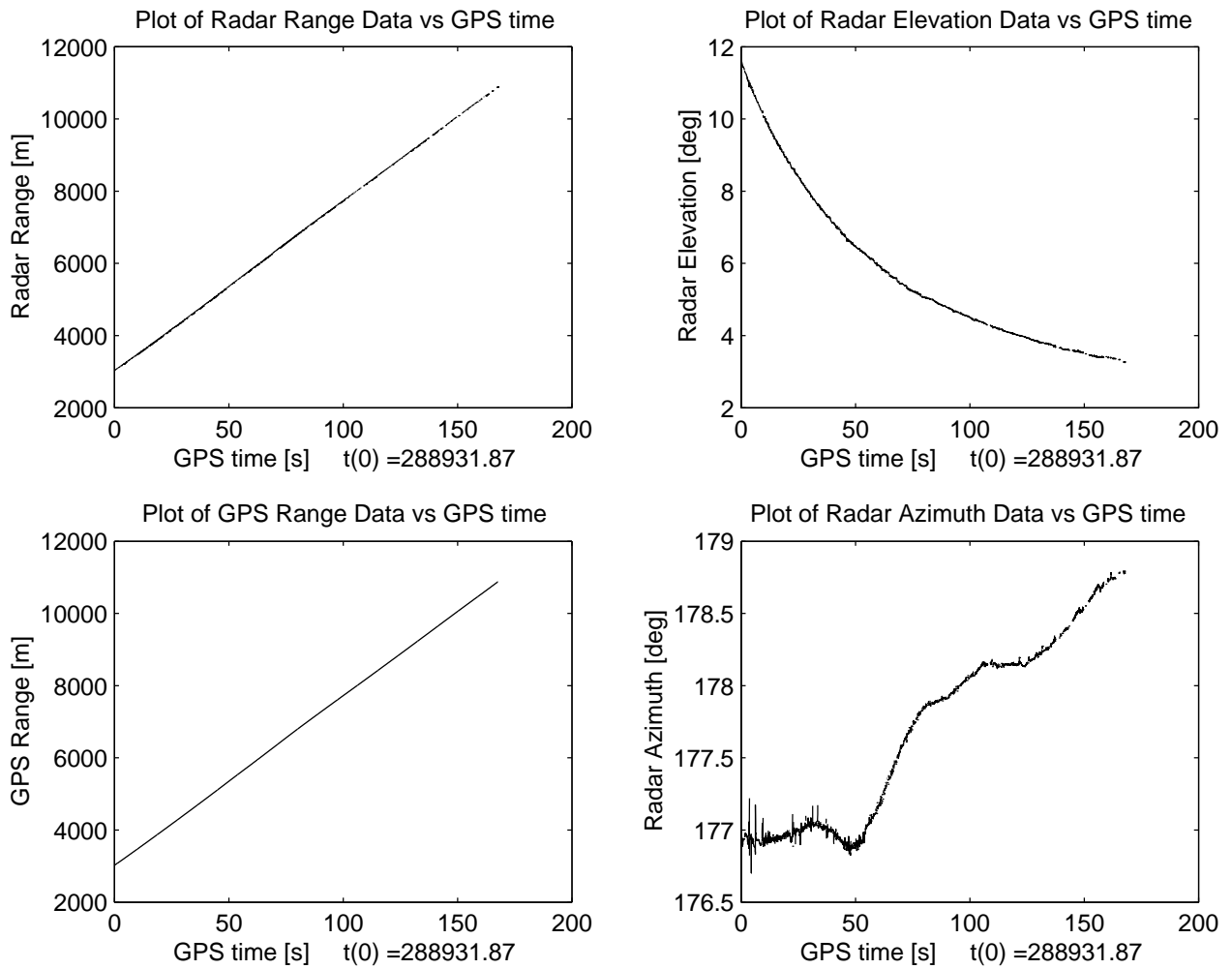


Figure B.4: Radar Segment 4 (ITB_FAT_WPN_Wed_10_15_54): Plots of radar range, elevation and azimuth data. The GPS-derived range data is also shown for comparison.

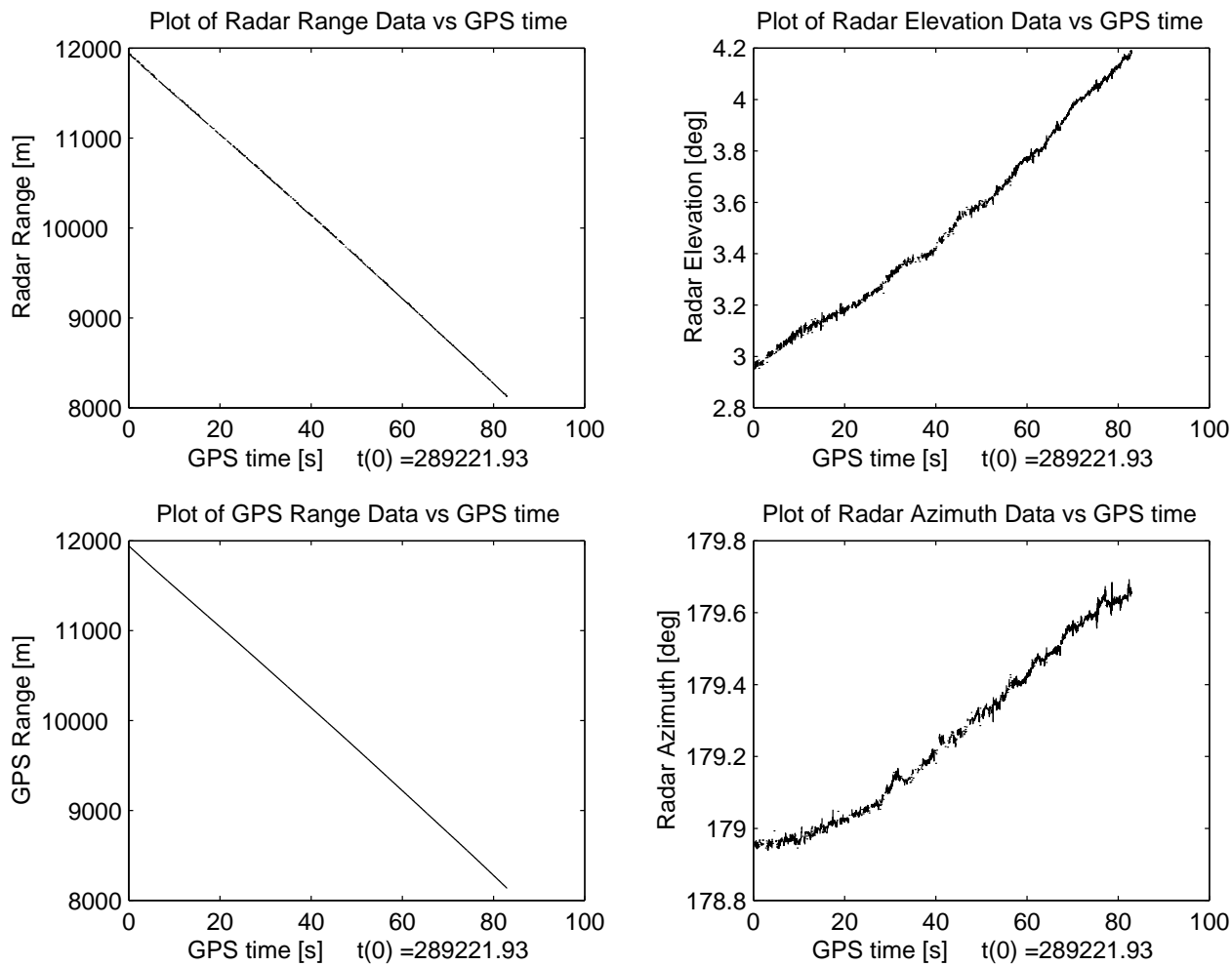


Figure B.5: Radar Segment 5 (ITB_FAT_WPN_Wed_10_19_56): Plots of radar range, elevation and azimuth data. The GPS-derived range data is also shown for comparison.

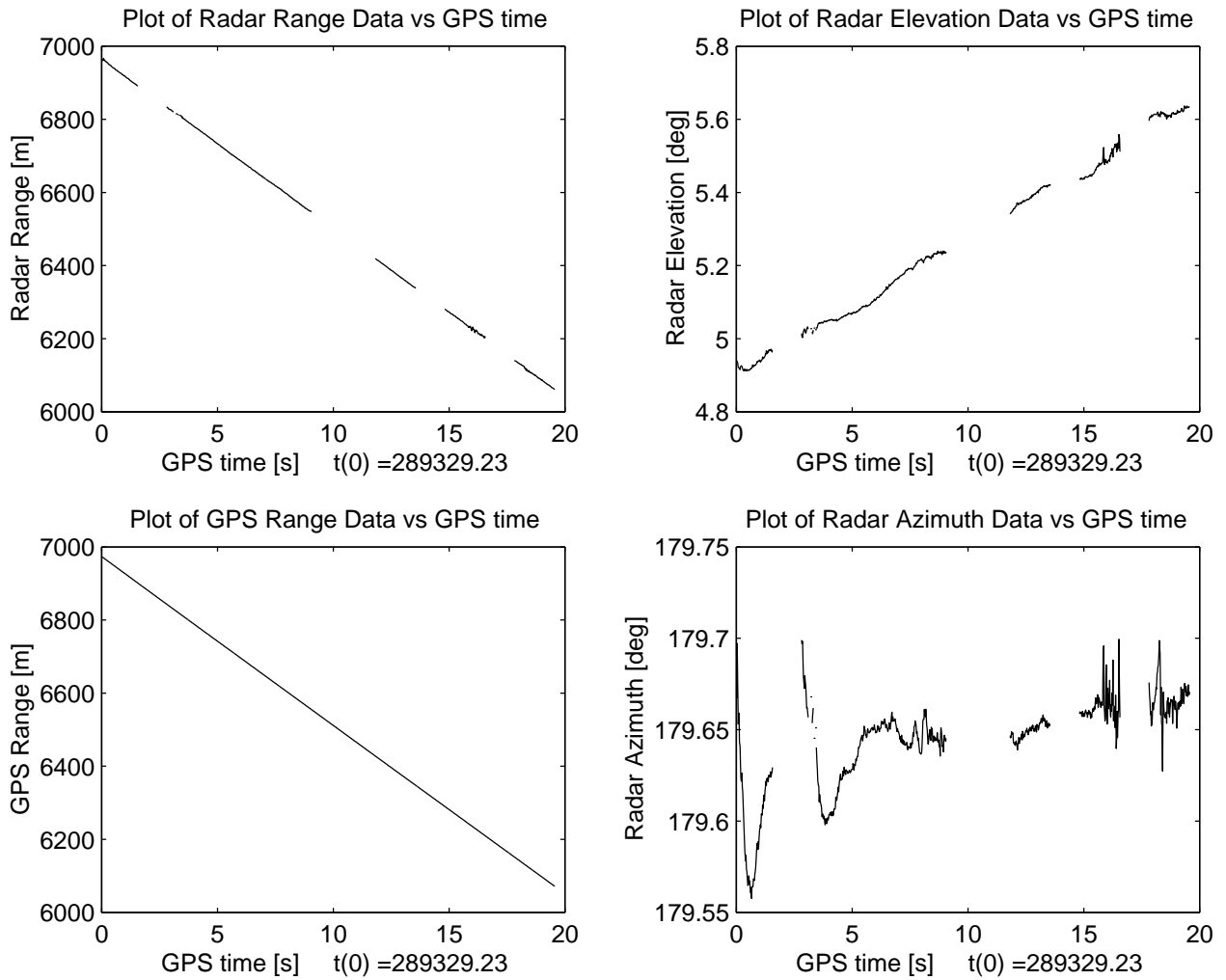


Figure B.6: Radar Segment 6 (ITB_FAT_WPN_Wed_10_19_56): Plots of radar range, elevation and azimuth data. The GPS-derived range data is also shown for comparison.

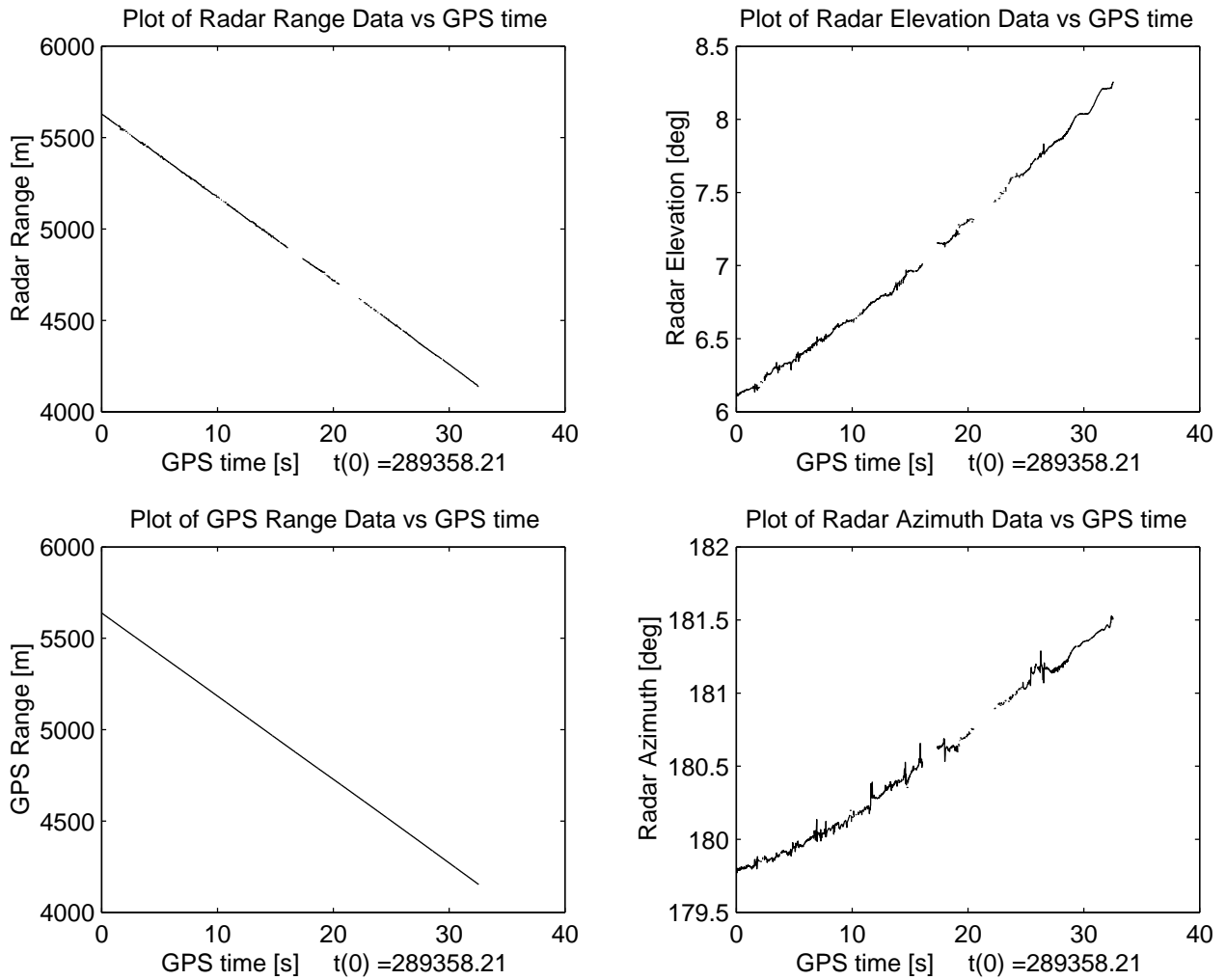


Figure B.7: Radar Segment 7 (ITB_FAT_WPN_Wed_10_19_56): Plots of radar range, elevation and azimuth data. The GPS-derived range data is also shown for comparison.

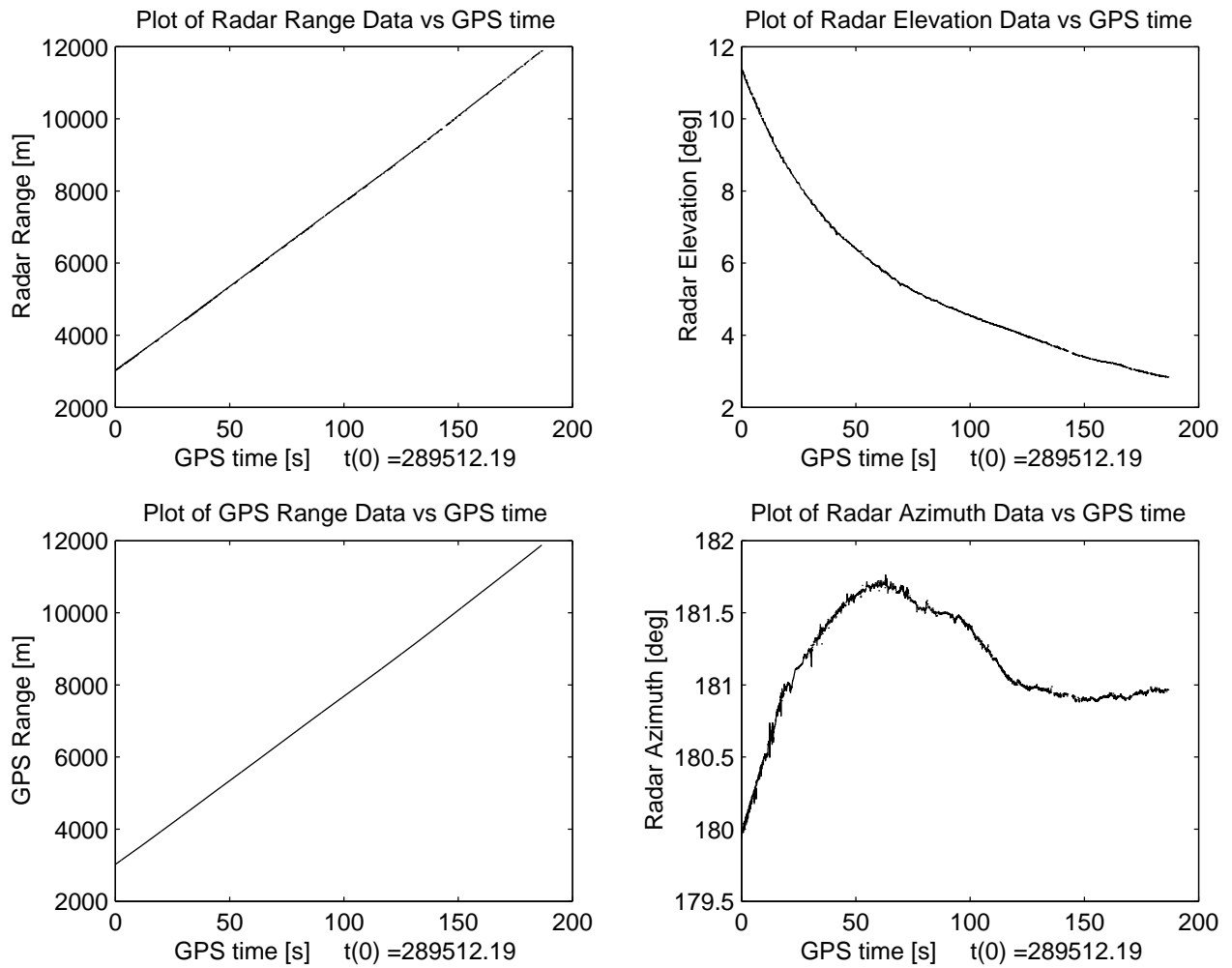


Figure B.8: Radar Segment 8 (ITB_FAT_WPN_Wed_10_25_04): Plots of radar range, elevation and azimuth data. The GPS-derived range data is also shown for comparison.

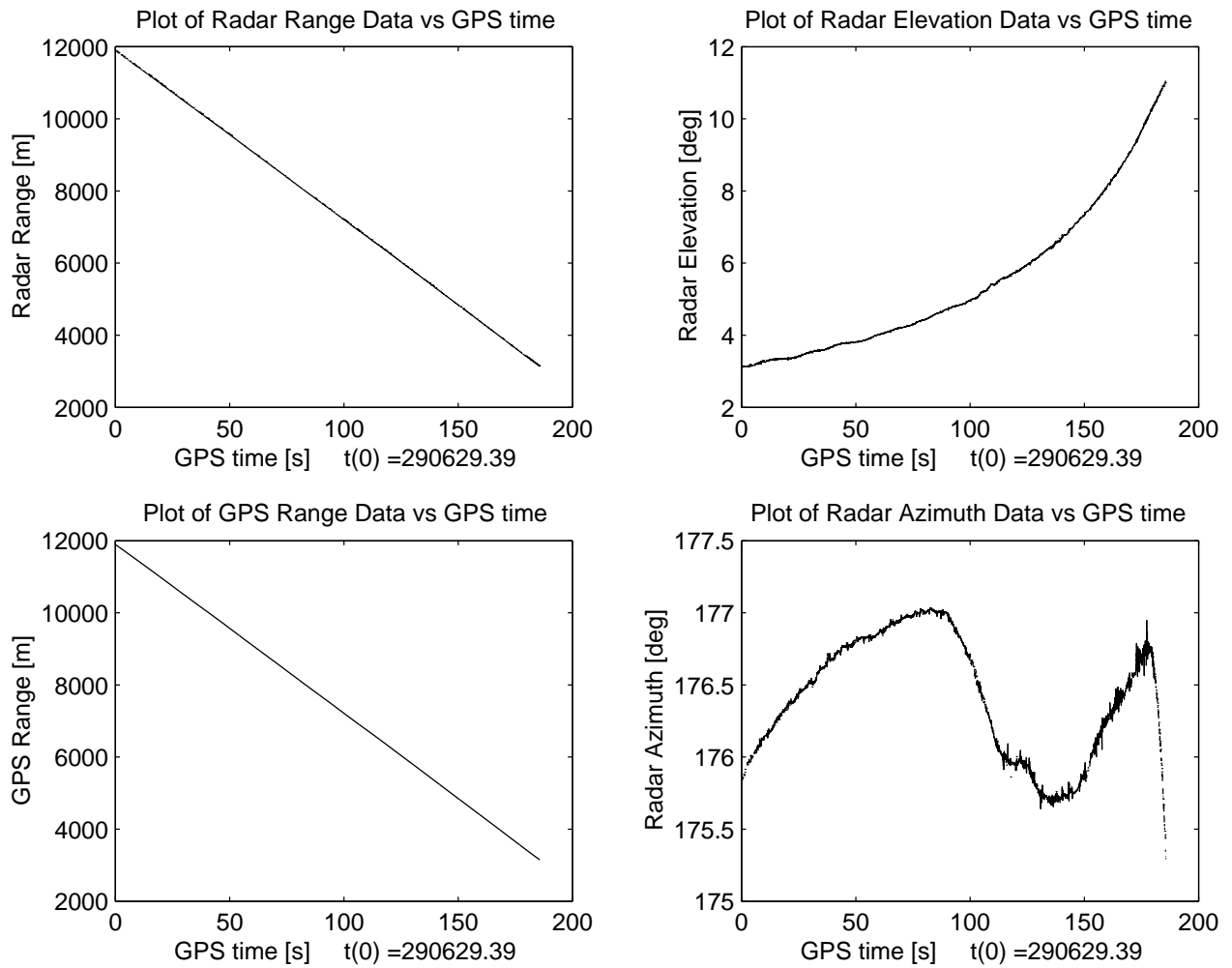


Figure B.9: Radar Segment 10 (ITB_FAT_WPN_Wed_10_43_27): Plots of radar range, elevation and azimuth data. The GPS-derived range data is also shown for comparison.

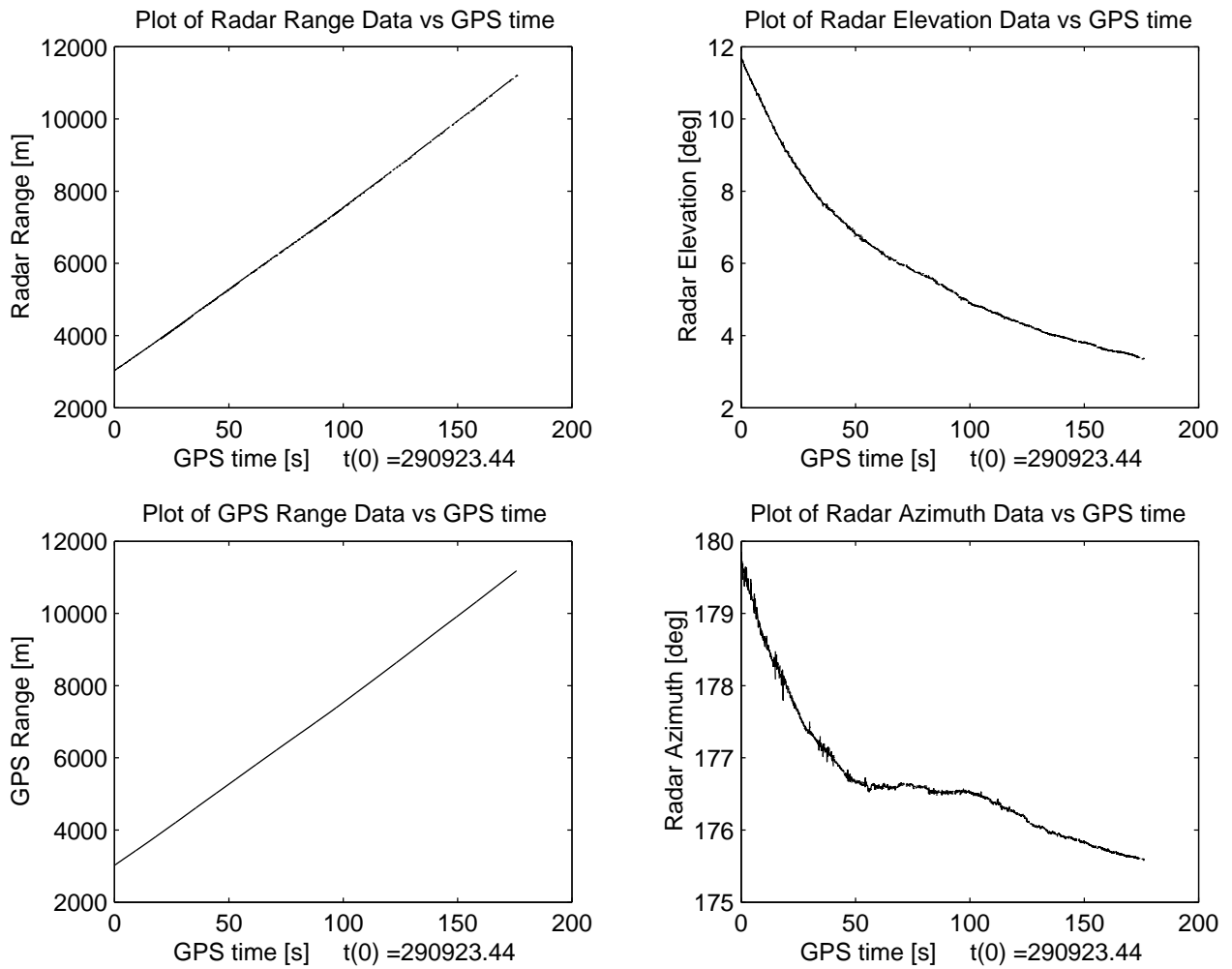


Figure B.10: Radar Segment 11 (ITB_FAT_WPN_Wed_10_48_28): Plots of radar range, elevation and azimuth data. The GPS-derived range data is also shown for comparison.

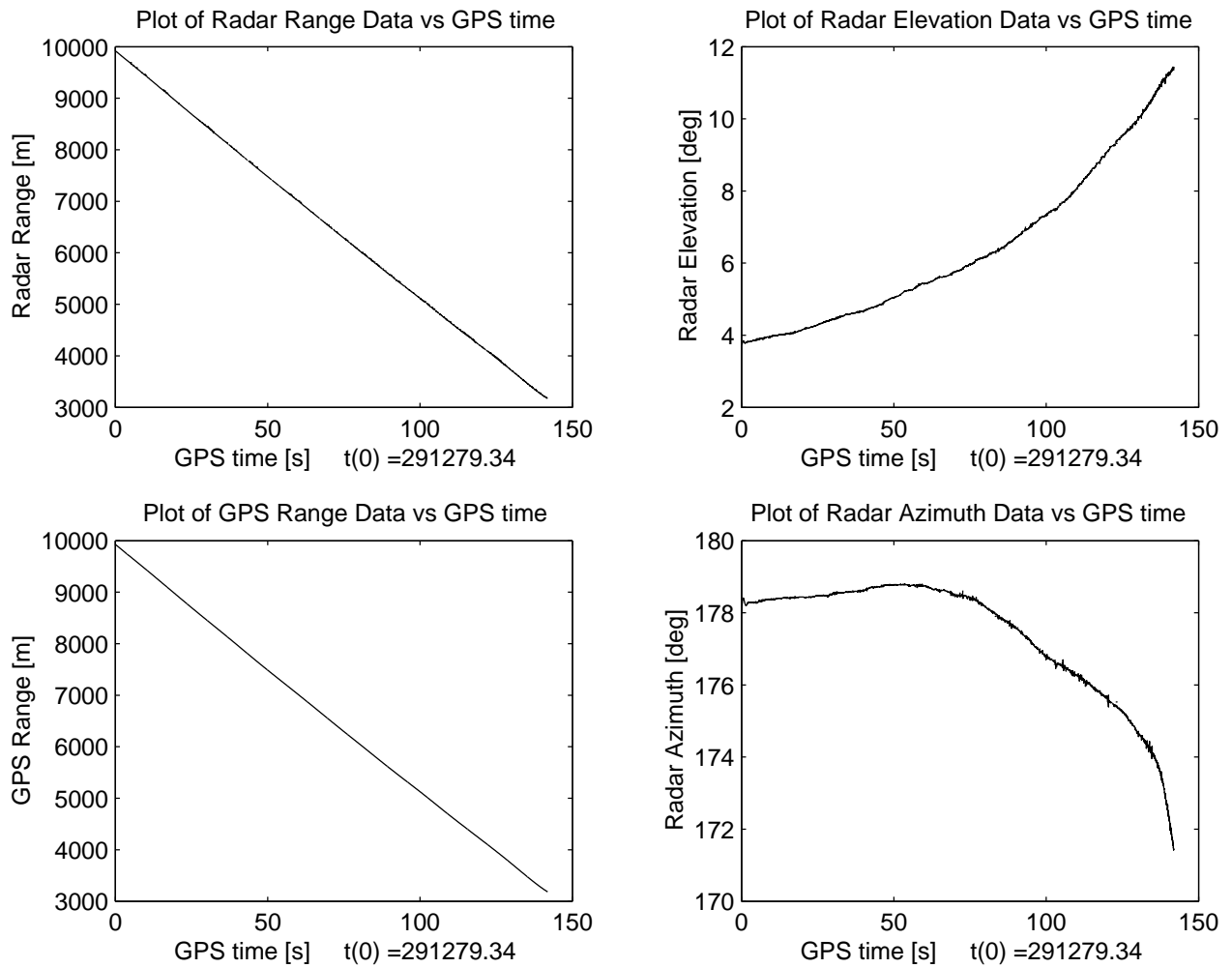


Figure B.11: Radar Segment 12 (ITB_FAT_WPN_Wed_10_53_19): Plots of radar range, elevation and azimuth data. The GPS-derived range data is also shown for comparison.

B.2 Results Overview

This appendix presents difference plots between the radar range, elevation and azimuth data respectively, for each of the analysed segments, with no data latency compensation applied to the data. Refer to Section 6.2.2.

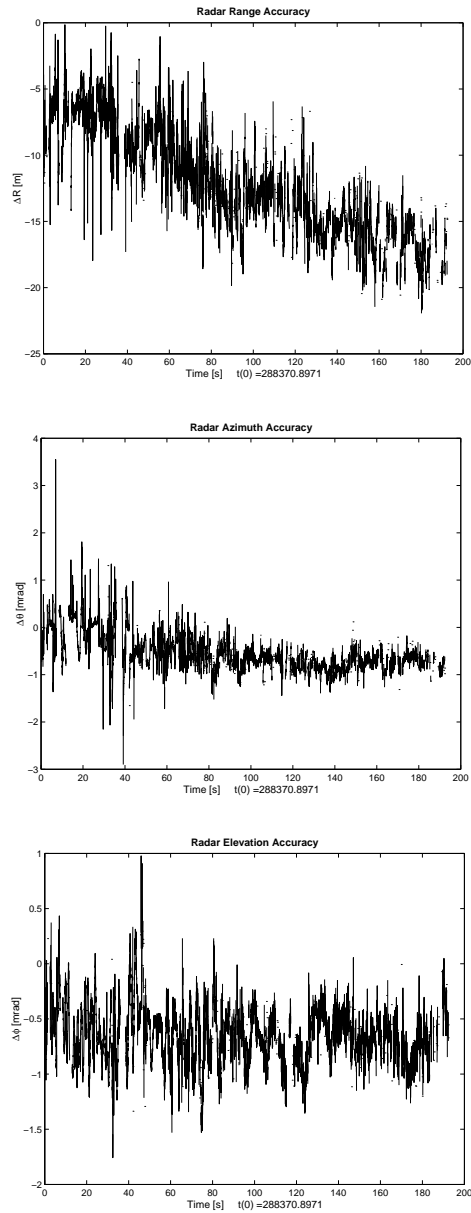


Figure B.12: Radar Segment 1: Difference between radar data and GPS-derived data for range, azimuth and elevation measurements (no latency compensation).

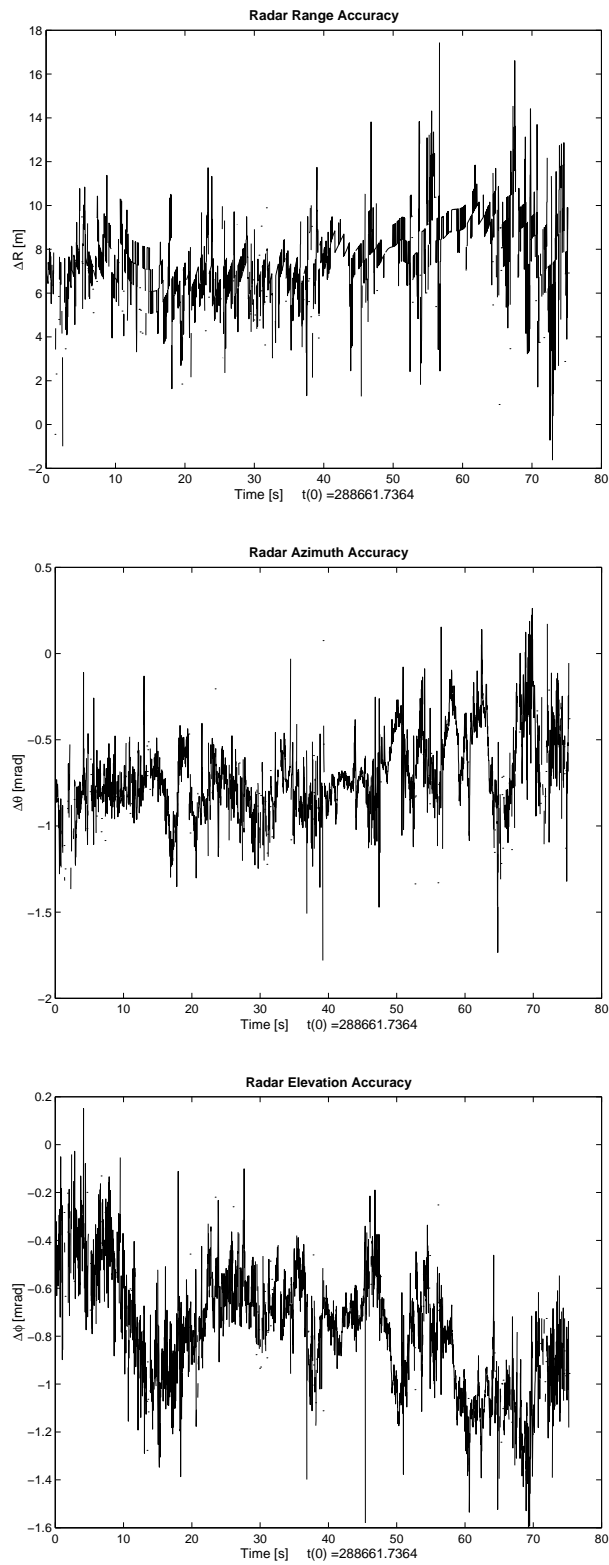


Figure B.13: Radar Segment 2: Difference between radar data and GPS-derived data for range, azimuth and elevation measurements (no latency compensation).

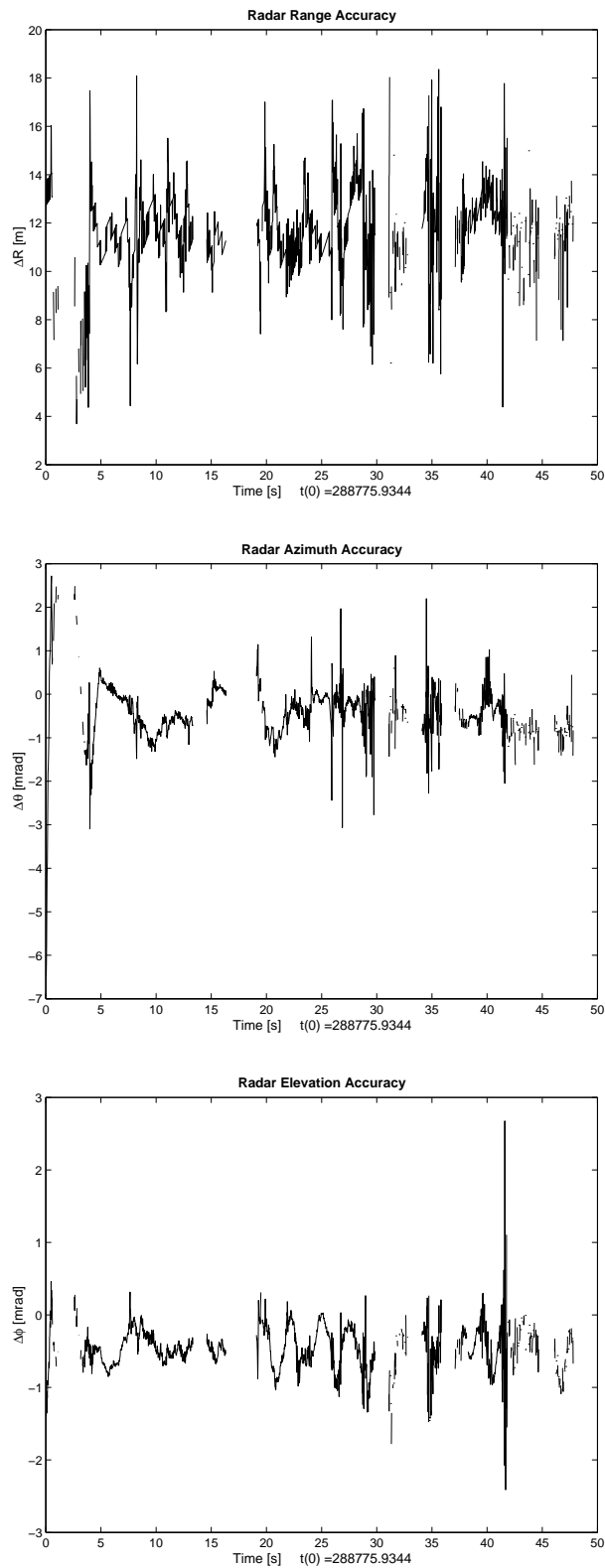


Figure B.14: Radar Segment 3: Difference between radar data and GPS-derived data for range, azimuth and elevation measurements (no latency compensation).

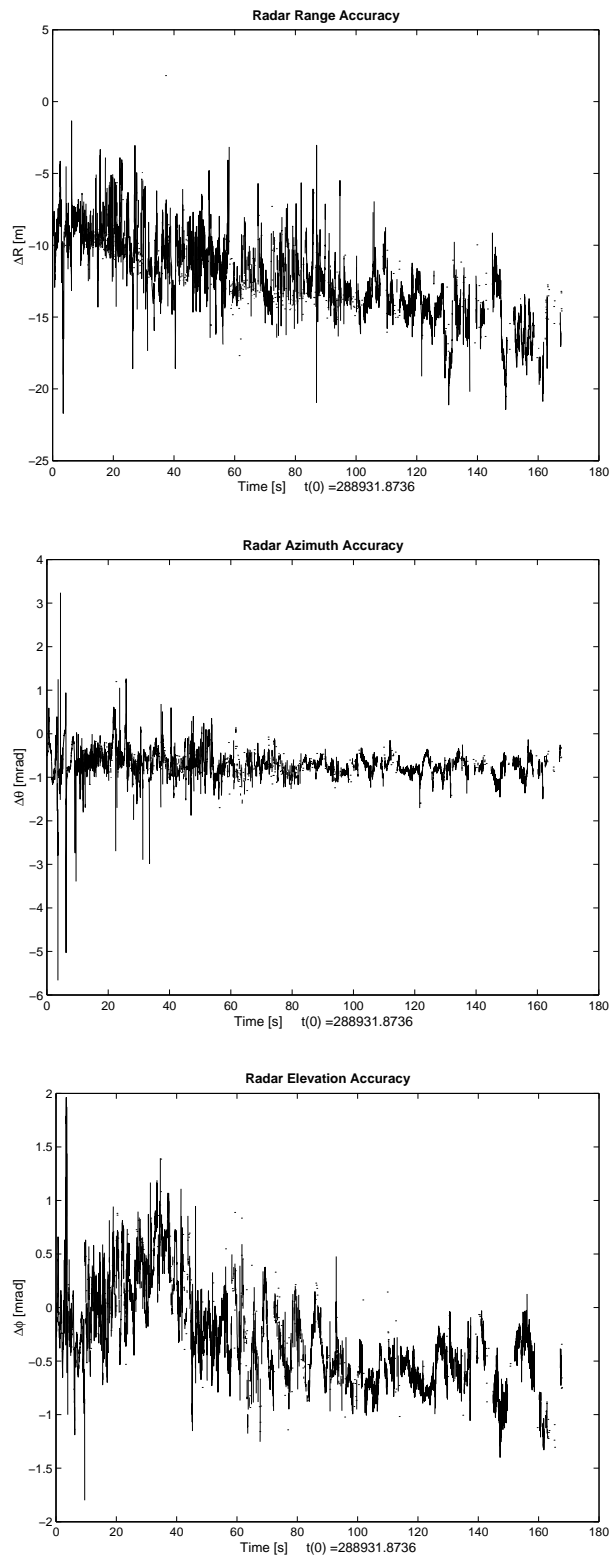


Figure B.15: Radar Segment 4: Difference between radar data and GPS-derived data for range, azimuth and elevation measurements (no latency compensation).

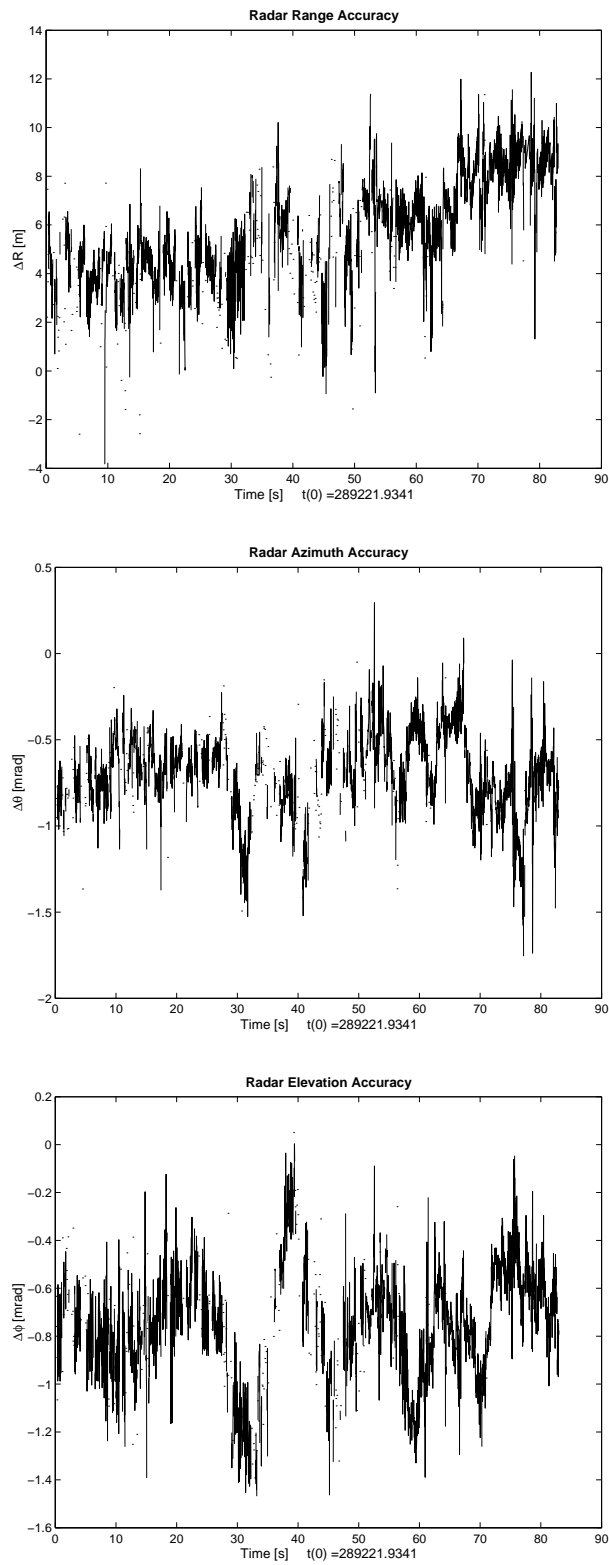


Figure B.16: Radar Segment 5: Difference between radar data and GPS-derived data for range, azimuth and elevation measurements (no latency compensation).

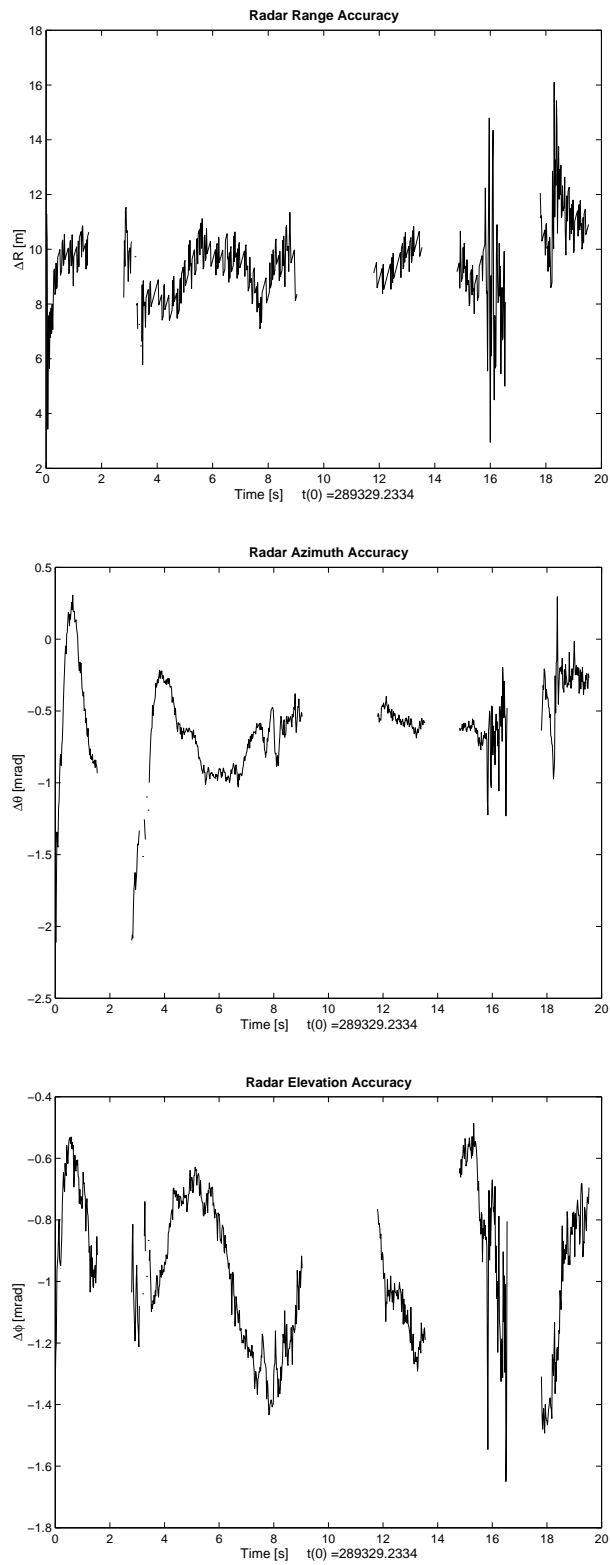


Figure B.17: Radar Segment 6: Difference between radar data and GPS-derived data for range, azimuth and elevation measurements (no latency compensation).

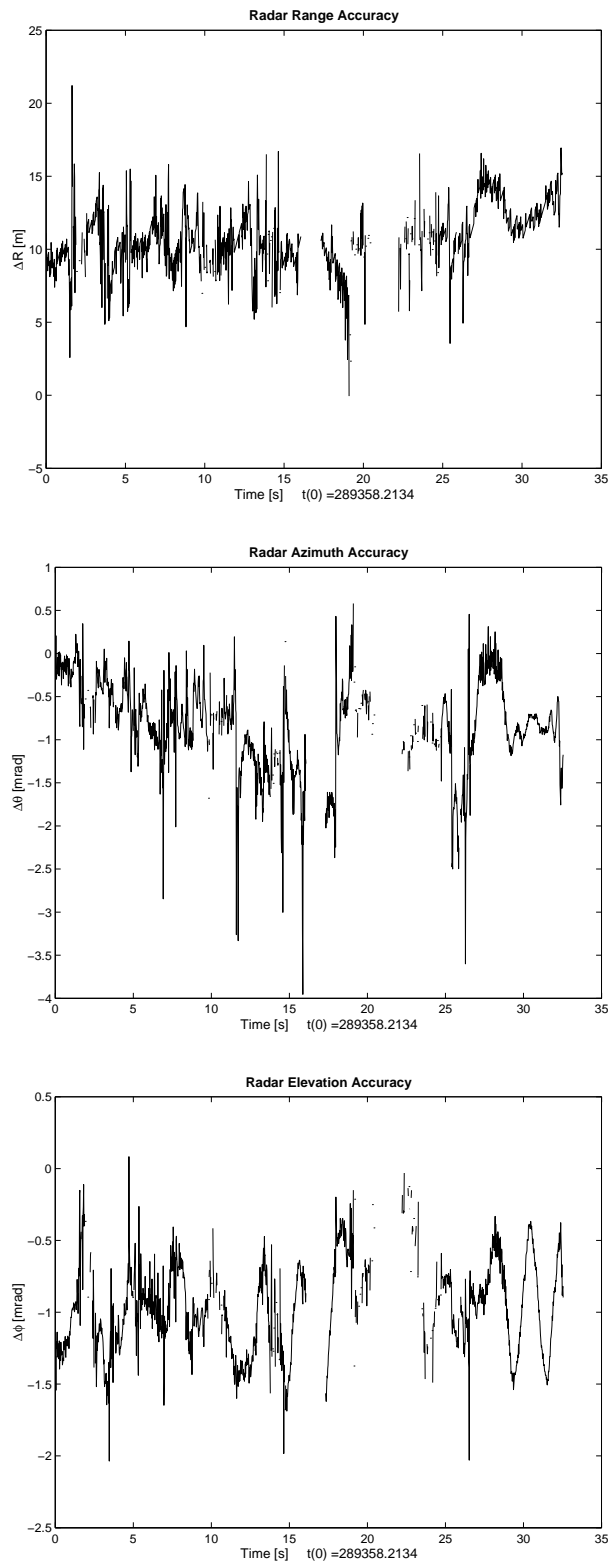


Figure B.18: Radar Segment 7: Difference between radar data and GPS-derived data for range, azimuth and elevation measurements (no latency compensation).

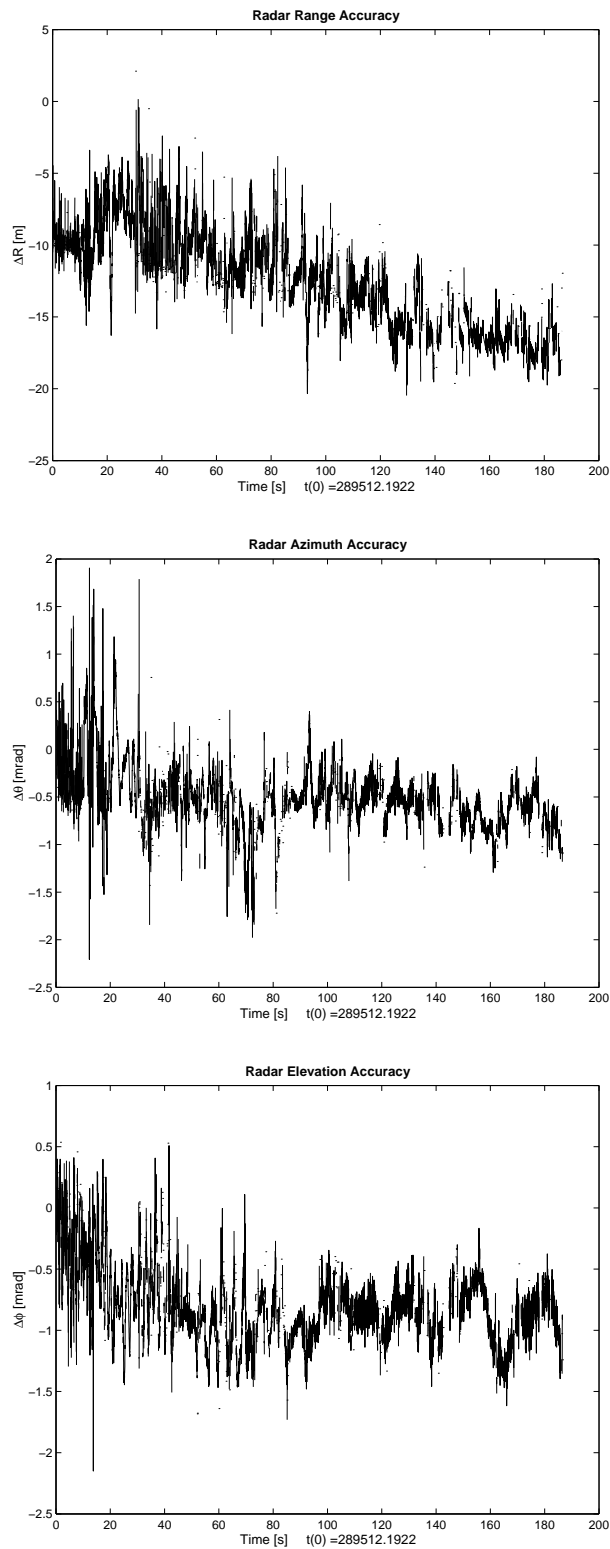


Figure B.19: Radar Segment 8: Difference between radar data and GPS-derived data for range, azimuth and elevation measurements (no latency compensation).

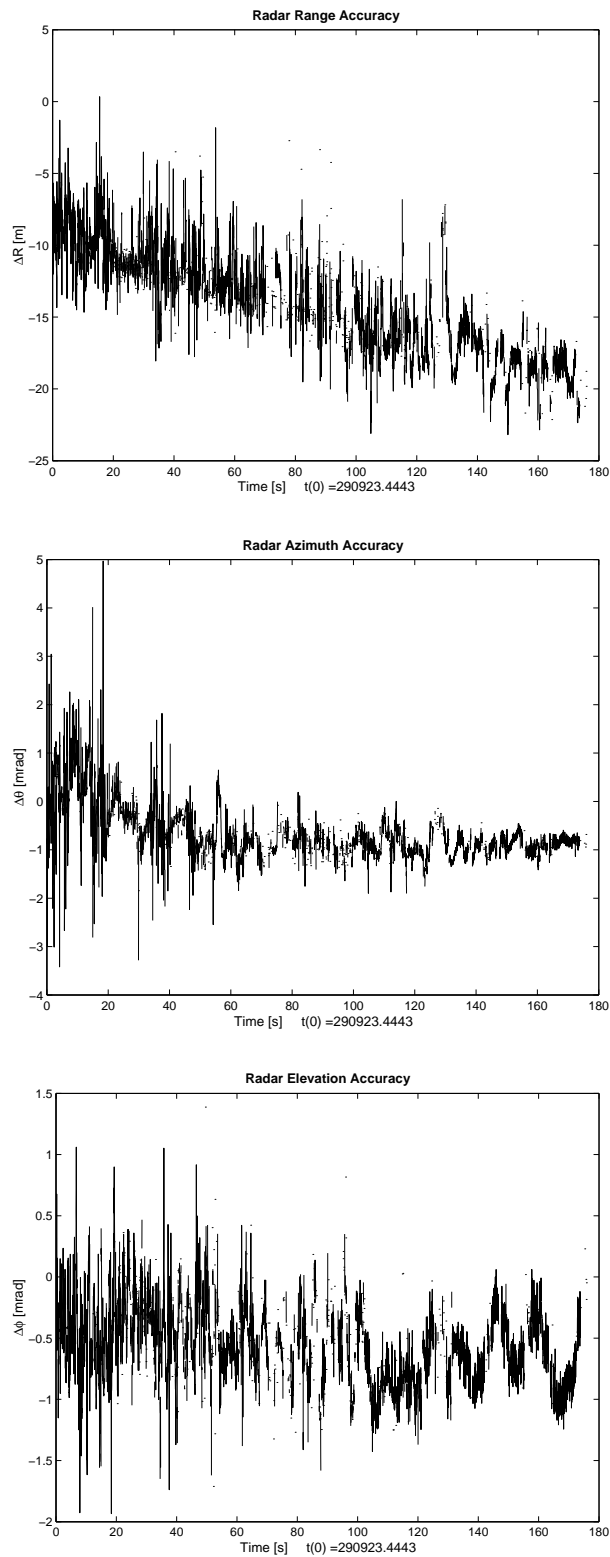


Figure B.20: Radar Segment 10: Difference between radar data and GPS-derived data for range, azimuth and elevation measurements (no latency compensation).

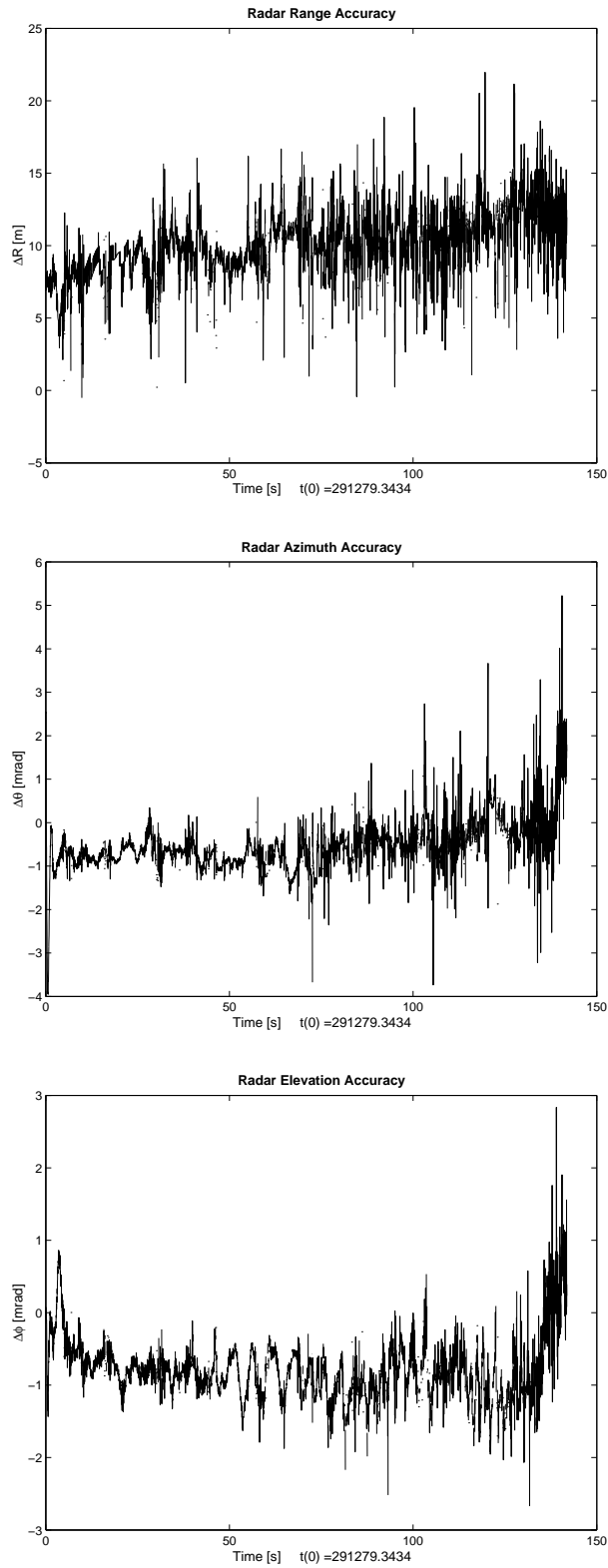


Figure B.21: Radar Segment 11: Difference between radar data and GPS-derived data for range, azimuth and elevation measurements (no latency compensation).

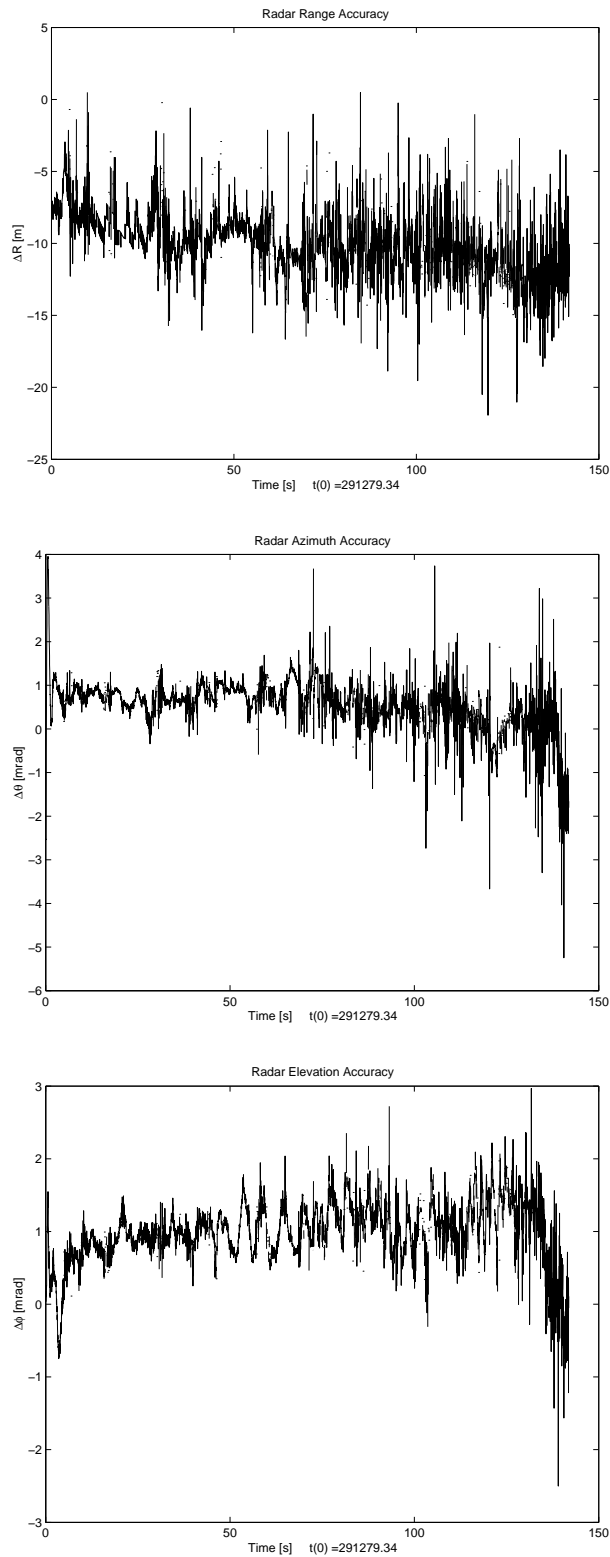


Figure B.22: Radar Segment 12: Difference between radar data and GPS-derived data for range, azimuth and elevation measurements (no latency compensation).

B.3 Results for ITB FAT - TAMS using LL data

Refer to Chapter 6.2.3.

B.3.1 Radar tracking accuracies for radar data latency compensation of 0 ms

Table B.1: Accuracy of azimuth data, radar time delay = 0 ms.

<i>Segment</i>	<i>min</i> [mrad]	<i>max</i> [mrad]	<i>mean</i> [mrad]	<i>std</i> [mrad]	<i>RMS</i> [mrad]	<i>Invalid data</i> [%]
1 (outbound)	-2.900	3.548	-0.514	0.394	0.647	24.672
2 (inbound)	-1.781	0.262	-0.708	0.233	0.745	14.301
3 (inbound)	-6.469	2.717	-0.428	0.689	0.811	32.144
4 (outbound)	-5.666	3.239	-0.704	0.331	0.778	33.460
5 (inbound)	-1.756	0.294	-0.697	0.236	0.736	26.902
6 (inbound)	2.112	0.307	-0.617	0.333	0.701	34.084
7 (inbound)	-3.955	0.581	-0.835	0.532	0.990	20.209
8 (outbound)	-2.207	1.904	-0.511	0.350	0.619	25.150
9 (not used)	n/a					
10 (inbound)	-3.234	3.077	-0.643	0.409	0.762	13.027
11 (outbound)	-3.420	4.970	-0.622	0.606	0.869	30.529
12 (inbound)	-3.952	5.223	-0.528	0.603	0.801	10.201

Table B.2: Accuracy of elevation data, radar time delay = 0 ms.

<i>Segment</i>	<i>min</i> [mrad]	<i>max</i> [mrad]	<i>mean</i> [mrad]	<i>std</i> [mrad]	<i>RMS</i> [mrad]	<i>Invalid data</i> [%]
1 (outbound)	-1.758	0.977	-0.647	0.260	0.697	24.672
2 (inbound)	-1.599	0.151	-0.777	0.245	0.814	14.301
3 (inbound)	-2.412	2.675	-0.464	0.308	0.558	32.144
4 (outbound)	-1.800	1.961	-0.295	0.442	0.532	33.460
5 (inbound)	-1.468	0.050	-0.752	0.234	0.787	26.902
6 (inbound)	-1.650	-0.486	-0.963	0.243	0.993	34.084
7 (inbound)	-2.036	0.083	-0.962	0.318	1.013	20.209
8 (outbound)	-2.150	0.537	-0.818	0.301	0.872	25.150
9 (not used)	n/a					
10 (inbound)	-2.491	0.929	-0.686	0.369	0.779	13.027
11 (outbound)	-1.934	1.388	-0.577	0.322	0.661	30.529
12 (inbound)	-2.665	2.834	-0.781	0.420	0.887	10.201

Table B.3: Accuracy of range data, radar time delay = 0 ms.

<i>Segment</i>	<i>min</i> [m]	<i>max</i> [m]	<i>mean</i> [m]	<i>std</i> [m]	<i>RMS</i> [m]	<i>Invalid data</i> [%]
1 (outbound)	-21.945	-0.149	-11.905	3.960	12.546	24.672
2 (inbound)	-1.617	17.437	7.589	1.792	7.798	14.301
3 (inbound)	3.692	18.359	11.673	1.712	11.798	32.144
4 (outbound)	-21.703	1.808	-12.397	2.797	12.708	33.460
5 (inbound)	-3.830	12.267	5.813	2.199	6.215	26.902
6 (inbound)	2.950	16.097	9.454	1.354	9.550	34.084
7 (inbound)	-0.052	21.209	10.723	2.185	10.943	20.209
8 (outbound)	-20.471	2.107	-12.678	3.393	13.125	25.150
9 (not used)	n/a					
10 (inbound)	-1.709	18.787	9.116	2.923	9.573	13.027
11 (outbound)	-23.189	0.335	-14.154	3.796	14.654	30.529
12 (inbound)	-0.512	21.968	10.030	2.191	10.266	10.201

Table B.4: Accuracies over all inbound flights, radar time delay = 0 ms.

<i>Measurement</i>	<i>min</i> [mrad, m]	<i>max</i> [mrad, m]	<i>mean</i> [mrad, m]	<i>std</i> [mrad, m]	<i>RMS</i> [mrad, m]
Azimuth	-6.469	5.223	-0.623	0.474	0.783
Elevation	-2.665	2.834	-0.739	0.361	0.822
Range	-3.830	21.968	9.006	2.845	9.445

Table B.5: Accuracies over all outbound flights, radar time delay = 0 ms.

<i>Measurement</i>	<i>min</i> [mrad, m]	<i>max</i> [mrad, m]	<i>mean</i> [mrad, m]	<i>std</i> [mrad, m]	<i>RMS</i> [mrad, m]
Azimuth	-5.666	4.970	-0.579	0.440	0.727
Elevation	-2.150	1.961	-0.603	0.378	0.711
Range	-23.189	2.107	-12.752	3.646	13.262

B.3.2 Radar tracking accuracies for radar data latency compensation of -204 ms

These are shown in Tables B.6 to B.10.

Table B.6: Accuracy of azimuth data, radar time delay = -204 ms.

<i>Segment</i>	<i>min</i> [mrad]	<i>max</i> [mrad]	<i>mean</i> [mrad]	<i>std</i> [mrad]	<i>RMS</i> [mrad]	<i>Invalid data</i> [%]
1 (outbound)	-2.969	3.502	-0.482	0.369	0.607	24.672
2 (inbound)	-1.797	0.312	-0.697	0.246	0.739	14.301
3 (inbound)	-6.375	2.811	-0.308	0.687	0.753	32.144
4 (outbound)	-5.699	3.222	-0.669	0.330	0.746	33.460
5 (inbound)	-1.729	0.324	-0.667	0.237	0.708	26.902
6 (inbound)	-2.119	0.327	-0.600	0.333	0.686	34.084
7 (inbound)	-3.739	0.806	-0.660	0.515	0.837	20.209
8 (outbound)	-2.013	2.108	-0.492	0.388	0.626	25.150
9 (not used)	n/a					
10 (inbound)	-3.193	3.172	-0.643	0.394	0.754	13.027
11 (outbound)	-3.785	4.720	-0.719	0.537	0.898	30.529
12 (inbound)	-3.937	3.425	-0.699	0.474	0.845	10.201

Table B.7: Accuracy of elevation data, radar time delay = -204 ms.

<i>Segment</i>	<i>min</i> [mrad]	<i>max</i> [mrad]	<i>mean</i> [mrad]	<i>std</i> [mrad]	<i>RMS</i> [mrad]	<i>Invalid data</i> [%]
1 (outbound)	-2.054	0.753	-0.811	0.268	0.854	24.672
2 (inbound)	-1.508	0.194	-0.708	0.239	0.748	14.301
3 (inbound)	-2.072	3.015	-0.244	0.308	0.393	32.144
4 (outbound)	-2.252	1.373	-0.488	0.383	0.621	33.460
5 (inbound)	-1.416	0.089	-0.698	0.234	0.736	26.902
6 (inbound)	-1.489	-0.367	-0.832	0.235	0.865	34.084
7 (inbound)	-1.870	0.289	-0.725	0.328	0.796	20.209
8 (outbound)	-2.605	0.281	-0.984	0.260	1.018	25.150
9 (not used)	n/a					
10 (inbound)	-2.042	1.272	-0.532	0.387	0.658	13.027
11 (outbound)	-2.406	1.157	-0.759	0.311	0.820	30.529
12 (inbound)	-2.272	3.257	-0.588	0.445	0.738	10.201

Table B.8: Accuracy of range data, radar time delay = -204 ms.

<i>Segment</i>	<i>min</i> [m]	<i>max</i> [m]	<i>mean</i> [m]	<i>std</i> [m]	<i>RMS</i> [m]	<i>Invalid data</i> [%]
1 (outbound)	-12.180	8.833	-2.583	3.722	4.530	24.672
2 (inbound)	-11.759	7.253	-2.537	1.787	3.102	14.301
3 (inbound)	-6.370	8.615	1.825	1.737	2.519	32.144
4 (outbound)	-12.568	11.455	-2.855	2.778	3.984	33.460
5 (inbound)	-12.909	2.440	-3.580	2.033	4.116	26.902
6 (inbound)	-6.445	6.728	0.043	1.358	1.357	34.084
7 (inbound)	-9.252	11.932	1.406	2.151	2.569	20.209
8 (outbound)	-10.835	11.668	-3.008	3.215	4.402	25.150
9 (not used)	n/a					
10 (inbound)	-11.024	9.114	-0.503	2.847	2.891	13.027
11 (outbound)	-13.484	9.431	-4.684	3.519	5.858	30.529
12 (inbound)	-10.453	12.726	0.326	2.295	2.318	10.201

Table B.9: Accuracies over all inbound flights, radar time delay = -204 ms.

<i>Measurement</i>	<i>min</i> [mrad, m]	<i>max</i> [mrad, m]	<i>mean</i> [mrad, m]	<i>std</i> [mrad, m]	<i>RMS</i> [mrad, m]
Azimuth	-6.375	3.425	-0.645	0.428	0.774
Elevation	-2.272	3.257	-0.590	0.381	0.702
Range	-12.909	12.726	-0.667	2.823	2.901

Table B.10: Accuracies over all outbound flights, radar time delay = -204 ms.

<i>Measurement</i>	<i>min</i> [mrad, m]	<i>max</i> [mrad, m]	<i>mean</i> [mrad, m]	<i>std</i> [mrad, m]	<i>RMS</i> [mrad, m]
Azimuth	-5.699	4.720	-0.580	0.426	0.720
Elevation	-2.605	1.373	-0.778	0.349	0.852
Range	-13.484	11.668	-3.254	3.453	4.744

Appendix C

Polynomial Coefficients

These appendices tabulate the coefficients for the polynomial to be fitted to the dGPS azimuth and elevation data.

Table C.1: Coefficients of dGPS **elevation** data for Optronics 5km range bin.

order of polynomial	a_1	a_2	a_3
1	1.5×10^{-3}	-4.435×10^2	0
2	2.212×10^{-5}	-13.082	1.934×10^6

Table C.2: Coefficients of dGPS **elevation** data for Radar 5km range bin.

order of polynomial	a_1	a_2	a_3
1	1.047×10^{-3}	-3.022×10^2	0
2	5.531×10^{-6}	-3.192	4.611×10^5

Table C.3: Coefficients of dGPS **elevation** data for Radar 10km range bin.

order of polynomial	a_1	a_2	a_3
1	3.111×10^{-4}	-89.756	0
2	-1.113×10^{-5}	6.429	-9.281×10^5

Table C.4: Coefficients of dGPS **azimuth** data for Optronics 5km range bin.

order of polynomial	a_1	a_2	a_3
1	-2.241×10^{-4}	69.469	0
2	-2.335×10^{-5}	13.811	-2.042×10^6

Table C.5: Coefficients of dGPS **azimuth** data for Radar 5km range bin.

order of polynomial	a_1	a_2	a_3
1	5.668×10^{-4}	5.668×10^7	0
2	2.011×10^{-5}	-11.618	1.676×10^6

Table C.6: Coefficients of dGPS **azimuth** data for Radar 10km range bin.

order of polynomial	a_1	a_2	a_3
1	-1.087×10^{-4}	34.501	0
2	1.018×10^{-5}	-5.881	8.489×10^5

End of Appendices